Minimization of Entropy Production in Diabatic Distillation Columns with Integrated Compression Resorption Heat Pumps

Author: Jasper de Kruif

Report number: 2327

Student number: 1178369

Final report, September 16, 2008

Supervisors:

Dr. Ir. C. A. Infante Ferreira

Prof. Dr. Ir. S. Kjelstrup

Prof. Dr. Eng. J. Gross

Process &Energy department
Delft University of Technology

Abstract

Minimization of the entropy production of different processes can be used to bring more insight in these processes. Diabatic distillation columns have heat transfer on every tray in the column, which means that a minimization of the entropy production in such a column can be favorable to obtain the optimal operating conditions.

Compression resorption heat pumps can be used to reduce the energy demand of diabatic columns. A diabatic column with a compression resorption heat pump is rejecting heat at the trays above the feed (rectifying section) and must be supplied of heat at the trays below the feed (stripping section). Compression resorption heat pumps are using the heat that is rejected from the diabatic column. This heat with a low temperature and pressure is converted to heat with a higher temperature and pressure, using a certain amount of compressor work. This high temperature heat is supplied to the column. In this configuration there is always a small external condenser needed at the top of the column. There are four components present in compression resorption heat pumps, namely a desorber, a resorber, a compressor and an expansion valve.

In the present study an optimization is performed minimizing the entropy production in diabatic columns with integrated compression resorption heat pumps. From this optimization, operating conditions are obtained that are favorable for the performance of the system. The working fluid in the compression resorption heat pump is an ammonia water mixture. The distillation concerns a Benzene / Toluene separation.

The optimization is done for a wide range of average ammonia concentrations in the mixture which is used in the compression resorption heat pump. Results have shown that the low average concentrations and the higher average concentrations gave the best results with respect to the entropy production. The minimum of entropy production is at an average concentration of 2wt% ammonia in the low concentration region, and 96wt% ammonia in the high concentration region. The compression resorption heat pump performance was stated as the Coefficient Of Performance (COP). The higher the COP the more efficient the heat pump operates. The highest COP was obtained at the concentrations causing the lowest entropy production (2wt% ammonia and 96wt% ammonia).

The heat loads required to perform the diabatic distillation were small i.e. supplied: 40.9 kW, rejected: 40.4 kW. This was due to the chosen purities and flows at the top and the bottom of the diabatic column. The heat load required to perform a conventional adiabatic distillation, with reboiler at the bottom and condenser at the top of the column and with the same purities and flows, is lower than the heat load required for the diabatic distillation process. However, due to the integration of the compression resorption heat pump the energy consumption of the diabatic column would become much lower than the energy consumption of the adiabatic column.

The tray in the diabatic distillation column with integrated compression resorption heat pump where the largest entropy production occurred, was modeled in two different detailed models. The first

model was a mass and heat transfer model. A tube of 0.6 m was used with a diameter of 30 mm. There where 20 parallel circuits needed for the heat transfer on the first desorber tray. The local entropy production increases rapidly in the first part of the tube due to the large heat supply. This heat supply is caused by the operating conditions, i.e. temperature differences between column and heat pump side and overall heat transfer coefficients. The total entropy production was lower than the entropy production calculated in the optimization model, but the order of magnitude was the same.

The second model was an irreversible thermodynamics based model. Due to time restrictions the irreversible thermodynamics model is not developed in a model properly. Therefore the results of this model are not evaluated in detail.

For future research it is recommended to implement the detailed models in the optimization model to improve the quality of the results.

Acknowledgements

First of all I would like to acknowledge my supervisor Carlos Infante Ferreira. I am very grateful for the many thing I have learned from him, and all the wise advices during my graduation, but also during my internship. He always encouraged me during my study at the TU Delft, and it was a pleasure working with him.

Many thanks are also go to my professor Signe Kjelstrup, who was very helpful during my graduation project especially when it came to irreversible thermodynamics.

I would like to acknowledge my parents, Ronald and Joke, who made it possible to do this study, and they always encouraged me in every possible way.

Denise I would like to thank you for your support, encouragement and patience during my study. You always believed in me.

I also want to thank my colleague students, Dennis, Jasper, Henk, Erik, Jordy, Marco, Mohammed, Sowande, Zhifang, for your help and support during my study at the TU Delft.

At last I want to sincerely thank Mr. Bernouw, who shared his expertise in mathematical problems with me.

Table of contents

Nomenclature

Latin symbols

B	Bottom product flow	[mol/s]
c_i	Concentration of molar density	[mol/m^3]
C_i	Molar concentration	[mol/mol]
c_p	Heat capacity at constant pressure	[J/kg K]
d	Diameter	[m]
D	Distillate product flow	[mol/s]
D	Diffusion coefficient	[m^2/s]
D_T	Thermal diffusion coefficient	[m^2/s K]
Ex	Specific exergy	[J/kg]
$\dot{ex}$	Exergy losses	[W]
$\hat{f}_i$	Fugacity of component i	[Pa]
F_i	Molar flow rate	[mol/s]
F	Feed flow	[mol/s]
g	Gravitational acceleration	[m/s^2]
G	Gibbs energy	[J]
$\Delta_r G$	Reaction Gibbs energy	[J/mol]
H	Enthalpy	[J]
h_i	Partial molar enthalpy	[J/mol]
h	Specific enthalpy	[J/kg]
h_F	Specific enthalpy feed	[J/mol]
h_n^L	Specific enthalpy tray n of the liquid stream	[J/mol]
h_n^V	Specific enthalpy tray n of the vapor stream	[J/mol]
$\dot{I}$	Irreversibility rate	[W]

J_i	Flux of component i	[mol /m^2 s]
J_s	Flux of entropy	[J m^2/K s]
k_i	Convective mass transfer coefficient	[m / s]
k_n	Equilibrium constant of the light component	
k_n'	Equilibrium constant of the heavy component	
l_{ik}	Phenomenological coefficient for coupling of diffusional fluxes i and k	
L_n	Liquid flow	[mol/s]
$\dot{m}_i$	Mass flow rate	[kg/s]
N	Total number of trays	
N_F	Feed tray	
P	Pressure	[Pa]
Q	Heat delivered to the system	[J]
$\dot{Q}$	Heat flux delivered to the system	[W]
q	Vapor quality	
q*	Heat of transfer	[J/mol]
R_{ik}	Resistivity coefficient for coupling of fluxes i and k	
R_i	Radius	[m]
R	Gas constant (=8.314)	[J/mol K]
S	Entropy of the system	[J/K]
$\Delta\dot{S}$	Sum of entropy production	[W/mK]
s^V	Entropy per volume	[J/K m^3]
s_F^L	Specific entropy of the liquid feed	[J/mol K]
s_D^L	Specific entropy of the liquid distillate	[J/mol K]
s_B^L	Specific entropy of the liquid bottom	[J/mol K]
s_n^L	Specific entropy tray n of the liquid stream	[J/mol K]
s_n^V	Specific entropy tray n of the vapor stream	[J/mol K]
S_i	Partial molar entropy	[J/K mol]

s	Specific entropy	[J/kg K]
dS_{irr}/dt	Total entropy production rate	[W/K]
T	Temperature	[K]
T_0	Temperature of environment	[K]
v_i	Specific volume	[m^3/kg]
V_n	Vapor flow	[mol/s]
$\dot{W}$	Power	[W]
x	Direction of transport	[m]
x_i	Mass fraction	[kg/kg]
X_i^c	Concentration of mass density	[kg/m^3]
x_n	mol fraction of the light component in the liquid streams	[mol/mol]
x_n'	Mol fraction of the heavy component in the liquid streams	[mol/mol]
X_i	General symbol for thermodynamic driving force	
y_n	mol fraction of the light component in the vapor streams	[mol/mol]
y_n'	Mol fraction of the heavy component in the vapor streams	[mol/mol]
z	height	[m]
z_F	Mol fraction of the light component in the feed stream	[mol/mol]

Greek symbols

α	Convective heat transfer coefficient	[W/m^2 K]
γ	Activity coefficient for non-electrolytes	[-]
Γ	Mass flow rate per wetted perimeter	[kg/m s]
δ	Film thickness	[m]
ϕ_i	Fugacity coefficient	
λ	Thermal conductivity	[W/K m]
λ	Lagrange multiplier	
μ	Dynamic viscosity	[N s/m^2]

μ_i	Chemical potential of i	[J/mol]
$\mu_{i,T}$	Chemical potential of i at constant T	[J/mol]
ρ	Density	[kg/m^3]
σ	Bulk entropy production rate	[W/K m^3]
σ_g	global entropy production rate	[W/K]
η	Efficiency	[-]
v	Kinematic viscosity	[m^2/s]

Subscripts

e	External
i	Internal
in	In
out	Out
pf	Process fluid
s	Solution
v	Vapor
l	Liquid
w	Wall
NH_3	Ammonia
H_2O	Water
R	Refrigerant mixture
Air	Air
n	Indicator for tray numbering
col	Column
hx	Heat exchanger (resorber and desorber)
0	Environment, or initial state
is	Isentropic

Superscripts

int	Interface
0	Environment, or initial state
s	Surface
v	Vapor
l	Liquid
irr	Irreversible

Abbreviations

COP	Coefficient of performance	[-]

Conductivity coefficients for bulk transport

l_{qq}	Main conductivity coefficient for heat transport	[J K/s m]
$l_{q\mu} = l_{\mu q}$	Coupling coefficient for heat and mass transport	[mol^2 K/m^2 s J]
$l_{\mu\mu}$	Main conductivity coefficient for mass transport	[mol^2 K/m s J]

Resistivity coefficients for bulk transport

r_{qq}	Main resistivity coefficient for heat transport	[J K/s m]
$r_{qs} = r_{sq}$	Coupling coefficient for heat and mass transport	[mol^2 K/m^2 s J]
r_{ss}	Main resistivity coefficient for mass transport	[mol^2 K/m s J]

1. Introduction

Nowadays the rapid depletion of energy resources is a world wide issue. The price of a liter of oil is increasing dramatically. The world population is using more and more energy over the last decades. Figure 1.1 shows the energy consumption of the world population over the last 43 years. From this figure it can be seen that the world energy consumption is increasing rapidly. The forecast for the energy consumption in the coming years can also be seen in this figure. The total energy consumption will increase more drastically in the next 12 years then it did before. To satisfy this energy need, people search for new (renewable) energy resources, but also the reduction of energy use is needed. Examples for renewable energy sources are e.g. wind-, water-, solar energy, biomass, etc. These renewable energy resources are also depicted in figure 1.1, and in figure 1.2. The forecast that is done in this figure projects the development of the last 43 years in renewable energy. The oil and natural gas are depleted in the end of this century. Therefore it is necessary to shift from fossil to renewable energy.

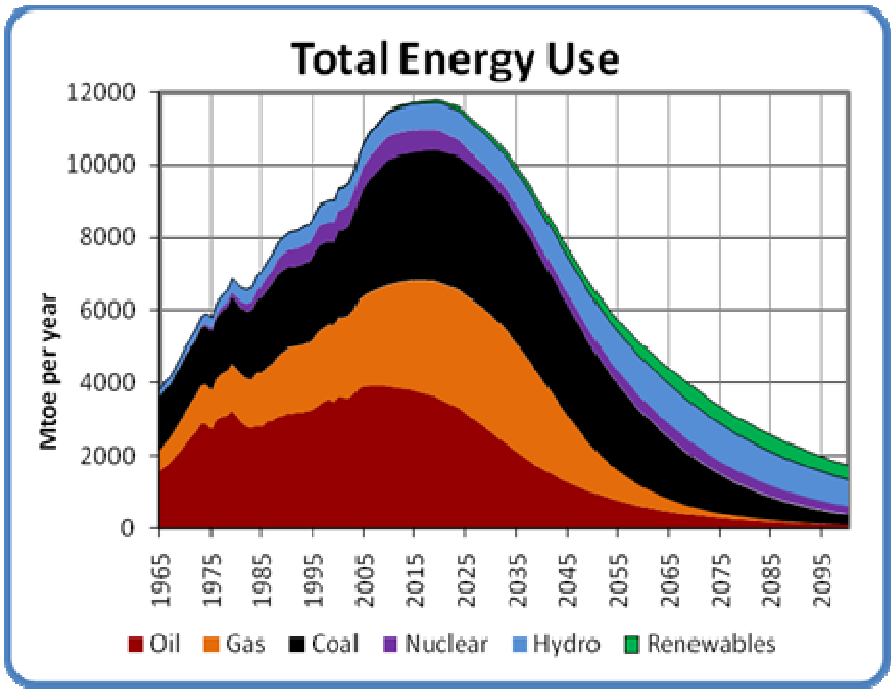

Figure 1.1 – Total energy use, 1965 – 2100[1]

Above some examples are given for renewable energy resources. Another way to reduce the energy consumption is to develop low energy consuming systems. A good example of such a system is a heat pump.

[1] www.paulchefurka.ca

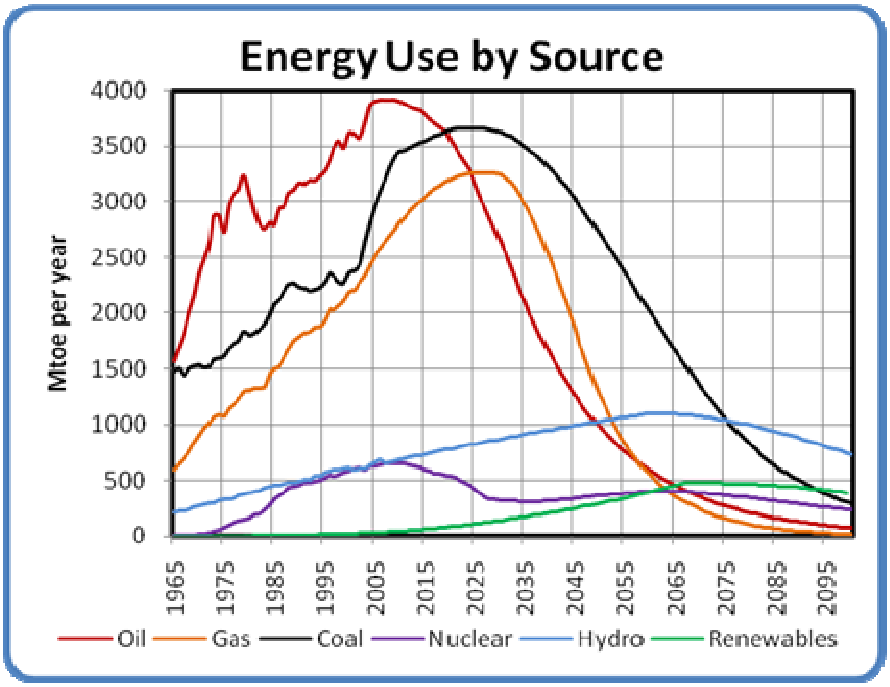

Figure 1.2 – Energy use by source, 1965 - 2100[2]

A heat pump uses energy (heat) with a low temperature. This energy is brought to a higher (pressure and) temperature level by using a compressor. This compressor uses energy like e.g. electricity. Energy is released from the system at a high temperature. Figure 1.3 is a graphical representation of the heat pump described above.

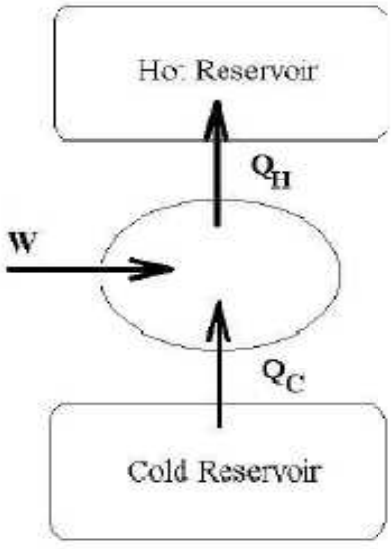

What can be seen in figure 1.3 is that the heat gained (Q_C) from the low temperature source and the work (W) that is applied on the system is equal to the heat that can be used by the heat user at high temperature level. The Coefficient of performance (COP) of a typical heat pump is in the range of 2-30 [3].

In recent years, the use of heat pumps has become more and more popular. Below some heat pump trends will be presented.

Figure 1.3 – heat pump principle Taboada (2007)

[2] www.paulchefurka.ca
[3] www.heatpumpcentre.org

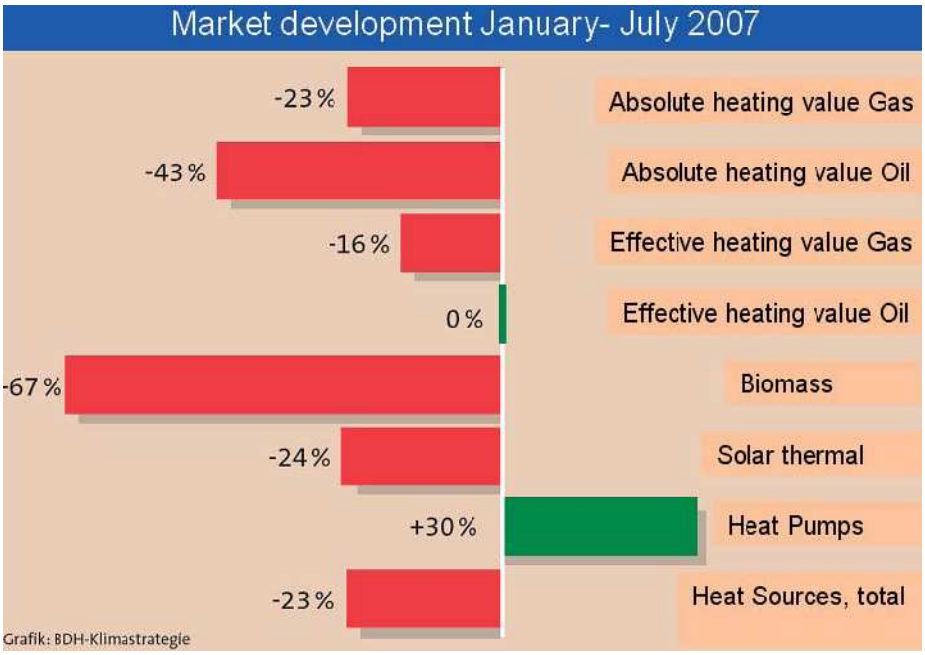

Figure 1.4 – Market analysis done by BDH

A market analysis, figure 1.4, done by the Association for House, Energy and Environmental Technology (BDH)[4] shows that the investment in almost all heating types, including solar thermal heating systems, has reduced. However, heat pumps show a market exception to this trend.

It is difficult to show a trend with the total installed capacity of heat pump because there is a wide range of different heat pumps. It is however, possible to show the trend for ground source heat pumps for a country like Korea. The trend of the installed capacity of ground source heat pumps is presented in figure 1.5.

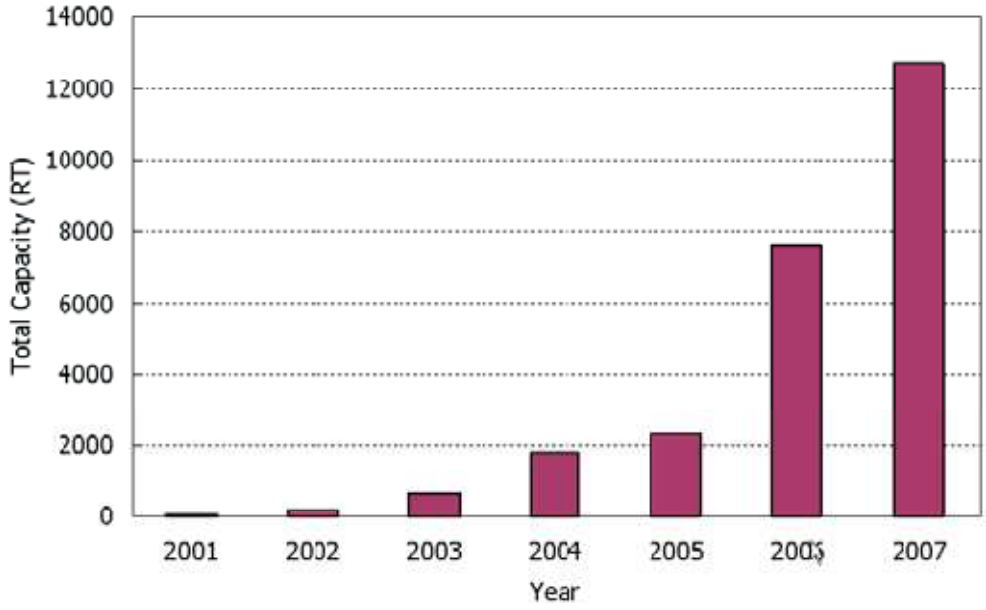

Figure 1.5 – Installed capacity of ground source heat pumps in Korea[4]

[4] www.heatpumpcentre.org

Another way to save energy is the optimization of current state-of-the-art processes. For example the heat pump discussed above can be optimized, by modifying the temperature driving forces in the heat exchangers or changing the working fluid, etc. By performing such an optimization the heat pump can become more efficient.

Energy can thus be saved by improving system performances. This can be realized by performing for example a second law optimization, or an exergy optimization.

This report will deal with a second law optimization, or entropy production, for a diabatic distillation column. In the next section some background will be presented about the topic of this report.

1.1 Background

Minimization of the entropy production of the different processes taking place in compression resorption cycles is thought to bring new insights in the analysis of these cycles. These new insights are expected to allow for optimization of the second law efficiency of these heat pumps and so to contribute also to first law efficiency improvements. Although the first extensive research on the application of the second law analysis in refrigeration and heat pump systems dates from 1984, (Auracher (1984)). Most of the publications limit themselves to component balances (e.g. Kilic and Kaynakli (2007) and Satapathy et al, (2004)). Kjelstrup & Bedeaux (2001), propose the use of local process side entropy production rate analysis for the optimization of heat and mass transfer processes. It is expected that application of this method to the different processes in compression resorption heat pumps will allow for significant improvements of the cycle.

Recently Taboada (2007), developed a model to predict the performance of diabatic distillation columns when the resorber of the heat pump is integrated in the stripping section of the column and its desorber is (partly) integrated in the rectification section of the column. With this model Taboada investigated the possible advantages of the heat pump integration and showed that enormous energy savings can be realized (e.g. from 2.0 MW energy required by an adiabatic column to 0.3 MW required by a diabatic column combined with a compression resorption heat pump).

1.2 Objectives

In Taboada's model the diabatic trays have been considered to operate with temperature differences between process side and heat pump fluid side of 5K. Both process side and heat pump side media have been assumed to be in equilibrium.

The objective of this study is to investigate the advantages of entropy production minimization in the evaluation / optimization of diabatic distillation column trays with integrated resorber / desorber of a compression resorption heat pump. Main goal is to identify the optimum operating conditions for the heat pump:

- thermal driving forces,
- operating pressure,
- refrigerant-absorbent average concentration

These objectives follows from the optimization by minimization of the entropy production in diabatic columns with integrated compression resorption heat pumps. To bring more detail in the cause of the entropy production on the trays, the tray in the column with the largest entropy production will be selected. For this tray (resorber of desorber) two detailed models will be developed. One model is taking the heat and mass transfer analogy into account, and the other model will be developed by using the theory of irreversible thermodynamics. In this way the local entropy production can be quantified.

1.3 Thesis overview

The main goal of this thesis is to present the results of the objectives above. To develop these results literature study is required. Results from this literature study are presented in chapter 2, where the first section presents a study on diabatic columns and compression resorption heat pumps. The second section presents the first and second law analysis. The second law analysis is discussed globally and locally. The last section of chapter 2 discusses the different components in the compression resorption heat pump, such as the compressor, resorber, desorber and expansion device.

Chapter 3 formulates the model that is used for the optimization by minimizing the entropy production in the diabatic columns with integrated compression resorption heat pumps. First the system is defined, i.e. the layout of the diabatic distillation columns with integrated compression resorption heat pumps, the first law analysis and the compression resorption heat pump cycle constraints. The second section discusses both global and local entropy production in the diabatic columns with integrated compression resorption heat pump, followed by the objective function and the constraints. The third section presents two detailed models of the resorber and the desorber. The first model is based on heat and mass transfer analogies, and the second model is based on the theory of irreversible thermodynamics. At last the conclusions of this chapter are presented in the fourth section.

The simulation approach is presented in chapter 4. First the program that has been used is discussed, thereafter the numerical solution procedure is presented for the optimization by minimizing the entropy production in compression resorption heat pumps. At last the approach for the detailed models is discussed.

The results of the present study are presented in chapter 5. First the results for the optimization by minimizing the entropy production in diabatic columns with integrated compression resorption heat pumps is presented. This section contains the results for the first part of the objectives above. The second part of this chapter presents the results for the detailed models (the second part of the objectives above). In the Appendices optimization results for a large number of operating conditions are also presented.

Chapter 6 gives a final conclusion of the present study, taking into account the objectives set above.

Finally in chapter 7 recommendations are done for future research on optimizations by minimizing the entropy production in diabatic columns with integrated compression resorption heat pumps.

2. Literature review

2.1 System description

2.1.1 Literature research on diabatic columns

Distillation columns are commonly used to separate two or more components from a feed stream with a certain purity. This is a continuous process in which heat is supplied to the bottom of the column and heat is rejected from the top of the column.

An adiabatic distillation column, figure 2.1 – a, is a column served by a reboiler and a condenser. The bottom product is a liquid, which is partly or fully evaporated (reboiler) and send back into the column for distillation. In the condenser the vapor, distillate product, is partially or fully condensed and send back into the column. In case of an adiabatic column the heat exchangers are outside the column.

A diabatic distillation column, figure 2.1 – b, has the same working principle as the adiabatic column only the heat exchangers (reboiler and condenser) are integrated in the column on each tray. The advantage of diabatic distillation is reducing the energy degradation (exergy losses). The result that has been obtained from earlier studies is that the exergy losses can be reduced up to 50%, Rivero (2002).

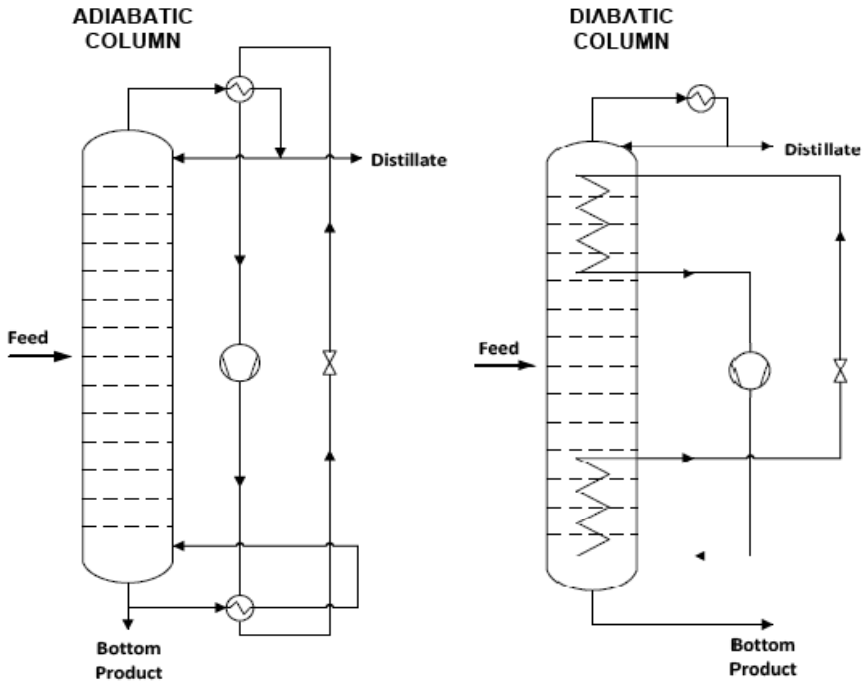

Figure 2.1- (a) adiabatic distillation column, (b) diabatic distillation column ,Taboada (2007)

A (diabatic) column consists of two parts namely a stripping section and a rectifying section. The stripping section is the part below the feed tray and the rectifying section is the part above the feed tray. In the stripping section heat is added to the distillation process by using a resorber. For the rectifying section a desorber is used to remove heat from the distillation process. In figure 2.1 –b a diabatic distillation column with integrated compression resorption heat pump is represented. This compression resorption heat pump is discussed in the following section.

The heat transfer from and to the distillation process on each tray is represented in figure 2.2 – a and b. Figure 2.2 – a is a cross sectional representation of the diabatic distillation column, where the trays are represented from side view. Figure 2.2 – b represents the trays with heat exchanger from top view.

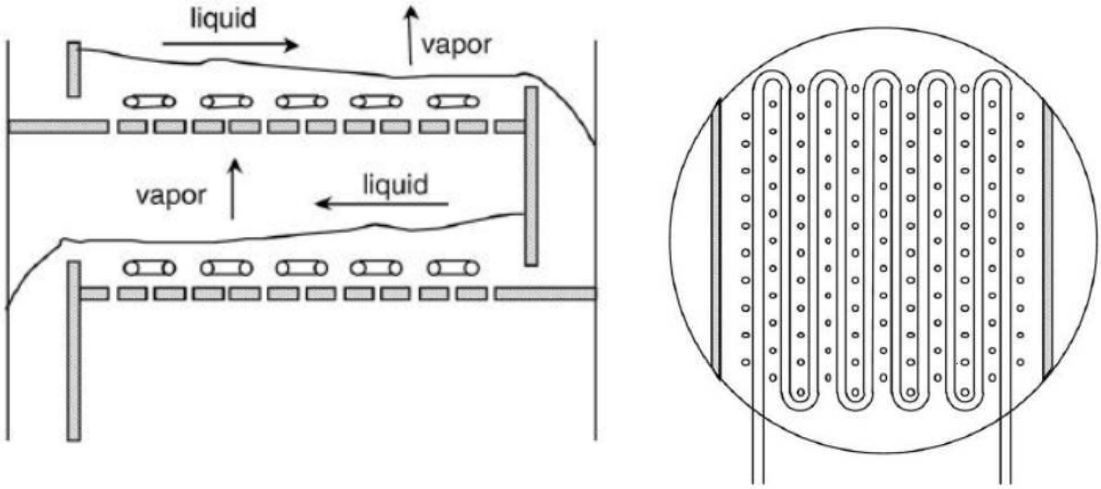

Figure 2.2 – (a) side view of diabatic distillation column, (b) top view of tray diabatic distillation column Rivero (2002)

Diabatic distillation can increase the second law efficiency drastically compared to adiabatic distillation, de Koeijer and Rivero (2003). Research was done to describe the entropy production rate in one adiabatic and one diabatic experimental water/ethanol rectifying column by applying the theory of irreversible thermodynamics. Result of this research was that the diabatic column looses 39% less exergy than the adiabatic column. The heat and mass transfer on the trays and in the heat exchangers determined the entropy production rate, and neither the pressure drop nor mixing effects played a large role in those columns.

To model this second law efficiency, analytical or numerical methods are required. De Koeijer et al. (2002) compared the entropy production rate and investigated its minimization for binary diabatic distillation. Two analytical methods, the equal thermodynamic distance method and the Lagrange minimization method applied to a model derived from irreversible thermodynamics, were compared with two numerical methods, the Powell and Monte Carlo algorithm's. Result from this research was that the Monte Carlo and Powell methods were giving similar results and the lowest entropy production rates. The analytical method based on applying Lagrange minimization on irreversible thermodynamics gave no direct result, but it's solution was in agreement with the numerically obtained minima.

Exergy analysis provides an assessment on the degree of thermodynamic perfection of a process, Labidi et al. (2000). The intrinsic exergy efficiency of absorption heat pumps is discussed in Labidi's

work. The intrinsic efficiency is based on the concept of transiting exergy. Result from this study is that when the analysis was only limited to heat fluxes, the intrinsic exergy efficiency becomes equivalent to a particular case of the well known thermodynamic efficiency based on the second law efficiency.

This exergy has also an economic and ecologic implication, Rivero (2002). The economic implication of exergy results from the fact that exergy is a measure of the quality of energy, of it's availability to perform work. The ecologic implication of exergy results from the fact that exergy is a measure of departure from equilibrium with the environment, of the difference in temperature, pressure, composition, etc. In Rivero's work a study is done on the three E's, energy-economy-ecology. The conclusion from his study is that exergy analysis is very important for process industries, such as e.g. diabatic distillation, which allows to simultaneously consider the three E's .

2.1.2 Literature research on compression resorption heat pumps

The compression resorption heat pump is also very often called a hybrid heat pump. This hybrid heat pump is a compression system working with an azeotropic mixture. In the desorber heat is added to the system, so evaporation takes place, which is not complete due to the fact that there is an azeotropic mixture present is the system. Therefore a two phase fluid , the weak solution and an ammonia rich gas phase, is present after the desorber. The pressure and temperature on this two phase fluid can be increased by using a wet compression (figure 2.3-b) or a dry compression with solution pump (figure 2.3-a). When the compression has taken place the mixture enters the resorber in which heat is removed from the system. The mixture, concentrated (strong) solution, leaves the resorber (as a liquid), to the expansion valve, after which it returns to the desorber as a two phase mixture.

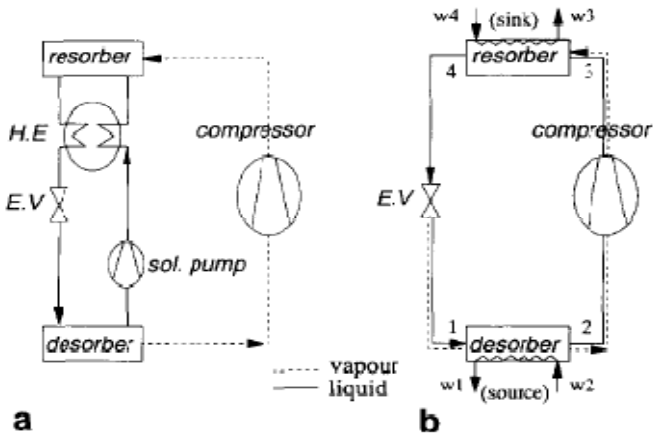

Figure 2.3 – (a) Hybrid heat pump with solution recirculation (Osenbrück cycle) (E.V. – expansion valve, H.E – heat exchanger); (b) hybrid wet compression cycle, Itard and Machielsen (1994)

In case all solution is recirculated the cycle is called a Osenbrück cycle. The wet compression, which was referred to in the above, shown in figure 2.3-b, is a two phase compression. In the desorber incomplete evaporation takes place, which means that at the outlet there is a two phase mixture. If the two phase mixture is compressed at once in the compressor, a wet compression has taken place. The second option, figure 2.3-a, is a dry compression in which the use of a solution pump makes it possible to pump the liquid phase to the resorber. The vapor phase is compressed by the dry compressor, after which it enters the resorber.

To increase the efficiency (COP) of the cycle, a mixture is used which allows for lower pressure levels and gliding temperatures during the desorption in the desorber and the absorption in the resorber.

Wet compression has in practice not often been used due to technical problems. In case wet compression can be used the heat pump efficiency (COP) will be improved, Itard and Machielsen (1994).

Kilic and Kaynakli (2007) and also Kaynakli and Yamankaradeniz (2007), did research on the second law efficiency for the components of an absorption cycle. For the system and conditions investigated, they concluded from the research that the maximum entropy production is in the desorber. The performance of the absorption refrigeration system increases with increasing desorber and evaporator temperatures, but decreases with increasing condenser and absorber temperatures. Exergy losses in the expansion valves and pump are small compared to other components. The highest exergy loss occurs in the desorber regardless of operating conditions, which therefore makes the desorber the most important component of the cycle in question. For this cycle extremely large temperature driving forces in the desorber were assumed. In this report the driving forces will be much smaller. Therefore the results from the above described study are an estimation for this report.

2.2 Thermodynamic analysis

2.2.1 First law analysis

For the thermodynamic analysis of the compression resorption heat pump with an azeotropic mixture, the principles of mass and energy conservation, first and second law efficiencies can be applied to every component of the system. Each component can be treated as a control volume with inlet and outlet streams, heat transfer and work interactions. In the system, mass conservation includes the mass balance of total mass and each component of the solution. In this report the solution considered is a mixture of water and ammonia. The equation that is describing the mass conservation in the system is the following:

$$\sum(\dot{m}x)_{in} - \sum(\dot{m}x)_{out} = 0 \quad [2.1]$$

Where $\dot{m}$ is the mass flow rate and x the mass fraction of ammonia in the solution.

Satapathy et al. (2004), studied compression resorption heat pumps for simultaneous cooling and heating. The results of the thermodynamic analysis of the compression resorption heat pumps are carried out in the equations below.

The energy balance is obtained by applying the first law of thermodynamics on every component of the compression resorption system :

$$\sum(\dot{m}h)_{in} - \sum(\dot{m}h)_{out} + \left[\sum \dot{Q}_{in} - \sum \dot{Q}_{out}\right] + \dot{W} = 0 \quad [2.2]$$

These mass and energy balances can be written for each component in the compression resorption heat pump (stationary state assumed), see figure 2.3:

Desorber mass and energy balance:

$$(x\dot{m})_{in} = (x\dot{m})_{out} \quad [2.3]$$

$$\dot{Q}_{desorber,in} = (\dot{m}h)_{out} - (\dot{m}h)_{in} \quad [2.4]$$

Resorber mass and energy balance:

$$(x\dot{m})_{in} = (x\dot{m})_{out} \quad [2.5]$$

$$\dot{Q}_{resorber,out} = (\dot{m}h)_{in} - (\dot{m}h)_{out} \quad [2.6]$$

Power input to the compressor (for dry compression only):

$$\dot{W}_{compressor,in} = \dot{m}_{in,v}(h_{out} - h_{in}) \quad [2.7]$$

Power input to the solution pump (for dry compression only):

$$\dot{W}_{solution\ pump,in} = \dot{m}_{in,l}(h_{out} - h_{in}) = \dot{m}_{in,liquid} \int_{P_{in}}^{P_{out}} v_{in}\, dP \times \frac{1}{\eta_{pump}} \quad [2.8]$$

At last the coefficient of performance COP can, for dry compression, be written as:

$$COP = \frac{\dot{Q}_{resorber,out}}{\dot{W}_{compressor,in} + \dot{W}_{solution\ pump,in}} \quad [2.9]$$

The second law analysis of the system will be discussed in the next sections.

2.2.2 Global second law analysis

The system performance can be investigated developing a second law analysis based on exergy flows. Exergy analysis is the combination of the first and second law of thermodynamics. Exergy is defined as the work potential of a material or fluid stream, when brought in equilibrium with the environment, Sencan et al. (2005).

When kinetic and potential energy effects may be considered negligible, the general expression for the exergy of a fluid stream is:

$$Ex = (h - h_0) - T_0(s - s_0) \quad [2.10]$$

Where Ex is the specific exergy, h the specific enthalpy and s the specific entropy of the fluid at temperature T, and h_0 and s_0 and the specific enthalpy and entropy respectively, of the fluid at environmental conditions including temperature T_0.

The expression for the exergy losses $\dot{ex}$ or irreversibility's that occur in each component of the process are defined as:

$$\sum \dot{ex} = \sum \dot{m}_{in} Ex_{in} - \sum \dot{m}_{out} Ex_{out} - \left[\left[\sum \dot{Q}\left(1 - \frac{T_0}{T}\right)\right]_{in} - \left[\sum \dot{Q}\left(1 - \frac{T_0}{T}\right)\right]_{out}\right] + \sum \dot{W} \quad [2.11]$$

Kilic and Kaynakli (2007) proposed a general equation for the irreversibility rate in a process, equation 2.12. This equation can be derived for the desorber and resorber of the cycle under study when all heat is transferred to the same environment, what will not be the case.

The irreversibility rate $\dot{I}$ per volume can be written as:

$$\dot{I} = T_0 \sigma_g = T_0 \left(\sum \dot{m}_{out}\, s_{out} - \sum \dot{m}_{in}\, s_{in} - {}^{\dot{Q}}/_{T} \right) \quad [2.12]$$

Whereby the entropy generation or entropy production σ_g can be calculated by using the thermodynamic analysis for absorption systems proposed by Kaynakli and Yamankaradeniz (2007).

Entropy production in the desorber (for constant desorber temperature):

$$\sigma_{g,desorber} = \dot{m}_{out} s_{out} - \dot{m}_{in} s_{in} - \frac{1}{T} \int_{desorber,in}^{desorber,out} d\dot{Q} \quad [2.14]$$

Entropy production in the resorber (for constant resorber temperature):

$$\sigma_{g,resorber} = \dot{m}_{out}s_{out} - \dot{m}_{in}s_{in} - \frac{1}{T}\int_{resorber,in}^{resorber,out} d\dot{Q} \quad [2.15]$$

Entropy production in the compressor (assuming it is adiabatic):

$$\sigma_{g,compressor} = \dot{m}_{out}s_{out} - \dot{m}_{in}s_{in} \quad [2.16]$$

Entropy production in the expansion valve:

$$\sigma_{g,expansion\ valve} = \dot{m}_{out}s_{out} - \dot{m}_{in}s_{in} \quad [2.17]$$

In the above a general formulation for entropy production and exergy loss per component was given. In the next section the local entropy production will be presented for every component in the compression resorption heat pump.

2.2.3 Local second law analysis

Kjelstrup and Bedeaux (2001), proposed a method to calculate the local entropy production rate for processes. The optimum process will have a minimum of entropy production (0 = reversible). In this section the local entropy production will be discussed.

Irreversible thermodynamics is the only method that can be used to assess the second law efficiency or indicate how valuable resources are exploited. In contradiction to what has been considered in section 2.2.2, local entropy production will be discussed in this section. The local entropy can be calculated by using fluxes, which are linear combinations of the forces in the system. The assumption of local equilibrium is used in this section to derive the entropy production. Below the (simple) flux equations are presented.

In section 2.2.2 only the entropy production due to heat transfer was considered. In reality there is also entropy production due to molar fluxes (concentrations), and electrical currents (electric potential). For this reason eq. 2.20 is presented for local entropy production.

Local entropy production rate (σ) by the second law:

$$\sigma = \sum_i J_i X_i \geq 0 \quad [2.20]$$

Where σ is the product sum of conjugated fluxes, J_i, and forces X_i. This equation converts easily to eq. 2.19, when its assumed that only heat transfer plays a role in eq. 2.20:

$$\sigma = \int \frac{d\dot{Q}}{T} = \left[-\lambda \frac{dT}{dx}\right]\left[\frac{\partial}{\partial x}\frac{1}{T}\right] = J_q' X \quad [2.21]$$

Where in this case X is the thermal force $d(\frac{1}{T})/dx$.

Heat flux in terms of the temperature gradient:

$$J'_q = -\lambda \frac{dT}{dx} \quad [2.22]$$

Molar flux of one of the components in terms of the gradient of its molar concentration c:

$$J_i = -D \frac{dc}{dx} \quad [2.23]$$

The driving force for eq. 2.23 is the chemical force $[-(1/T)(d\mu_T/dx)]$.

The change in local entropy can be described by equation 2.24 for stationary state, where the result is given by the flow of entropy through a volume element, and the entropy production rate (σ):

$$\frac{\partial s}{\partial t} = -\frac{\partial}{\partial x} J_s + \sigma \quad [2.24]$$

Where s the entropy per volume and J_s the entropy flux. From this equation it is obvious that the entropy production rate (σ) must be written in terms of conjugate forces and fluxes.

2.3 Component description

In this section the different components of the compression resorption heat pump will be discussed. The heat pump contains four different components namely a desorber, a resorber, a compressor and an expansion valve.

To minimize the entropy production in the compression resorption heat pump it is necessary to assume a geometry for the different components.

2.3.1 Desorber geometry

The desorber is an application that removes heat from a process flow. In this report the process flow is the one that has to be separated by using distillation. In the compression resorption heat pump a two component mixture, ammonia / water, is present. A strong solution enters the desorber, where it absorbs heat. By absorbing this heat, a lower concentration of ammonia is obtained. This weak solution leaves the desorber and enters the compressor.

The entering flow of the desorber is at the top of the distillation column. This flow leaves the desorber at approximately the feed stage of the column. The mixture is thus flowing from a high to a lower level. In this case a falling film desorber can be used as geometry.

Kim (2007), presented a falling film type desorber, where a refrigerant vapor is produced by adding heat to the refrigerant-rich interface. This is a somewhat complex model because the entrance effects are also taken into account as well as the different film types.

Islam (2007), investigated the experimental and theoretical heat and mass transfer that takes place in the falling film absorber of a vapor absorption cooling system. There was a satisfactory agreement between the analytical model and the experimental results. The equations of this theoretical model were solved by using the Laplace Transformation technique.

Xiaofeng et al.(2007), proposed a numerical analysis of a falling film absorption with ammonia / water in a magnetic field. The result of this study was that in some degree the magnetic field has a positive effect of the ammonia / water falling film absorption.

Medrano et al. (2003), presented a simple model for falling film absorption on vertical tubes for Lithium-Bromide water systems. This model will be adopted to describe the desorber by rewriting the mass and energy balances presented by these authors.

2.3.2 Resorber geometry

The resorber is working in an opposite direction as de desorber, because it adds heat to the process (distillation) flow. The ammonia / water mixture enters the resorber at a higher pressure and temperature level than applies the desorber. This is due to the compression that is done before the mixture enters the resorber.

A weak solution and ammonia vapor enter the resorber where it adds heat to the distillation process. Therefore the concentration of ammonia in the solution will increase during the resorption process. The leaving strong solution flows out to the expansion valve, where the pressure and temperature of the mixture decrease.

The resorption process takes place in the lower part of the column. The mixture enters the column at the bottom, and leaves at approximately the feed stage. Therefore a falling film absorber cannot be used for this process. A geometry of the resorption system that can be used in this case is a bubble absorber.

A bubble absorption process is characterized by simultaneous heat and mass transfer phenomena. Infante Ferreira (1985), presented a study of the combined momentum, heat and mass transfer processes in two-phase vertical slug flow. Infante Ferreira et al. (1984), investigated heat and mass transfer is vertical tubular bubble absorbers, figure 2.4, for ammonia / water absorption systems. They presented correlations of the mass transfer coefficients resulting from experiments in the form of a modified Sherwood relation. Also an iterative procedure was presented which allows design of vertical tubular bubble absorbers for ammonia / water absorption refrigeration systems.

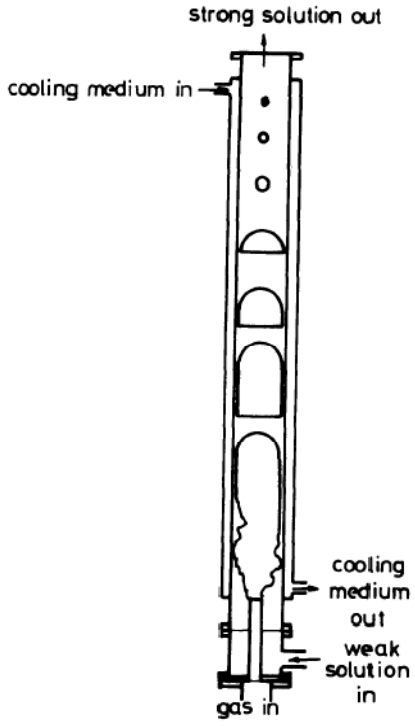

Figure 2.4 – Vertical tubular absorber, (Infante Ferreira et al. 1984)

The visualization of bubble behavior and bubble diameter correlation for ammonia /water bubble absorption was presented by Kang et al.(2002). The research that was presented was too specific on the bubble dynamics which is out of the scope for the “simple” model that has to be developed for this research.

The model presented by Infante Ferreira et al. (1984), will be adopted to describe the mathematical model for the resorber.

2.3.3 Compressor and expansion valve geometry

From section 2.1.2 two possible types of compression resorption heat pumps were discussed. The first heat pump makes use of dry compression, which means that the two phases (liquid and vapor) after the desorber are separated. The vapor phase is compressed by the compressor (dry compression) and the liquid phase is pumped by a solution pump to the resorber. The two phases enter the resorber where they are absorbed.

The second option is a wet compression. In this case the two phases that leave the desorber are not separated, but compressed at once, by the compressor. In practice the wet compression has not been often applied.

Zamfirescu et al. (2004) investigated the heat and mass transfer phenomena for wet compression. However, due to the fact that previous studies indicate that the most important components that determine the entropy production, are the resorber and the desorber (section 2.1.2), the heat and mass balances are not modeled in detail for the compressor. Only the global entropy production is taken into account in this report.

Like the compressor the expansion valve will be modeled as a global component, with global entropy production.

3. Model formulation

In this chapter the mathematical model of diabatic columns with integrated compression resorption heat pump will be formulated. Section 3.1 starts with the definition of the whole system, followed with a first law analysis for the system. The approach and assumptions to calculate the different states in the heat pump is presented in section 3.1.3.

The entropy production of the total system, heat pump plus diabatic column, is described in section 3.2.1, by using entropy balances. Global entropy production balances are used to determine the entropy production on every tray in the column, using the assumption of vapor – liquid equilibrium at the outlet of each tray. These balances are presented in section 3.2.2. Using these balances the objective function, the total entropy production, can be defined, which is done in 3.2.3. This objective function will be optimized, searching for the solution with lowest entropy production.

From the above optimization the tray with the largest entropy production will be selected. For this tray a dynamic model will be developed. The related dynamic models are presented in section 3.3. The model, for the resorber and desorber trays is presented in section 3.3.1.1 and 3.3.1.2 respectively. In these models several correlations for mass and heat transfer are used.

The above can also be done using irreversible thermodynamics theory, Kjelstrup and Bedeaux (2008), which is presented in a second model. The assumption of equilibrium at the outlet of each tray is then not needed for this model. This method is presented in section 3.3.2, where the mathematical models for the desorber and resorber from 3.3.1.1 and 3.3.1.2 are coupled with the irreversible thermodynamics theory.

The conclusions of this chapter are presented in section 3.5. The optimization of the process by minimization of the entropy production in diabatic columns with integrated compression resorption heat pump will be worked out in a Matlab environment. The tray with the largest entropy production will be modeled, taking the local driving forces and fluxes into account.

3.1 System definition

3.1.1 Layout of distillation column with integrated compression resorption heat pump

In section 2.1.1 the general working principle of the diabatic distillation column has been described. When possible heat is transferred on every tray in the distillation column, with exception of the feed tray. The advantage of this distillation method, is the reduction of exergy losses in comparison with

adiabatic distillation columns. Disadvantages are the extra investment costs associated with the heat exchangers.

The compression resorption heat pump that supplies and rejects heat to and from the column operates, as described in section 2.1.2, with an ammonia / water mixture.

Figure 3.1 represents the diabatic column with the integrated compression resorption heat pump. It is assumed that the total number of trays in the column is fixed. The number of trays that transfer heat with the resorber, and the number of trays that transfer heat with the desorber are also fixed. Røsjorde (2004), modeled Benzene / Toluene diabatic columns. His model optimizes the entropy production in diabatic columns. From the existing model the heat transfer from and to each tray of the column is obtained as well as the temperature profile of the column.

The compression resorption heat pump has to supply and reject the heat required by the column. The heat will be supplied by the resorber, and rejected to the desorber. For a heat pump, the rejected heat must be equal to the supplied heat plus the compressor work. For the diabatic column in question the supplied heat is given by the requirement that there is no external reboiler present in the system. An external condenser is needed to reject the remaining heat. In formula form this can be written as follows.

First law of thermodynamics for a heat pump:

$$\dot{W}_{compressor} = \dot{Q}_{desorber} - \dot{Q}_{resorber} \qquad [3.1]$$

The heat load of the external condenser can then be determined by:

$$\left|\dot{Q}_{removal\_column}\right| = \left|\dot{Q}_{desorber}\right| + \left|\dot{Q}_{ext.condenser}\right| \qquad [3.2]$$

Initially a temperature difference between the column side and the heat pump side (mixture) has to be assumed. Taboada (2007), assumed 5K for this temperature difference.

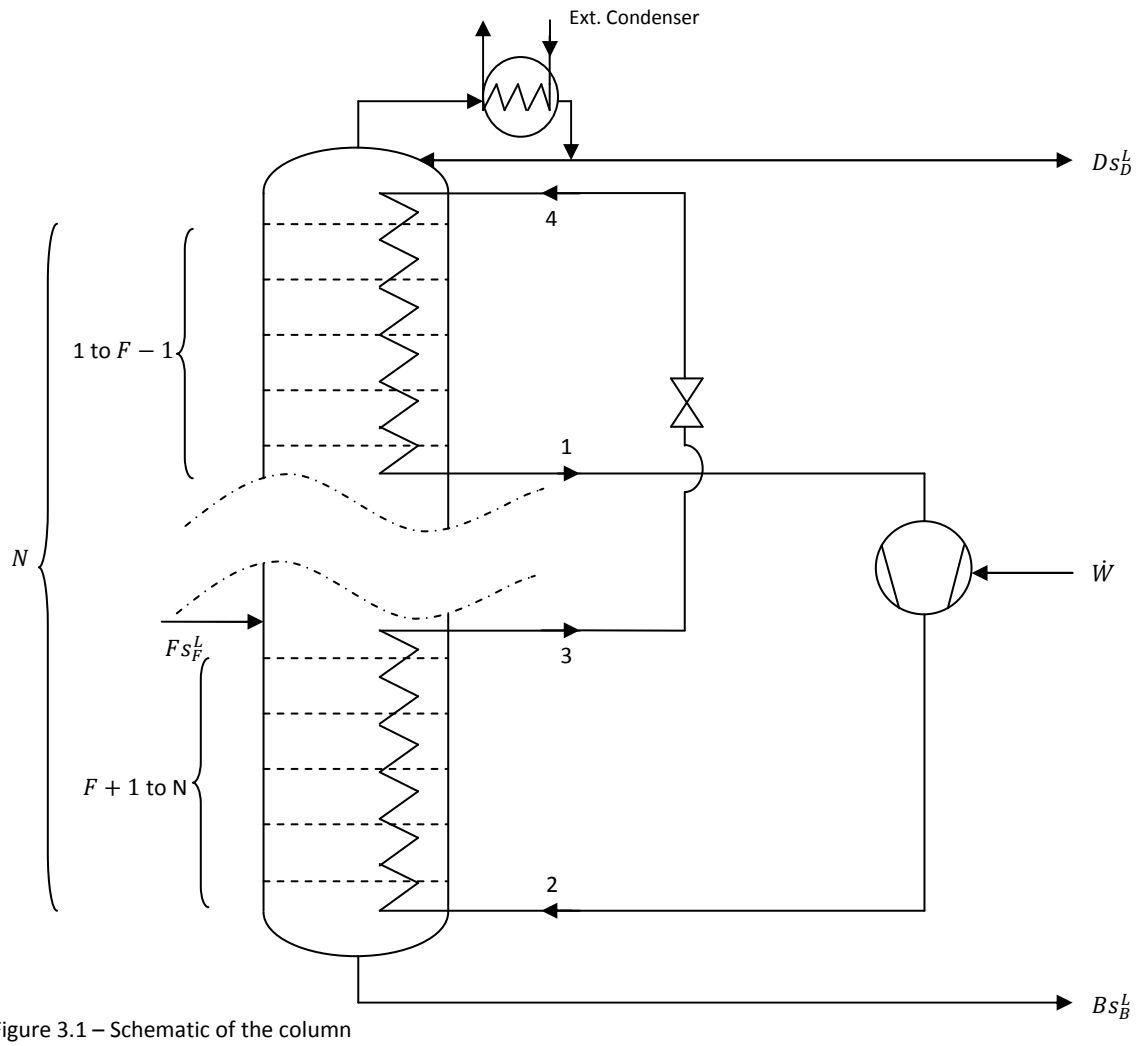

Figure 3.1 – Schematic of the column

3.1.2 First law analysis diabatic columns with integrated compression resorption heat pump

The first law analysis for compression resorption heat pumps done in section 2.2.1, can be expanded with a first law analysis for the diabatic column. This analysis will be done by making use of mass and energy balances. Below the first law analysis is done for the diabatic column with integrated compression resorption heat pump.

The main equations for binary tray distillation (diabatic column) are obtained from Taboada (2007):

The equations for a typical tray n, figure 3.2, are given below (where F is only at the feed tray):

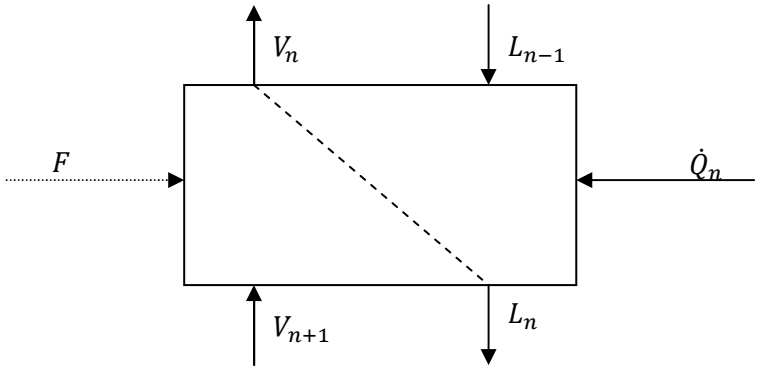

Figure 3.2 – Typical tray n

Total mol balance:

$$V_n + L_n = V_{n+1} + L_{n-1} \quad [3.3]$$

Mol balance for the light component:

$$V_n y_n + L_n x_n = V_{n+1} y_{n+1} + L_{n-1} x_{n-1} + (F z_F) \quad [3.4]$$

Energy balance equation:

$$V_n h_n^V + L_n h_n^L = V_{n+1} h_{n+1}^V + L_{n-1} h_{n-1}^L + (F h_F) + \dot{Q}_n \quad [3.5]$$

Equilibrium relations between vapor and liquid phases:

$$y_n = k_n x_n \quad [3.6]$$

$$y_n' = k_n' x_n' \quad [3.7]$$

Where k_n the equilibrium constant of the light component, k_n' the equilibrium constant of the heavy component, x_n' the mol fraction of the heavy component in the liquid streams and y_n' the mol fraction of the heavy component in the vapor streams.

Summation equation for the liquid and vapor compositions:

$$x_n + x_n' = 1 \quad [3.8]$$

$$y_n + y_n' = 1 \quad [3.9]$$

From eq. 3.5, the energy balance for the column at each tray can be given by the following equation:

$$\dot{Q}_n = V_n h_n^V + L_n h_n^L - V_{n+1} h_{n+1}^V - L_{n-1} h_{n-1}^L - k \quad [3.10]$$

Where k is defined as:

$$k = \begin{cases} qFh_F^V & \mathrm{n} = \mathrm{N_{F-1}} \\ (1-q)Fh_F^L & \mathrm{n} = \mathrm{N_F} \\ 0 & \text{otherwise} \end{cases} \quad [3.11]$$

k is graphically represented in figure 3.3:

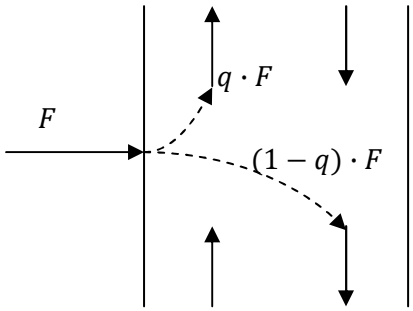

Figure 3.3 – Distribution of the feed flow above and below the feed entrance

The energy balance for the lowest tray:

$$\dot{Q}_N = V_N h_N^V + B h_N^L - L_{N-1} h_{N-1}^L \quad [3.12]$$

The first law analysis for the compression resorption heat pump (at each heat transferring tray) can be described using the following equations:

Desorber for $n = 1$ to $F - 1$:

$$\dot{m}_{s+1} x_{n+1} + \dot{m}_{v+1} y_{n+1} = \dot{m}_s x_n + \dot{m}_v y_n \quad [3.13]$$

$$\dot{Q}_{desorber,in,n} = \dot{m}_R h_n - \dot{m}_R h_{n+1} \quad [3.14]$$

Resorber for $n = F + 1$ to N:

$$\dot{m}_{s+1} x_{n+1} + \dot{m}_{v+1} y_{n+1} = \dot{m}_s x_n + \dot{m}_v y_n \quad [3.15]$$

$$\dot{Q}_{resorber,out,n} = \dot{m}_R h_{n+1} - \dot{m}_R h_n \quad [3.16]$$

Compressor work:

$$\dot{W}_{compressor} = \dot{m}_R (h_{F-1} - h_N) \quad [3.17]$$

The above equations are presenting the first law analysis for diabatic columns with integrated compression resorption heat pump.

3.1.3 Heat pump cycle constraints

The operating conditions, such as e.g. pressure levels between resorber and desorber, can be determined by using 4 state points in the heat pump cycle. These state points are located at the in- and outlet of the resorber and desorber, see figure 3.1. Using these four states, the pressure levels, the refrigerant mass flow, the compressor work, the desorber load, the temperatures, entropies and enthalpies can be determined. Below a procedure to calculate these state points is presented.

To start the calculations assumptions have been made:

- Temperature difference of n K between the column fluid and the heat pump mixture in state 2, 3 and 4 (initially n is taken equal to 5 K).
- Isentropic efficiency of 70% assumed, because of the irreversibilities in the compressor.
- Isenthalpic expansion ($h_3 = h_4$).
- No pressure drop in the resorber and the desorber.
- Mixture is saturated liquid in state 3 (all ammonia is absorbed into the ammonia / water mixture).

The parameters that are varied, in the optimization, are the average concentration of ammonia in water and the related high and low operating pressures.

If an average concentration of ammonia in the water is assumed, the pressure in the resorber at the heat pump side can be determined due to the fact that the mixture is assumed to be a saturated liquid at the outlet of the resorber (state 3), and that a temperature difference of n K can be assumed between the column fluid side and the heat pump mixture. The pressure is thus determined as function of vapor quality and temperature: $P = f(T, q)$. The same applies for the enthalpy and entropy: $h = f(T, q)$ and $s = f(T, q)$.

The pressure and concentration in state 4 can be determined by the assumption of isenthalpic expansion between state 3 and 4. Due to this isenthalpic expansion the enthalpy in state 4 is known ($h_3 = h_4$), as well as the temperature, because a temperature difference of n K is assumed between the column fluid side and the heat pump mixture: $P = f(T, h)$. The entropy can also be determined using $s = f(T, h)$.

The conditions in state 2 can be determined using the pressure and the assumed temperature difference between the column fluid side and the heat pump mixture: $h = f(P, T)$, $s = f(P, T)$.

From the column requirements the heat load of the resorber is known. The mass flow of the ammonia / water solution can now be calculated using the following equation:

$$\dot{Q}_{resorber} = \dot{m}_R(h_3 - h_2) \quad [3.18]$$

The enthalpy of state 1 can be determined using the equations 3.1, 3.18, 3.19, 3.20 and 3.21:

$$\dot{W}_{compressor} = \dot{m}_R(h_2 - h_1) \quad [3.19]$$

$$\dot{Q}_{desorber} = \dot{m}_R(h_1 - h_4) \quad [3.20]$$

$$\eta_{is} = \frac{(\dot{W}/\dot{m}_R)_{is}}{\dot{W}/\dot{m}_R} = \frac{h_{2s}-h_1}{h_2-h_1} = 0.7 \qquad [3.21]$$

First an initial value is assumed for the enthalpy of state 1. This enthalpy gives also an entropy ($s = f(P,h)$). For isentropic compression $s_1 = s_{2s}$, which gives h_{2s} ($h = f(P,s)$), and consequently also h_2, from the isentropic efficiency (eq. 3.21). The real enthalpy in state 1 can now be found by iteration.

Using the enthalpy in state 1 the desorber load and the compressor work can be determined (eq. 3.19 and 3.20).

Finally the heat load of the external condenser can be determined using equation 3.2.

The above approach is represented in a temperature – entropy diagram, figure 3.4, where the states are obtained from Taboada's model.

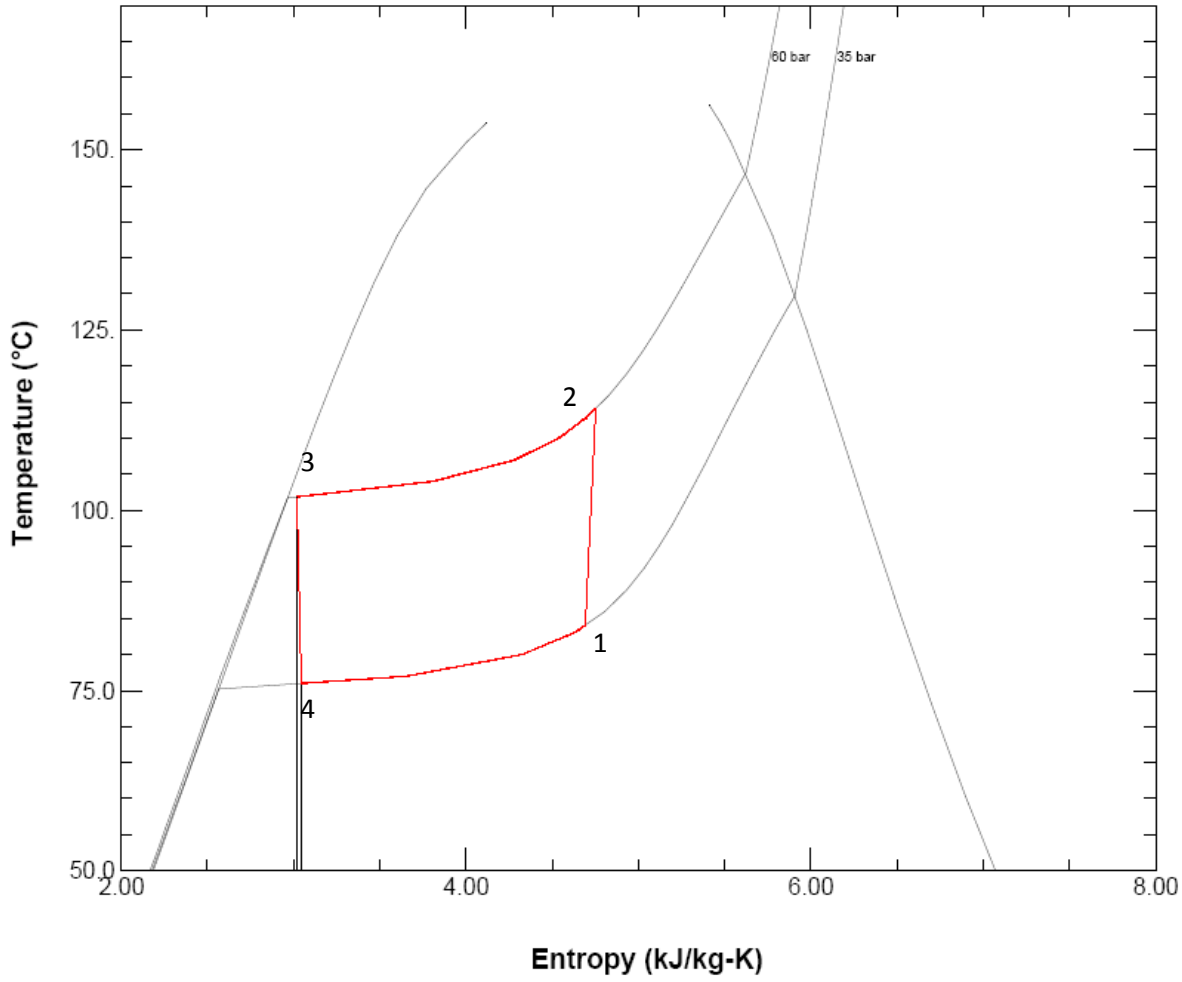

Figure 3.4 – Temperature – Entropy diagram (95wt% ammonia in ammonia / water solution)

3.2 Entropy production in diabatic distillation columns with integrated heat pump

3.2.1 Global entropy production in diabatic distillation columns with integrated heat pump

The global entropy production in diabatic distillation columns will be described in this section. In section 2.2.2 the global entropy production has already been introduced. The global entropy production of the total column can be described using the following balance:

$$\Delta\dot{S} = Bs_B^L + Ds_D^L + \dot{m}_{air,out}s_{air,out} - Fs_F^L - \dot{m}_R(s_2 - s_1) - \dot{m}_{air,in}s_{air,in} \quad [3.22]$$

Figure 3.5 represents the total column with the entropy flows. This global entropy production of the total column can be developed in more detail, by quantifying the entropy production on every tray instead of the total column.

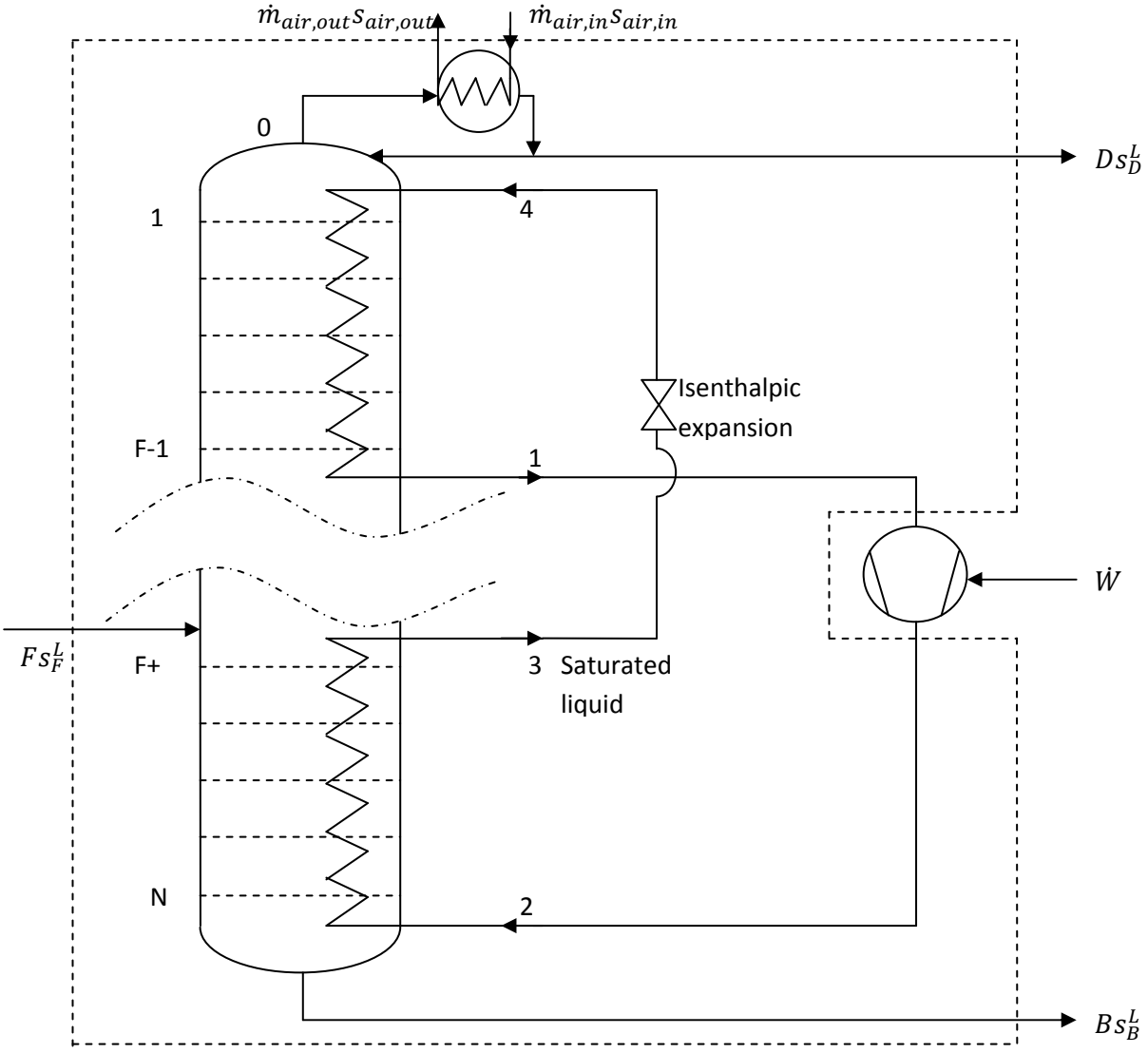

Figure 3.5 – Global entropy production of the diabatic column with integrated heat pump

3.2.2 Local entropy production in diabatic distillation columns with integrated heat pump

Equations 3.23 – 3.26 describe the entropy production in each tray. Figure 3.6 represents tray 0, 1, N-1 and N with the appropriate entropy flows.

Tray 0 (external condenser):

$$\Delta\dot{S}_0 = L_0 s_0^L + D s_D^L + \dot{m}_{air,out} s_{air,out} - V_1 s_1^V - \dot{m}_{air,in} s_{air,in} \quad [3.23]$$

Tray 1:

$$\Delta\dot{S}_1 = L_1 s_1^L + V_1 s_1^V + \dot{m}_R s_{R,1,out} - L_0 s_0^L - V_2 s_2^V - \dot{m}_R s_{R,1,in} \quad [3.24]$$

Tray N-1:

$$\Delta\dot{S}_{N-1} = V_{N-1} s_{N-1}^V + L_{N-1} s_{N-1}^L + \dot{m}_R s_{R,N-1,out} - L_{N-2} s_{N-2}^L - V_N s_N^V - \dot{m}_R s_{R,N-1,in} \quad [3.25]$$

Tray N:

$$\Delta\dot{S}_N = V_N s_N^V + B s_B^L + \dot{m}_R s_{R,N,out} - L_{N-1} s_{N-1}^L - \dot{m}_R s_{R,N,in} \quad [3.26]$$

The entropy production on every tray can be rewritten in one equation, which predicts the global entropy production of the total column evaluated on every tray.

$$\Delta\dot{S} = L_0 s_0^L + D s_D^L + \dot{m}_{air,out} s_{air,out} - V_1 s_1^V - F s_F^L - \dot{m}_{air,in} s_{air,in} + \cdots$$

$$\ldots + \sum_1^N L_n s_n^L + V_n s_n^V - L_{n-1} s_{n-1}^L - V_{n+1} s_{n+1}^V + \cdots$$

$$\ldots + \underbrace{\sum_1^{F-1} \dot{m}_R \left(s_{R,n,out} - s_{R,n,in}\right)}_{Desorber} + \underbrace{\sum_{F+1}^N \dot{m}_R \left(s_{R,n,out} - s_{R,n,in}\right)}_{Resorber} + \ldots$$

$$\ldots - \underbrace{\dot{m}_R \left(s_{R,F-1,out} - s_{R,N,in}\right)}_{Compressor} - \underbrace{\dot{m}_R \left(s_{R,F+1,out} - s_{R,1,in}\right)}_{Expansion\ Valve} \quad [3.27]$$

Where $L_N s_N^L = B s_B^L$ and $V_{N+1} s_{N+1}^V = 0$.

This equation must be equal to the equation found above (eq. 3.22). The purpose of an optimization based on equation 3.27 is to minimize the compressor work $\dot{W}$, by minimizing $\Delta\dot{S}$. The variables are the temperature differences (ΔT_N) and the average concentration of ammonia in water.

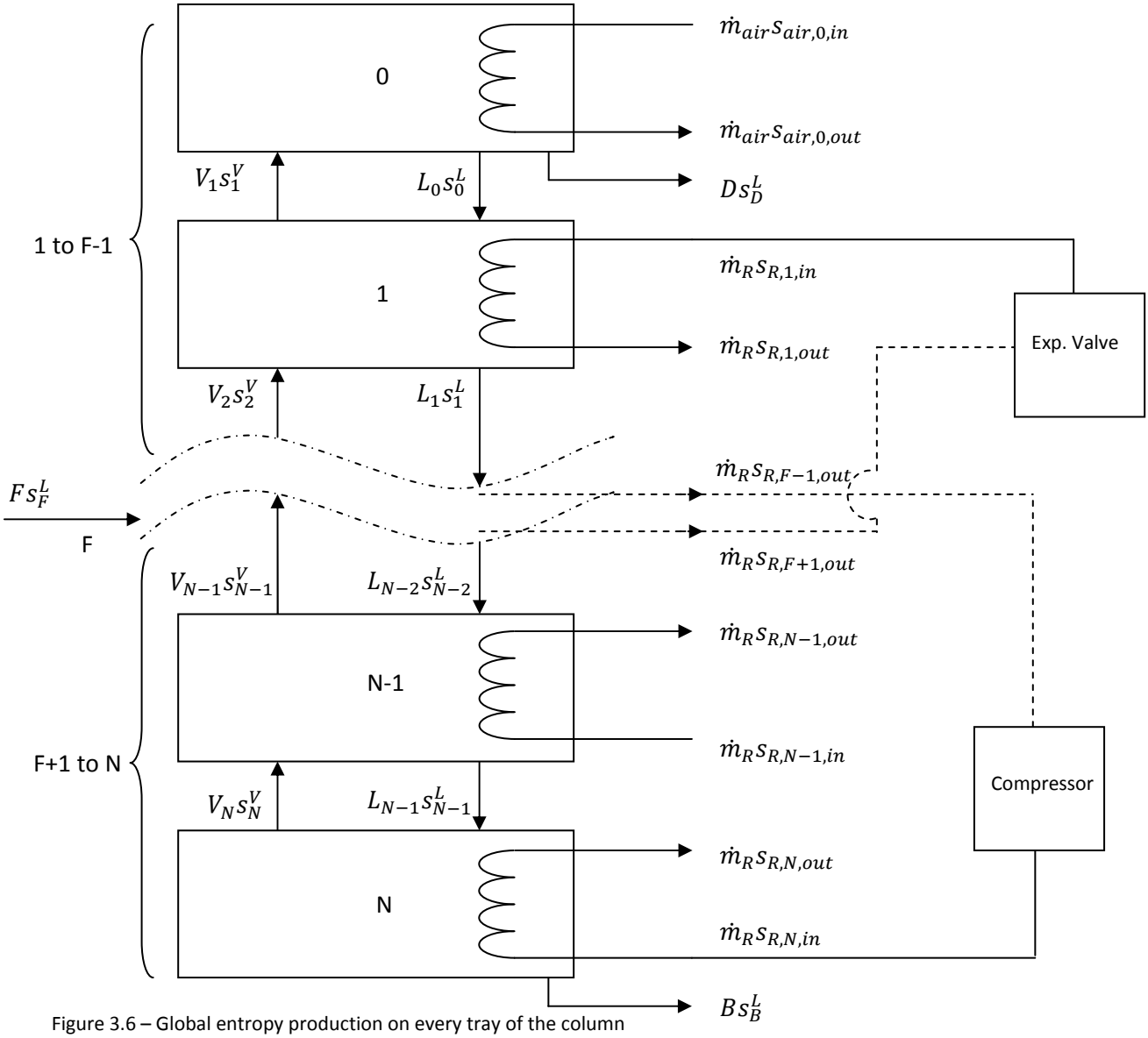

Figure 3.6 – Global entropy production on every tray of the column

3.2.3 Objective function

The (objective) function to be minimized is the entropy production of the column with integrated heat pump.

In the column, there is entropy production due to heat and mass transfer between the fluid streams. Previously, an optimization study of diabatic distillation columns has been developed by Røsjorde (2004).

In the heat exchangers, there is entropy production due to heat and mass transfer. Røsjorde has optimized only the column, and did not consider a heat pump. A source for the heat addition / removal was not included in Røsjorde's study.

From section 3.2.2 the objective function can be derived:

$$\left(\frac{dS}{dt}\right)^{irr} = \sum_{n=0}^{N+1}\left(\frac{dS}{dt}\right)_{col,n}^{irr} + \left(\frac{dS}{dt}\right)_{hx,n}^{irr} \qquad [3.28]$$

$$\left(\frac{dS}{dt}\right)^{irr} = L_0 s_0^L + D s_D^L + B s_B^L + \dot{m}_{air,out} s_{air,out} - V_1 s_1^V - F s_F^L - \dot{m}_{air,in} s_{air,in} + \cdots$$

$$\ldots + \sum_{1}^{N} L_n s_n^L + V_n s_n^V - L_{n-1} s_{n-1}^L - V_{n+1} s_{n+1}^V + \cdots$$

$$\ldots + \underbrace{\sum_{1}^{F-1} \dot{m}_R\left(s_{R,n,out} - s_{R,n,in}\right)}_{Desorber} + \underbrace{\sum_{F+1}^{N} \dot{m}_R\left(s_{R,n,out} - s_{R,n,in}\right)}_{Resorber} + \ldots$$

$$\ldots - \underbrace{\dot{m}_R\left(s_{R,F-1,out} - s_{R,N,in}\right)}_{Compressor} - \underbrace{\dot{m}_R\left(s_{R,F+1,out} - s_{R,1,in}\right)}_{Expansion\ Valve} \qquad [3.29]$$

Where $L_N s_N^L = B s_B^L$ and $V_{N+1} s_{N+1}^v = 0$.

This (objective) function can be compared with the one used by Røsjorde (2004). In the present case the entropy production in the heat exchangers (desorber and resorber) are defined in a different way. The entropy production at every tray on the heat pump side can be calculated using the mathematical models for heat and mass transfer in the desorber and resorber, which are presented in section 3.3.

3.2.3 Constraints

The constraints needed for the optimization of the objective function are:

1. Product purity distillate and bottom products are fixed.
2. The vapor flow leaving tray 1 must be equal to or greater than the distillate flow: $V_1 \geq D$.
3. The liquid flow leaving tray N must be equal to or greater than the bottom product flow: $L_N = B$ or equivalently $V_{N+1} = 0$.
4. Temperature difference between the column fluid side and the heat pump mixture is n K at the in-and outlet of the resorber and at the inlet of the desorber (with n a constant varied in the range 5 to 15 K).
5. $\dot{W}_{compressor} = \dot{Q}_{desorber} - \dot{Q}_{resorber}$ and $\dot{Q}_{removal\_column} = \dot{Q}_{desorber} + \dot{Q}_{ext.condenser}$.
6. Isentropic efficiency of the compressor is 70%.
7. The column has 20 trays.
8. The feed enters at tray 8.
9. Feed enters as saturated liquid.
10. The mixture leaving the resorber is a saturated liquid.

3.3 Models of a tray in the resorber/desorber

In this section models are presented that describe the heat and mass transfer on a tray in the resorber and desorber. These models are used to define the contributions that cause entropy production. In section 3.2 the equations for the optimization of the entropy production in diabatic columns with integrated compression resorption heat pumps have already been presented.

Only the tray with the largest entropy production will be investigated with detailed models. These detailed models are presented in the following sections.

3.3.1 Model A: Heat and mass transfer models

3.3.1.1 Resorber

The model for the resorber is based on previous research, see Infante Ferreira et al. (1984). The geometry that is used for the resorber is a bubble absorber as discussed in section 2.3.3. First the heat and mass balances are formulated for any differential element dz along the tube length, by using figure 3.7:

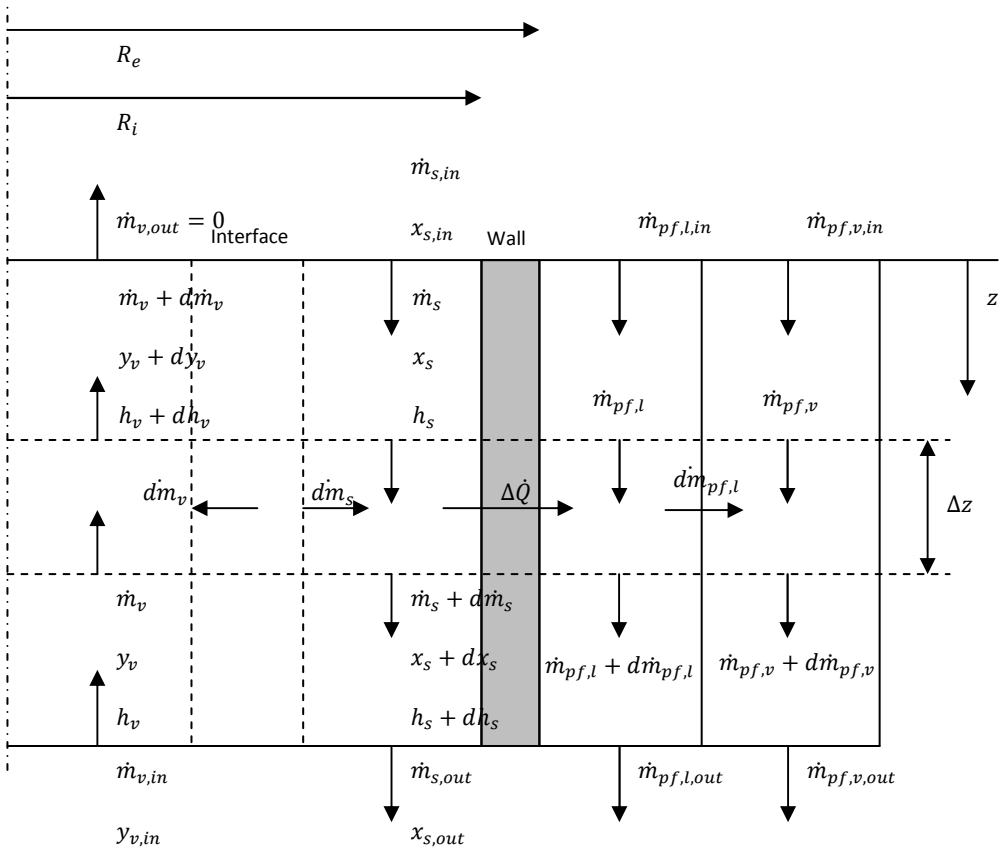

Figure 3.7 – Schematic model of differential element of the resorber

Overall balance equations

In the top of the absorber all gas has to be absorbed:

$$\dot{m}_{v,out} = 0 \quad [3.30]$$

First the balances for the total system are written, starting with the overall mass balance:

$$\dot{m}_{s,out} = \dot{m}_{s,in} + \dot{m}_{v,in} \quad [3.31]$$

The overall mass balance for ammonia becomes (with x and y the mass fraction of ammonia):

$$x_{s,out} = \left(\dot{m}_{v,in} y_{v,in} + \dot{m}_{s,in} x_{s,in}\right)/\dot{m}_{s,out} \quad [3.32]$$

The mass balances for a control volume Δz:

$$d\dot{m}_v = d\dot{m}_s \quad [3.33]$$

The mass balance for the control volume Δz for the ammonia component:

$$\dot{m}_v y_v + \dot{m}_s x_s = (\dot{m}_v + d\dot{m}_v)(y_v + dy_v) + (\dot{m}_s + d\dot{m}_s)(x_s + dx_s) \quad [3.34]$$

The energy balance is presented as an enthalpy balance:

$$\dot{m}_v h_v + \dot{m}_s h_s = (\dot{m}_v + d\dot{m}_v)(h_v + dh_v) + (\dot{m}_s + d\dot{m}_s)(h_s + dh_s) + d\dot{Q} \quad [3.35]$$

The entropy balance becomes:

$$\dot{m}_v s_v + \dot{m}_s s_s = (\dot{m}_v + d\dot{m}_v)(s_v + ds_v) + (\dot{m}_s + d\dot{m}_s)(s_s + ds_s) + \frac{d\dot{Q}}{T_{wall}} \quad [3.36]$$

Where the heat transfer is given by:

$$d\dot{Q} = UA\left(T_{s,bulk} - T_{pf}\right) \quad [3.37]$$

And,

$$\frac{1}{U} = \frac{1}{\alpha_{c,s}} + \frac{d}{2\lambda} ln \frac{d_o}{d} + \frac{d}{d_o} \frac{1}{\alpha_{c,pf}} \quad [3.38]$$

The heat transfer coefficients in eq. 3.38 can be determined from empirical correlations. The selected correlations are listed in Appendix A.

Interface equations

In the next part of this section the liquid vapor interface equations are presented:

Mass transfer equations:

$$d\dot{m}_v = k_v\left(y_v - y_v^{int}\right)\pi ddz \quad [3.39]$$

$$d\dot{m}_s = -k_s\left(x_s - x_s^{int}\right)\pi ddz \quad [3.40]$$

$$y_v^{int} = f\left(T^{int}, P\right),\ x_s^{int} = f\left(T^{int}, P\right) \quad [3.41]$$

In the above mass transfer equation k_s and k_v are mass transfer coefficients. These are determined by using the correlations presented by Chilton and Colburn (1934), see Hobler (1966), Appendix A.

Heat transfer equations (figure 3.8):

$$d\dot{Q}_v = -\alpha_v\left(T^{int} - T_v\right)\pi ddz \quad [3.42]$$

$$d\dot{Q}_s = \alpha_s\left(T^{int} - T_s\right)\pi ddz \quad [3.43]$$

$$d\dot{Q}_v + d\dot{Q}_s = d\dot{m}_v h_{sv} \quad \text{, with } h_{sv} \text{ heat of solution plus vaporization} \quad [3.44]$$

The heat transfer coefficients in eq. 3.42 and 3.43 are also determined by using the Nusselt theory, see Appendix A.

With this set of equations a resorber can be sized.

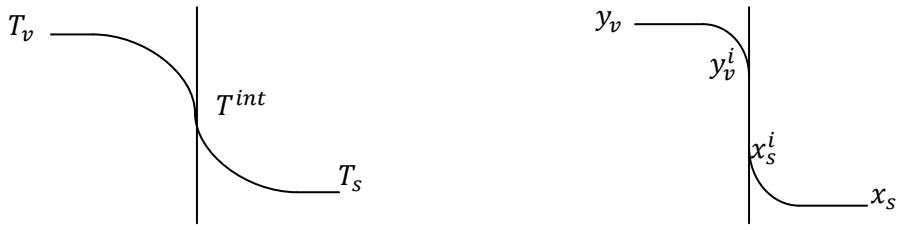

Figure 3.8 – Interface temperature profile (left), Concentration profile (right)

3.3.1.2 Desorber

The model for the desorber is based on research by Medrano et al. (2003). The geometry that is used for the desorber is a falling film absorber, see section 2.3.1. First the heat and mass balances are formulated for any differential element dz along the tube length, by using figure 3.9.

Overall balance equations

Top desorber (enthalpy and pressure are known after the expansion valve):

$P = f(h, T)$, and $q = f(h, P)$ (with q the vapor quality) [3.45][3.46]

$\dot{m}_{v,in} = f(\dot{m}_{s+v}, q)$ $\dot{m}_{s,in} = \dot{m}_{s+v} - \dot{m}_{v,in}$ [3.47][3.48]

The inlet concentrations for the desorber can be obtained by using the Fluidprop database (Colonna and v.d. Stelt (2004)), because the enthalpy and the pressure are known and equilibrium is assumed. This database includes water / ammonia data.

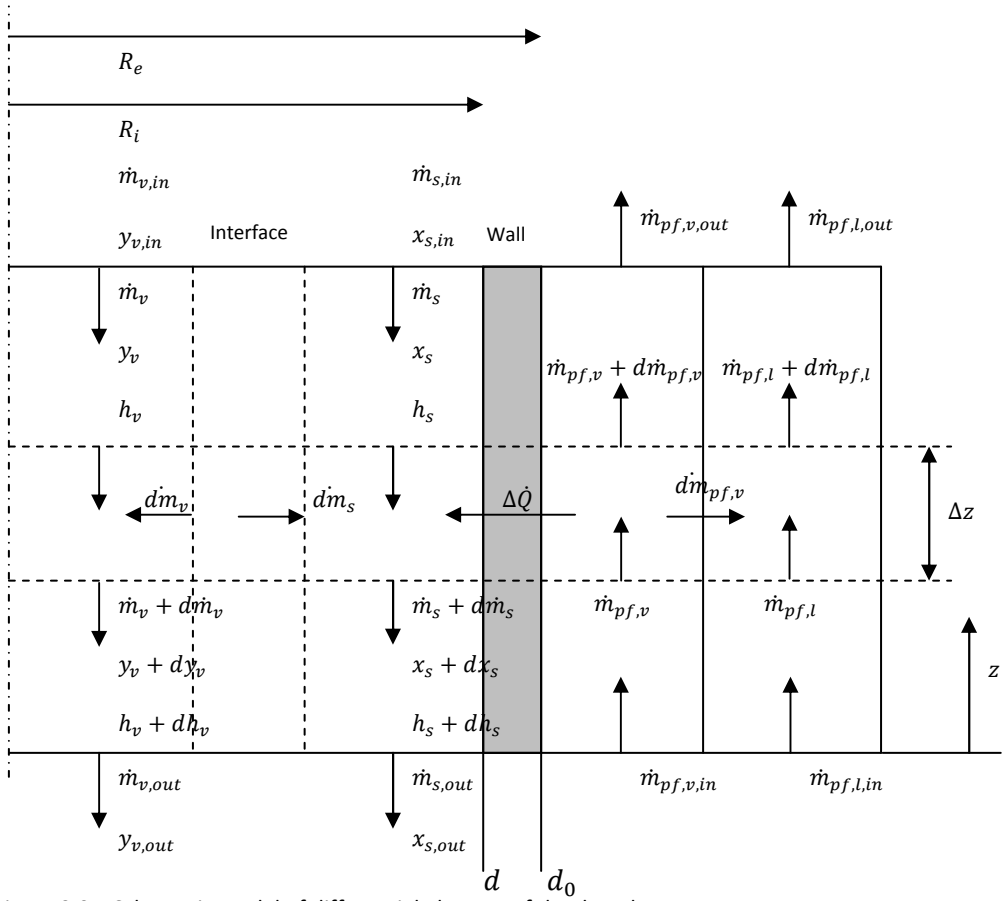

Figure 3.9 – Schematic model of differential element of the desorber

First the balances for the total system are written, starting with the overall mass balance:

$\dot{m}_{s,out} + \dot{m}_{v,out} = \dot{m}_{s,in} + \dot{m}_{v,in}$ [3.49]

The overall mass balance for ammonia becomes (with x and y the mass fraction of ammonia):

$\dot{m}_{s,out} x_{s,out} + \dot{m}_{v,out} y_{v,out} = \dot{m}_{v,in} y_{v,in} + \dot{m}_{s,in} x_{s,in}$ [3.50]

The mass balances for a control volume Δz:

$d\dot{m}_v = d\dot{m}_s$ [3.51]

The mass balance for the control volume Δz for the ammonia component:

$$\dot{m}_v y_v + \dot{m}_s x_s = (\dot{m}_v + d\dot{m}_v)(y_v + dy_v) + (\dot{m}_s + d\dot{m}_s)(x_s + dx_s) \quad [3.52]$$

The energy balance is presented as an enthalpy balance:

$$\dot{m}_v h_v + \dot{m}_s h_s = (\dot{m}_v + d\dot{m}_v)(h_v + dh_v) + (\dot{m}_s + d\dot{m}_s)(h_s + dh_s) - d\dot{Q} \quad [3.53]$$

The entropy balance becomes:

$$\dot{m}_v s_v + \dot{m}_s s_s = (\dot{m}_v + d\dot{m}_v)(s_v + ds_v) + (\dot{m}_s + d\dot{m}_s)(s_s + ds_s) - \frac{d\dot{Q}}{T_{wall}} \quad [3.54]$$

Where the heat transfer is given by:

$$d\dot{Q} = UA\left(T_{pf} - T_{s,bulk}\right) \quad [3.55]$$

And,

$$\frac{1}{U} = \frac{1}{\alpha_{c,s}} + \frac{d}{2\lambda} ln \frac{d_o}{d} + \frac{d}{d_o}\frac{1}{\alpha_{c,pf}} \quad [3.56]$$

The heat transfer coefficients in eq. 3.56 can be determined from empirical correlations. The correlations used are listed in Appendix A.

Interface equations

In the next part of this section the liquid vapor interface equations are presented:

Mass transfer equations:

$$d\dot{m}_v = k_v\left(y_v^{int} - y_v\right)\pi d dz \quad [3.57]$$

$$d\dot{m}_s = k_s\left(x_s - x_s^{int}\right)\pi d dz \quad [3.58]$$

$$y_v^{int} = f\left(T^{int}, P\right),\ x_s^{int} = f\left(T^{int}, P\right) \quad [3.59]$$

In the above mass transfer equation k_s and k_v are mass transfer coefficients. These are determined by using mass transfer correlations.

Hobler (1966), presented mass transfer correlations for the gaseous and liquid phase of falling film absorbers. The mass transfer coefficient can be calculated using dimensionless Sherwood number correlations, Appendix A.

Heat transfer equations (figure 3.10):

$$d\dot{Q}_v = \alpha_v\left(T_v - T^{int}\right)\pi ddz \quad [3.60]$$

$$d\dot{Q}_s = \alpha_s\left(T_s - T^{int}\right)\pi ddz \quad [3.61]$$

$$d\dot{Q}_v + d\dot{Q}_s = d\dot{m}_s h_{sv} \quad \text{, with } h_{sv} \text{ heat of solution plus vaporization} \quad [3.62]$$

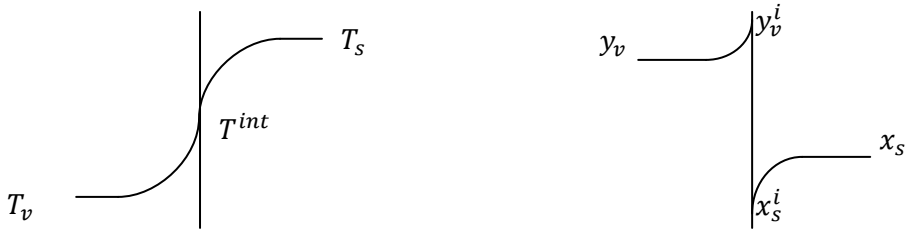

Figure 3.10 – Interface temperature profile (left), Concentration profile (right)

The heat transfer coefficients in eq. 3.60 and 3.61 are also determined by using the Nusselt theory, see Appendix A.

With this set of equations a desorber can be sized.

3.3.2 Model B: Irreversible thermodynamics model

In section 2.2.3 the basics on local entropy production using irreversible thermodynamics has been presented. To develop a model, based on this irreversible thermodynamics theory, linear flux relations are required. In the section below a linear flux force relations model is presented that describes the entropy production, in particular in the phase transition, in the resorber and desorber.

3.3.2. Linear flux relations (Kjelstrup and Bedeaux, (2001))

The entropy production rate, as was discussed in section 2.2.3, determines the conjugate thermodynamic forces and fluxes of the system. In this section the major assumption in irreversible thermodynamics is used, namely the assumption of linear flux-force relations. With this assumption the Onsager relations apply for the coupling coefficients.

The fluxes J_i that are used in the equation for local entropy production (2.20) are linear functions of all forces, X_j. In general this can be written as:

$$J_i = \sum_{k=1}^{n} L_{ik} X_k \qquad \text{for} \qquad i = 1, 2, \dots, n \qquad [3.63]$$

The forces can also be expressed as linear function of all fluxes:

$$X_k = \sum_j R_{kj} J_j \qquad \text{for} \qquad k = 1, 2, \dots, n \qquad [3.64]$$

These linear relations are assumed to be valid locally. If eq. 3.64 would be substituted in the entropy production rate eq. 2.20 one obtains the following:

$$\sigma = \sum_i X_i \sum_k L_{ik} X_k = \sum_{i,k} X_i L_{ik} X_k = \sum_{i,k} J_i R_{ik} J_k \geq 0 \qquad [3.65]$$

3.3.2.2 Mathematical model for a binary mixture

Kjelstrup and Bedeaux (2008), discussed evaporation and condensation in a two-component fluid. The equations that they found can be rewritten for absorption and desorption.

The mathematical models for the resorber and desorber, presented in sections 3.3.1.1 and 3.3.1.2, are rewritten by using the theory of irreversible thermodynamics. This theory makes use of fluxes and forces to determine the entropy production.

In this section the liquid phase and the gas phase will be discussed separately. At the end of this section the contributions of the two phases will be combined to one relation to describe the entropy production. To illustrate the mass, entropy and energy balances, figure 3.11 representing the

desorber is used. *A major assumption done writing these equations is that the vapor phase is pure ammonia.* This means that $J_{H2O} = 0$.

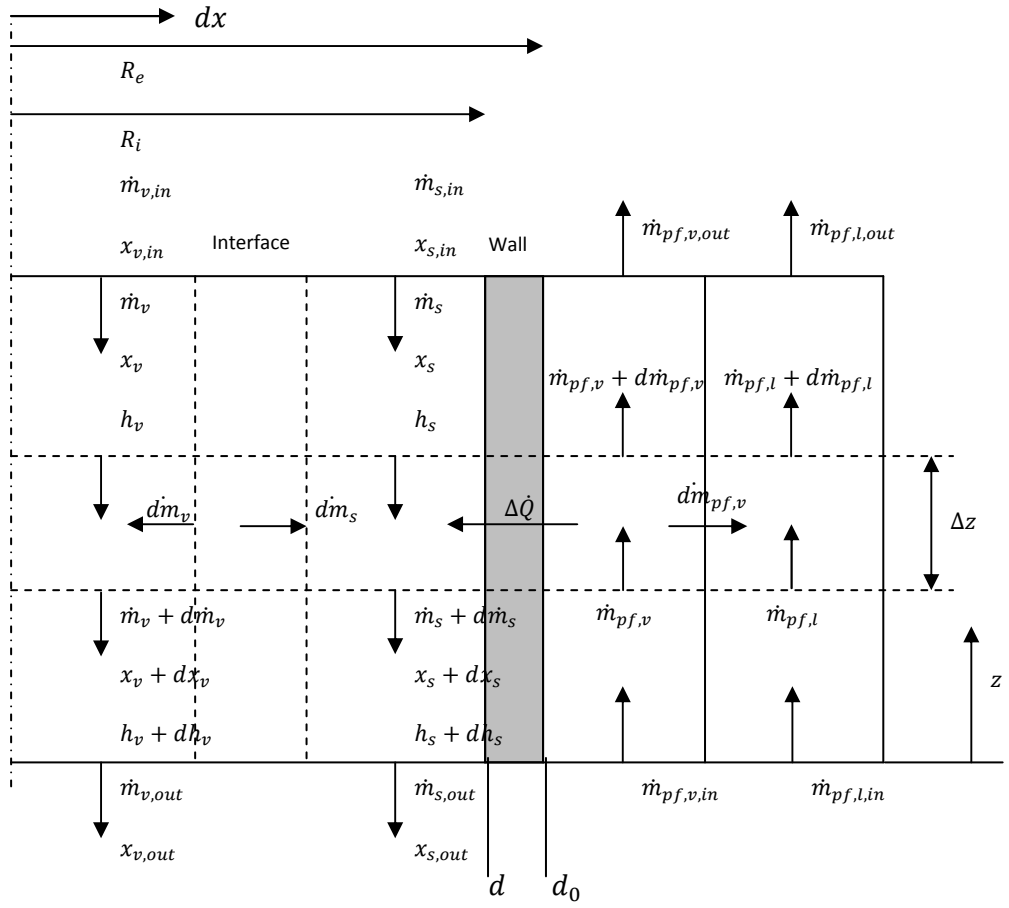

Figure 3.11 - Schematic of the desorber (see also figure 3.9)

Entropy production liquid phase

The entropy production in the liquid phase can be given in general by:

$$\sigma^l = J_q'^l \frac{\partial}{\partial x}\left(\frac{1}{T^l}\right) + J_{NH3}^l \left[-\frac{1}{T^l}\frac{\partial \mu_{NH3,T}^l}{\partial x}\right] \quad [3.66]$$

Where $J_q'^l$, the measurable heat flux and J_{NH3}^l the molar flux.

Entropy production gas phase

The entropy production in the gas phase can generally be represented by:

$$\sigma^g = J_q'^g \frac{\partial}{\partial x}\left(\frac{1}{T^g}\right) + J_{NH3}^g \left[-\frac{1}{T^g}\frac{\partial \mu_{NH3,T}^g}{\partial x}\right] \quad [3.67]$$

Where $J_q'^g$, the measurable heat flux and J_{NH3}^g the molar flux.

Comparison with model A

The heat fluxes $J_q^{\prime l}$ and $J_q^{\prime g}$ from the irreversible thermodynamics theory are comparable with the $d\dot{q}_v$ and $d\dot{q}_s$ from figure 3.11. The relations are as follows:

$$J_q^{\prime l} = \frac{d\dot{Q}_s}{A} = -\lambda_{NH3}^{l}\frac{\partial T}{\partial x}, \text{ so} \qquad d\dot{Q}_s = A\left(-\lambda_{NH3}^{l}\frac{\partial T}{\partial x}\right) \qquad [3.68]$$

$$J_q^{\prime g} = \frac{d\dot{Q}_v}{A} = -\lambda_{NH3}^{g}\frac{\partial T}{\partial x}, \text{ so} \qquad d\dot{Q}_v = A\left(-\lambda_{NH3}^{g}\frac{\partial T}{\partial x}\right) \qquad [3.69]$$

The coupling coefficients in the liquid and gas phases are small, so therefore they are neglected.

The molar fluxes J_{NH3}^{l} and J_{NH3}^{g} from the irreversible thermodynamics theory are comparable with the $d\dot{m}_s$ and $d\dot{m}_v$ from figure 3.11. The relations are as follows:

$$J_{NH3}^{l} = \frac{d\dot{m}_s M_s}{A} = -k_s\frac{M_s\partial x_s}{\partial x} = -D_{NH3}^{l}\frac{\partial c_{NH3}^{l}}{\partial x}, \text{ so} \qquad d\dot{m}_s = \frac{A}{M_s}\left(-D_{NH3}^{l}\frac{\partial c_{NH3}}{\partial x}\right) \qquad [3.70]$$

$$J_{NH3}^{g} = \frac{d\dot{m}_v M_v}{A} = -k_v\frac{M_v\partial x_v}{\partial x} = -D_{NH3}^{g}\frac{\partial c_{NH3}^{g}}{\partial x}, \text{ so} \qquad d\dot{m}_v = \frac{A}{M_v}\left(-D_{NH3}^{g}\frac{\partial c_{NH3}}{\partial x}\right) \qquad [3.71]$$

The interface

The equimolar surface, figure 3.12, of the solvent is used as the frame of reference. The solvent flux, J_{H2O}, is then zero through the surface. The solute flux is not zero through the surface. Adsorption of solute generally takes place at the surface, which reduces to surface tension:

$$\frac{d\Gamma_{NH3}}{dt} = J_{NH3}^{l} - J_{NH3}^{g} \qquad [3.72]$$

For this study, steady state is assumed, so $\frac{d\Gamma_{NH3}}{dt} = 0$

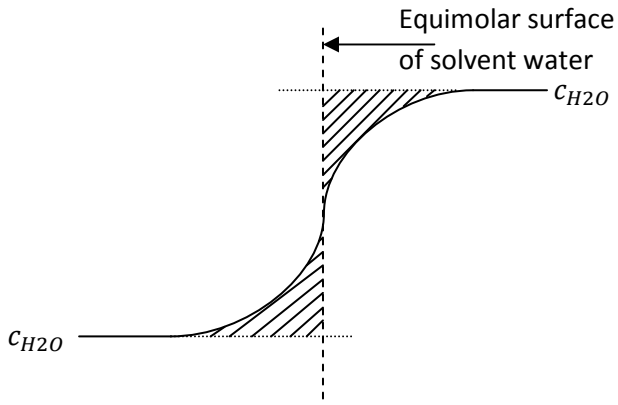

Figure 3.12 – Graphical representation of the equimolar surface

There are two measurable heat fluxes namely the heat flux from the liquid ($J_q^{\prime l}$) into the surface, and the heat flux out of the surface into the gas ($J_q^{\prime g}$). These fluxes are not the same because the enthalpies differ in the two phases. The total heat flux in the system, J_q, is the conserved flux, which is in stationary state represented by:

$$J_q = J_q^{'g} + H_{NH3}^{g} J_{NH3} = J_q^{'l} + H_{NH3}^{l} J_{NH3}, \text{ so } J_q^{'l} = J_q^{'g} + J_{NH3}\left(H_{NH3}^{g} - H_{NH3}^{l}\right) \quad [3.73]$$

This enthalpy balance is comparable with the enthalpy balances (equations 3.35 and 3.53) presented in sections 3.3.1.1 and 3.3.1.2.

Equation 3.73 is schematically represented in figure 3.13.

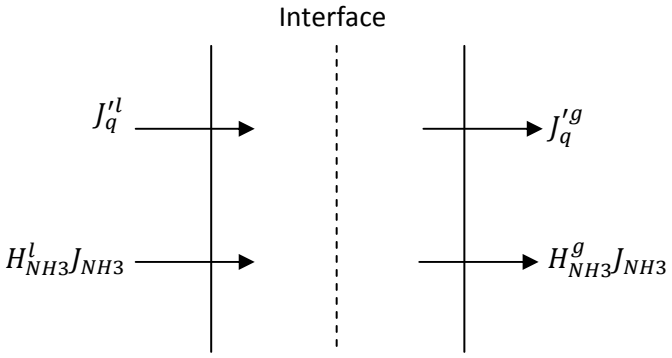

Figure 3.13 – Schematic representation equation 3.75

From a matrix of four forces linearly related to four fluxes, the following equations can be written:

$$q_{NH3}^{*s,g} = \left(\frac{J_q^{'g}}{J_{NH3}}\right)_{\Delta_{g,l}T=0} = -\frac{r_{qs}^{s,lhs}}{r_{qq}^{s}} = \frac{r_{qq}^{s,g} q_{NH3}^{*g} + r_{qq}^{s,l}\left(q_{NH3}^{*l} + \Delta_{g,l} H_{NH3}\right)}{r_{qq}^{s,g} + r_{qq}^{s,l}} \quad [3.74]$$

$$q_{NH3}^{*s,l} = \left(\frac{J_q^{'l}}{J_{NH3}}\right)_{\Delta_{g,l}T=0} = -\frac{r_{qs}^{s,rhs}}{r_{qq}^{s}} = \frac{r_{qq}^{s,g}\left(q_{NH3}^{*g} + \Delta_{g,l} H_{NH3}\right) + r_{qq}^{s,l} q_{NH3}^{*l}}{r_{qq}^{s,g} + r_{qq}^{s,l}} \quad [3.75]$$

Where the superscripts RHS and LHS indicate the right hand side and left hand side respectively of the surface.

The expression for σ^s with the four fluxes is given by:

$$\sigma^s = J_q^{'g} \Delta_{l,s}\left(\frac{1}{T}\right) + J_q^{'l} \Delta_{s,g}\left(\frac{1}{T}\right) + J_{NH3}\left[-\frac{1}{T^s}\Delta_{l,g}\mu_{NH3,T}(T^s)\right] + J_{H2O}\left[-\frac{1}{T^s}\Delta_{l,g}\mu_{H2O,T}(T^s)\right] \quad [3.76]$$

The reduction of σ can be done assuming steady state (1) and using the energy balance (2):

(1) $J_{NH3}^{g} = J_{NH3}^{l} = J_{NH3}$ [3.77]

(2) $J_q^{'g} - J_q^{'l} = J_{NH3}\left(H_{NH3}^{g} - H_{NH3}^{l}\right)$ [3.78]

The entropy production can now be written as:

$$\sigma^s = J_{NH3}\left[-\frac{1}{T^s}\Delta_{l,g}\mu_{NH3,T}(T^s)\right] + J_q^{'g}\Delta_{s,g}\left(\frac{1}{T^s}\right) + \left(J_q^{'g} - J_{NH3}\Delta_{l,g}H\right)\Delta_{s,l}\left(\frac{1}{T^s}\right) \quad [3.79]$$

By applying the method below, it can be seen that the heat flux in the liquid may be eliminated:

Gibbs Helmholtz'equation:

$$\frac{\partial(\mu/T)}{\partial(1/T)} = H \quad [3.80]$$

Then:

$$\frac{1}{T^s}[\mu^g(T^s) - \mu^l(T^s)] = \frac{1}{T^l}\left[\mu^g\left(T^l\right) - \mu^l\left(T^l\right)\right] + \left\{\frac{\partial}{\partial(1/T)}\left[\frac{\mu^g(T) - \mu^l(T)}{T}\right]\right\}_{T=T^l}\left(\frac{1}{T^s} - \frac{1}{T^l}\right) \quad [3.81]$$

$$= \left[\frac{\mu^g\left(T^l\right) - \mu^l\left(T^l\right)}{T^l}\right] + \left(H^g - H^l\right)\left(\frac{1}{T^s} - \frac{1}{T^l}\right)$$

The entropy balance found by the irreversible thermodynamics theory (using the energy balance (3.73)) is:

$$\sigma^s = J_q'^g \Delta_{g,l}\left(\frac{1}{T}\right) + J_{NH3}\left[-\frac{1}{T^l}\Delta_{g,l}\mu_{NH3,T}\left(T^l\right)\right] \quad [3.82]$$

Where the chemical potential differences are evaluated at the liquid temperature T^l. For the full derivation see Kjelstrup and Bedeaux, chapter 11.1 (2008).

The chemical potentials used above can be represented as:

$$\mu^l(T) = \mu^{g,0}(T) + RTln\frac{p^*(T)}{p_0} \quad [3.83]$$

With $p^*(T)$ the pressure of the vapor in equilibrium with the liquid at temperature T, also called the saturation pressure. Then the chemical potential of an ideal vapor at the temperature T and at the real pressure, p, is (note that the superscript g,0 means ideal gas):

$$\mu^g(T) = \mu^{g,0}(T) + RTln\frac{p}{p_0} \quad [3.84]$$

The force conjugate to J_{NH3} is:

$$-\frac{1}{T^l}\Delta_{l,g}\mu_{NH3,T}\left(T^l\right) = -Rln\frac{p_{NH3}}{p^*_{NH3}(T^l)} = -R\frac{(p_{NH3} - p^*_{NH3})}{p^*_{NH3}(T^l)} \quad [3.85]$$

Using the resistivity formulation, the linear relations across the surface become:

$$r^s_{qq}J_q'^g + r^s_{qs}J_{NH3} = \Delta_{l,g}\left(\frac{1}{T}\right) \quad [3.86]$$

$$r^s_{sq}J_q'^g + r^s_{ss}J_{NH3} = -R\frac{(p_{NH3} - p^*_{NH3})}{p^*_{NH3}(T^l)} \quad [3.87]$$

In the above linear relations there are three unknown coefficients because $r^s_{sq} = r^s_{qs}$.

This can be rewritten using the heat of transfer q^*_{NH3}:

Using the heat flux of the gas side as a variable:

(1) $\Delta_{g,s}\left(\frac{1}{T}\right) = r^{s,g}_{qq}\left(J_q'^g - q^{*s,g}_{NH3}J^g_{NH3}\right)$ [3.88]

(2) $\frac{1}{T^s}\Delta_{g,s}\mu_{NH3,T}(T^s) = r^{s,g}_{qq}q^{*s,g}_{NH3}J_q'^g - r^{s,g}_{ss}J^g_{NH3}$ [3.89]

Using the heat flux of the liquid side as a variable:

(3) $\Delta_{s,l}\left(\frac{1}{T}\right) = r_{qq}^{s,l}\left(J_q'^{g} - q_{NH3}^{*s,l}J_{NH3}^{l}\right)$ [3.90]

(4) $\frac{1}{T^s}\Delta_{s,l}\mu_{NH3,T}(T^s) = r_{qq}^{s,l}q_{NH3}^{*s,l}J_q'^{l} - r_{ss}^{s,l}J_{NH3}^{l}$ [3.91]

For one-component systems $q_{NH3}^{*l} = q_{NH3}^{*g} = 0$, and thus equations 3.74 - 3.75 reduce to:

$q_{NH3}^{*s} = -\frac{r_{qs}^{s}}{r_{qq}^{s}} \equiv \frac{r_{qq}^{s,l}\Delta_{g,l}H_{NH3}}{r_{qq}^{s,l}+r_{qq}^{s,g}} = -k\Delta_{g,l}H_{NH3}$, where 0<k<1 [3.92]

For absorption a typical value for $k = 0.2$.

The resistivities can be calculated using the kinetic theory presented by Kjelstrup and de Koeijer (2003):

$r_{qq}^{s,g} = \frac{\sqrt{\pi}}{4R(T^s)^2 c_{eq}^{g}(T^s)v_{mp}(T^s)}\left(1 + \frac{104}{25\pi}\right)$ [3.93]

$r_{ss}^{s,g} = \frac{2R\sqrt{\pi}}{c_{eq}^{g}(T^s)v_{mp}(T^s)}\left(\frac{1}{\pi} - \frac{23}{32}\right)$ [3.94]

In the above equations $v_{mp}(T^s)$ is the average of the most probable velocities of the two components at temperature T^s:

$v_{mp}(T^s) \equiv \frac{\left(c_{NH3}^{g}v_{NH3,mp}\right)}{c_{NH3}^{g}}$ [3.95]

With $v_{NH3,mp} = \sqrt{2RT^s/M_{NH3}}$ [3.96]

Another method to find r_{qq}^{s} and r_{ss}^{s}

Heat transfer resistivity: r_{qq}^{s}

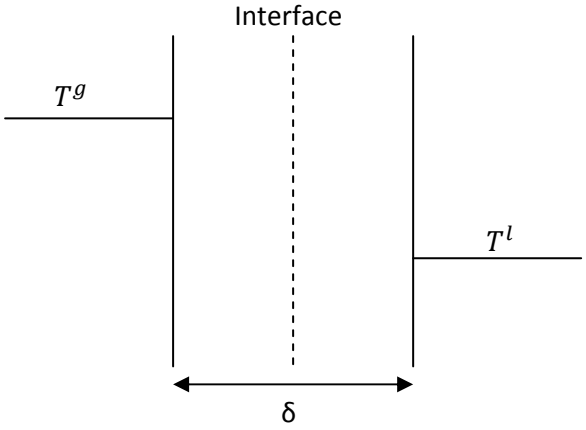

Figure 3.14 – Interface presenting heat transfer

$$\frac{1}{r_{qq}^{s}}\frac{\Delta_{l,g}T}{T^2} = U\Delta_{l,g}T = J_q^{\prime g} \quad [3.97]$$

If $\Delta_{l,g}T \approx \Delta_{s,g}T$:

$$r_{qq}^{s} = \frac{1}{UT^2} \quad [3.98]$$

Where U is given by:

$$\frac{1}{U} = \frac{1}{\alpha_{c,g}} + \frac{\delta}{\lambda_{NH3}} \quad [3.99]$$

Mass transfer resistivity: r_{ss}^{s}

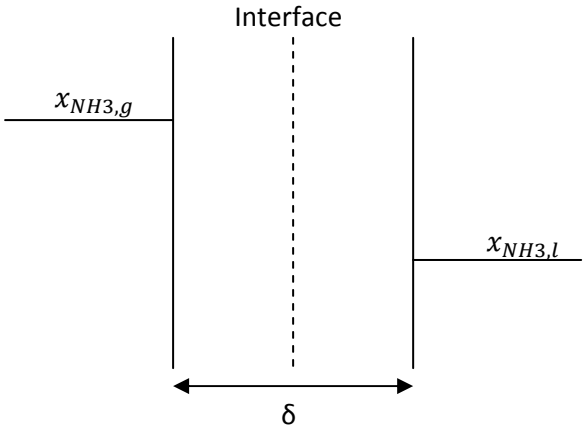

Figure 3.15 – Interface presenting mass transfer

$$\frac{1}{r_{ss}^{S}} R \frac{(p_{NH3}-p_{NH3}^{*})}{p_{NH3}^{*}(T^{l})} = K\Delta_{l,g} x_{NH3} = J_{NH3} \quad [3.100]$$

$$r_{ss}^{S} = \frac{1}{K\Delta_{l,g} x_{NH3}} R \frac{(p_{NH3}-p_{NH3}^{*})}{p_{NH3}^{*}(T^{l})} = \frac{1}{J_{NH3}} R \frac{(p_{NH3}-p_{NH3}^{*})}{p_{NH3}^{*}(T^{l})} \quad [3.101]$$

Where K is given by:

$$\frac{1}{K} = \frac{1}{\rho_{NH3} A k_g} + \frac{\delta}{\rho_{NH3} A D_{NH3}} + \frac{1}{\rho_{NH3} A k_l} \quad [3.102]$$

3.4 Conclusion

Equations are derived that describe the entropy production in diabatic columns with an integrated compression resorption heat pump. The first set gives the global entropy production of the system, and the second set gives the local entropy production at each tray of the column.

The objective function that should be minimized is the entropy production of the whole diabatic column with integrated compression resorption heat pump.

The global entropy production will be used to determine the temperatures of the trays when the total entropy production of the system is minimum.

The tray with the highest entropy production will be used for a detailed model. This detailed model uses the local entropy production model, based heat and mass transfer resistivity's. In this model the heat and mass transfer between the column fluid side and the heat pump mixture is taken into account. Result from this detailed model is to quantify the local entropy production along the tube length of the resorber or desorber. Due to time restrictions the results of the irreversible thermodynamics model will not be evaluated in detail.

4. Simulation

The optimization goal of the present study is the minimization of the entropy production in compression resorption heat pumps integrated in diabatic distillation columns. The global entropy production will be minimized in the system, which will be done by optimizing the variables described in section 3.1.3. After the optimization for the entropy production is done, a detailed model will be developed to quantify the local entropy production. This model will only be developed for the tray with the largest entropy production.

The first section of this chapter will describe which software package will be used for the optimization and for the development of the detailed models. The numerical solution procedure is discussed in section 4.2. Notes on running the simulation are exposed in section 4.3. At last the implementation of the detailed models is described in section 4.4.

4.1 Software package

For the optimization of the objective function, minimization of the entropy production in a compression resorption heat pump integrated in diabatic distillation columns, several software packages can be used, such as: Microsoft Excel, Matlab R2007a, MathWorks Inc., etc.

In the present study Matlab R2007a, MathWorks Inc. is chosen to solve the optimization problem due to the large number of variables in the diabatic distillation column and in the compression resorption heat pump. Thereby, a Matlab simulation is obtained from Røsjorde (2004), which optimizes the entropy production in diabatic distillation columns.

An advantage of using Matlab is the wide variety of built-in solvers that can be used, which makes the programming less time consuming.

4.2 Numerical solution procedure

The minimization problem is a nonlinear constrained optimization problem. Røsjorde (2004) tried to optimize the diabatic column by minimizing the objective function as it is given in eq. 4.1, by varying the independent variables.

$$\left(\frac{dS}{dt}\right)^{irr} = Bs^B + Ds^D - Fs^F + \sum_{n=0}^{N+1}\left(-\frac{Q_n}{T_n} + Q_n X_n\right) \quad [4.1]$$

The problem was that this method converged only for a small set of initial conditions, and then very slowly. Another method investigated by Røsjorde is to solves analytically derived equations. This was also not successful.

Therefore a different approach was adopted by Røsjorde due to the nature of the objective function. The objective function was, like it is in the diabatic distillation column with integrated compression resorption heat pump optimization, the sum of many contributions. Each contribution may or may not be affected by the different variables. The sum, however, will always depend on all of the variables.

Røsjorde therefore used the least square regression method including each of the terms in the summation. This means that if there are N+2 terms due to the internal entropy production and N+2 terms due to entropy production in the heat pump. A general formulation of then sum is given in the following equation:

$$F(x) = [f_1(x)]^2 + [f_2(x)]^2 + \cdots + \left[f_{2(N+2)}(x)\right]^2 \quad [4.2]$$

Where $F(x)$ the objective function, and $f_i(x)$ the square root of each contribution to the total entropy production. Experience has shown that least square regression converges much faster and more stable than other optimization methods.

To solve the least square regression problem Matlab R2007a, MathWorks Inc. is used as discussed above. Matlab has a nonlinear least squares function called lsqnonlin. This function can be found in the Optimization Toolbox in the Matlab environment. This algorithm uses a Gauss-Newton method with line search.

Before the actual optimization took place, the diabatic column and the heat pump were modelled separately using the fsolve function. This function iterates a function F, using a set of initial conditions, such that $F(x) = 0$.

For the diabatic column the function F consists of the mass and energy balances, which are given in equations 3.3 - 3.12, section 3.1.2.

For the heat pump the function F consists of equations 3.18 – 3.21. These equations were used as described in section 3.1.3.

The optimization was done using the fmincon command in Matlab. This command minimizes the objective function, using a set of initial conditions, upper and lower bounds, and constraints. Three separated m files were needed to perform the optimization:

- Optimize.m
- Nonlcon.m
- Objective_function.m

In the optimization file, the optimization, the upper and lower bounds and the initial conditions are described. The output of the file is transferred to the nonlcon and the objective_function files.

In the nonlcon file, the constraints are given. There are two different kind of constraints, namely the $Ceq(x)$ (nonlinear equalities at x) and the $C(x)$ (nonlinear inequalities at x) constraints. The $Ceq(x)$ constraint sets the equation equal to zero: $Ceq(x) = 0$. The $C(x)$ constraint set the equation smaller than zero: $C(x) < 0$.

The objective_function file, describes the objective function to be minimized. In case of the diabatic column with integrated compression resorption heat pump, this equation is equal to equation 3.29, section 3.2.3.

4.3 Simulations of the diabatic column with integrated compression resorption heat pump

Running the simulation, first the diabatic distillation column was optimized. The results of this column were used for the optimization of the compression resorption heat pump. This means that the compression resorption heat pump was optimized using a fixed (optimized) column, i.e. temperature profile, heat load and entropy production (in the column). Using this column data, temperature profiles of the resorber and desorber were optimized while minimizing the entropy production of the total system.

The simulation was performed at a constant average concentration of ammonia in the heat pump solution. To optimize the average concentration the total optimization was repeated for different concentrations.

Results of the optimization are presented in the following chapter.

4.4 Detailed models

First the heat and mass transfer model is implemented in the Matlab software program. A data file is created containing the tray inlet conditions, the tube dimensions, and the transport properties. These data is used in the dimensionless numbers file, where the dimensionless numbers needed for the heat and mass transfer were calculated, and in the falling film file, where the mass and energy balances were solved.

This falling film file solves the mass and energy balances on the solution side, the interface and the vapour side. First this is done for a single control volume, where after it is repeated for more control volumes. The balances used in the falling film file are represented below:

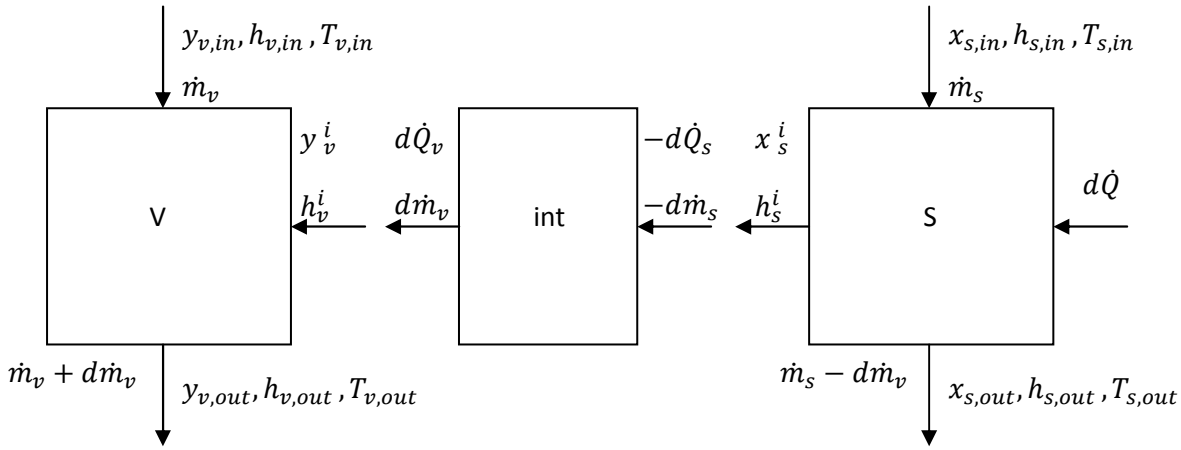

Figure 4.1 – Falling film balances

The balances were solved by iterating the interface temperature. The procedure is as follows:

$$y_v^{int} = f\left(T^{int}, P\right),\ x_s^{int} = f\left(T^{int}, P\right) \quad [3.59]$$

$$d\dot{m}_v = k_v\left(y_v^{int} - y_v\right)\pi d dz \quad [3.57]$$

Mass balance solution side:

$$x_{s,out} = \frac{\dot{m}_s x_{s,in} - d\dot{m}_v x_s^i}{(\dot{m}_s - d\dot{m}_v)} \quad [4.3]$$

Mass balance vapor side:

$$y_{v,out} = \frac{\dot{m}_v y_{v,in} + d\dot{m}_v y_v^i}{(\dot{m}_v + d\dot{m}_v)} \quad [4.4]$$

Mass balance interface:

$$d\dot{m}_v = -d\dot{m}_s \quad [3.51]$$

Energy balance solution side:

$$h_{s,out} = \frac{\dot{m}_s h_{s,in} - d\dot{m}_v h_s^i + d\dot{Q}}{(\dot{m}_s - d\dot{m}_v)} \quad [4.5]$$

Energy balance vapor side:

$$h_{v,out} = \frac{\dot{m}_v h_{v,in} + d\dot{m}_v h_v^i}{(\dot{m}_v + d\dot{m}_v)} \quad [4.6]$$

Interface heat transfer:

$$d\dot{Q}_v = \alpha_v \left(T_v - T^{int}\right) \pi d dz \quad [3.60]$$

$$d\dot{Q}_s = \alpha_s \left(T_s - T^{int}\right) \pi d dz \quad [3.61]$$

The interface is iterated by solving equation 3.62:

$$d\dot{Q}_v + d\dot{Q}_s - d\dot{m}_s h_{sv} = 0 \quad [3.62]$$

To determine the entropy production along the tube length the entropy is calculated using the Fluidprop database for the different control volumes.

The irreversible thermodynamics model is based on the values obtained from the heat and mass transfer model. The procedure for this model is as follows:

The resistivities can be found by using eq.3.98 and 3.101:

$$r_{qq}^s = \frac{1}{UT^2} \quad [3.98]$$

Where U is given by:

$$\frac{1}{U} = \frac{1}{\alpha_v} + \frac{\delta}{\lambda_{NH3}} \quad [3.99]$$

Where δ, the interface thickness, is infinitely small and λ_{NH3} is in the vapor phase.

$$r_{ss}^s = \frac{1}{K \Delta_{l,g} x_{NH3}} R \frac{(p_{NH3} - p_{NH3}^*)}{p_{NH3}^*(T^l)} = \frac{1}{J_{NH3}} R \frac{(p_{NH3} - p_{NH3}^*)}{p_{NH3}^*(T^l)} \quad [3.101]$$

Where K is given by:

$$\frac{1}{K} = \frac{1}{\rho_{NH3} A k_g} + \frac{\delta}{\rho_{NH3} A D_{NH3}} + \frac{1}{\rho_{NH3} A k_l} \quad [3.102]$$

For the heat of transfer the latent heat is used. With the heat of transfer the last resistivity can be calculated:

$$q_{NH3}^{*s} = -\frac{r_{qs}^s}{r_{qq}^s} \equiv \frac{r_{qq}^{s,l} \Delta_{g,l} H_{NH3}}{r_{qq}^{s,l} + r_{qq}^{s,g}} = -k \Delta_{g,l} H_{NH3}, \text{ where } 0<k<1 \quad [3.92]$$

The fluxes can be calculated using values from the heat and mass transfer model:

$$J_{NH3}^{l} = \frac{d\dot{m}_s M_s}{A} \quad [3.70]$$

$$J_{NH3}^{g} = \frac{d\dot{m}_v M_v}{A} \quad [3.71]$$

Combining those fluxes with the resistivities gives the driving forces:

$$r_{qq}^{s} J_q^{'g} + r_{qs}^{s} J_{NH3} = \Delta_{l,g}\left(\frac{1}{T}\right) \quad [3.86]$$

$$r_{sq}^{s} J_q^{'g} + r_{ss}^{s} J_{NH3} = -R\frac{(p_{NH3} - p_{NH3}^{*})}{p_{NH3}^{*}(T^l)} \quad [3.87]$$

$$-\frac{1}{T^l}\Delta_{l,g}\mu_{NH3,T}(T^l) = -R\frac{(p_{NH3} - p_{NH3}^{*})}{p_{NH3}^{*}(T^l)} \quad [3.85]$$

Finally the entropy production can be calculated

$$\sigma^s = J_q^{'g}\Delta_{g,l}\left(\frac{1}{T}\right) + J_{NH3}\left[-\frac{1}{T^l}\Delta_{g,l}\mu_{NH3,T}(T^l)\right] \quad [3.82]$$

For the second, irreversible thermodynamics, method the values from the first heat and mass transfer model are used. Another possibility to simulate the second model is to use the chemical potentials, diffusivities, etc (section 3.3.2). The results should be the same, however this was not validated due to time restrictions.

5. Results

The optimization which minimizes the entropy production in a diabatic column with integrated heat pump will be discussed in the first part of this chapter. The second part of this chapter presents the results of the detailed models, which are applied to the tray of the diabatic column which produces the highest entropy production.

5.1 Optimization of entropy production in diabatic distillation column with integrated compression resorption heat pump

The first part of this section exposes the results for the optimization of entropy production minimization for the diabatic column. The model is obtained from the PhD research of Røsjorde (2004). The results for this model are presented in appendix B.

Figure 5.1 presents the temperature profile, obtained from the entropy production optimization, of the diabatic column. What can be seen from this result is that the temperature profile is almost linear, which was expected since the lowest entropy production will be obtained if the temperature gradient within the column is constant. The heat load profile, figure 5.2, that is obtained from the optimization of entropy production in the diabatic column is a consequence of the linear temperature profile, and is similar to the heat load of an adiabatic column.

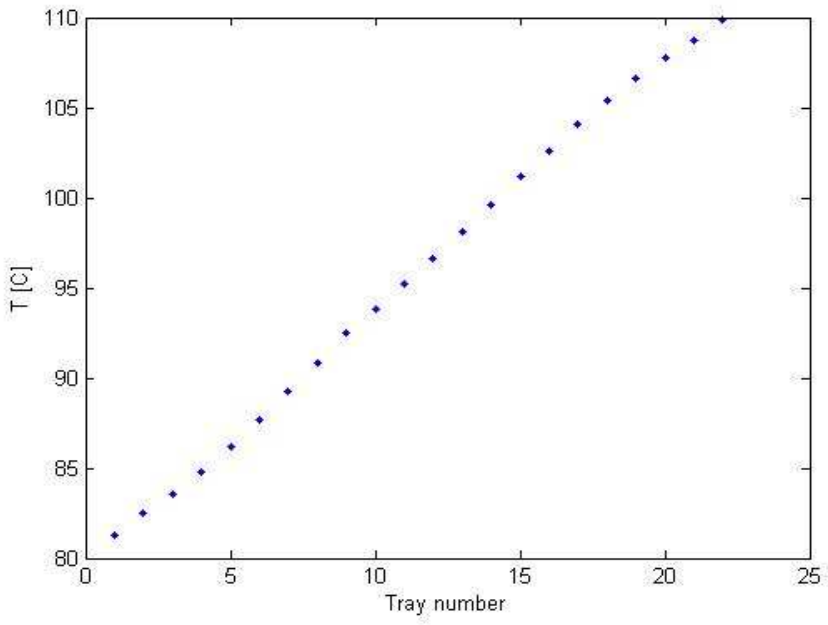

Figure 5.1 – Temperature profile of the diabatic column

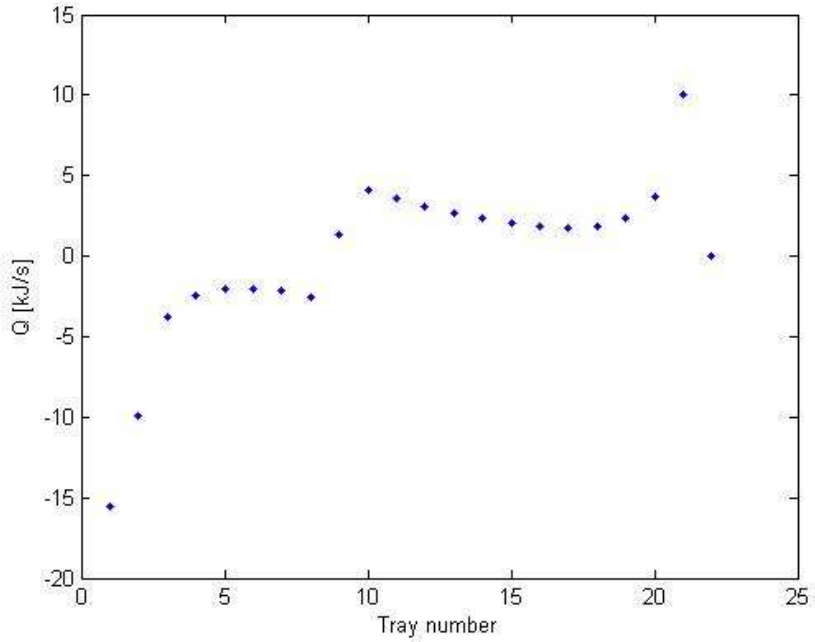

Figure 5.2 – Heat load in the diabatic column

The optimization resulted in a minimum entropy production of 0.529 [kW/K] in the diabatic column. The entropy change per tray (multiplied with mass flow) in the diabatic column is presented in figure 5.3.

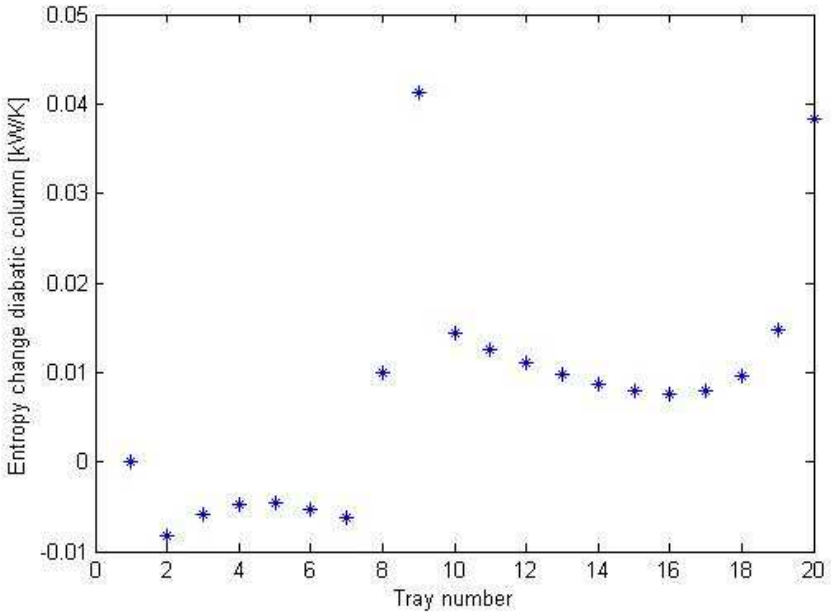

Figure 5.3 – Entropy production per tray in the diabatic column

It can be seen from figure 5.3 that the largest entropy change is at the feed location. This was expected due to the mixing effects of the feed stream into the column.

For the optimization of the compression resorption heat pump the optimized column is taken as a constant input i.e. the results of the optimization of the diabatic column are used as input for the optimization for the compression resorption heat pump. The next part of this section exposes the optimization of this compression resorption heat pump while minimizing the entropy production.

The optimization of entropy production in the compression resorption heat pump, is as stated above, performed using a "fixed, optimized" diabatic column. The optimization is done by varying the average ammonia concentration, which resulted in different pressure levels, and temperature driving forces between the diabatic column and the compression resorption heat pump. The detailed results of the optimization for different average ammonia concentrations is presented in appendix C. The overall results are presented below. The entropy change (multiplied with mass flow) for an ammonia / water mixture with an average concentration of 96 wt% in the compression resorption heat pump is presented in figure 5.4.

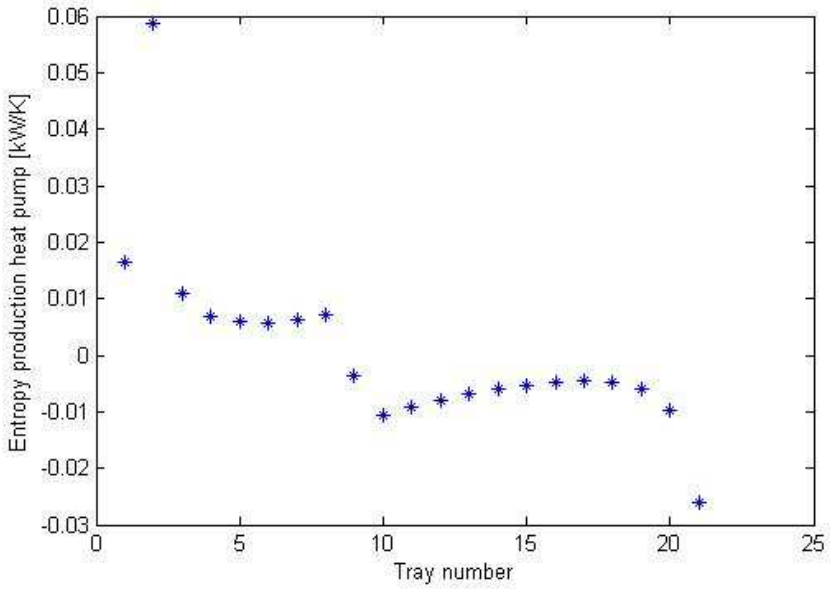

Figure 5.4 – Entropy production in the compression resorption heat pump

From figure 5.4 it can be seen that there is a large entropy change in the first tray. The model for the column calculates the external condenser heat load (tray 1 in figure 5.2). If the compression resorption heat pump is implemented, this external condenser does not fit into the heat pump requirements. Therefore the heat that is required for the compression resorption heat pump is exchanged on the first tray of the diabatic column, which results in smaller external condenser duty. Therefore a large entropy change occurs at the second tray, because the heat load is much higher than on the other trays. This small external condenser not represented in figure 5.2. In this figure the external condenser of the column optimization is shown.

From figure 5.4 it also can be observed that the entropy has a very small value. However the total entropy production for the compression resorption heat pump should be larger, according to the

results. This is due to the fact that the entropy change in the compressor and in the expansion valve are not included in this figure. The entropy changes presented, are only related to the trays.

The main result of the optimization is the entropy production in the diabatic distillation column with integrated compression resorption heat pump. Figures 5.5 and 5.6 presents the entropy production of this system. Figures 5.3 and 5.4 present the entropy changes on the different trays. Those figures are combined for the entropy production in the diabatic column with integrated compression resorption heat pump.

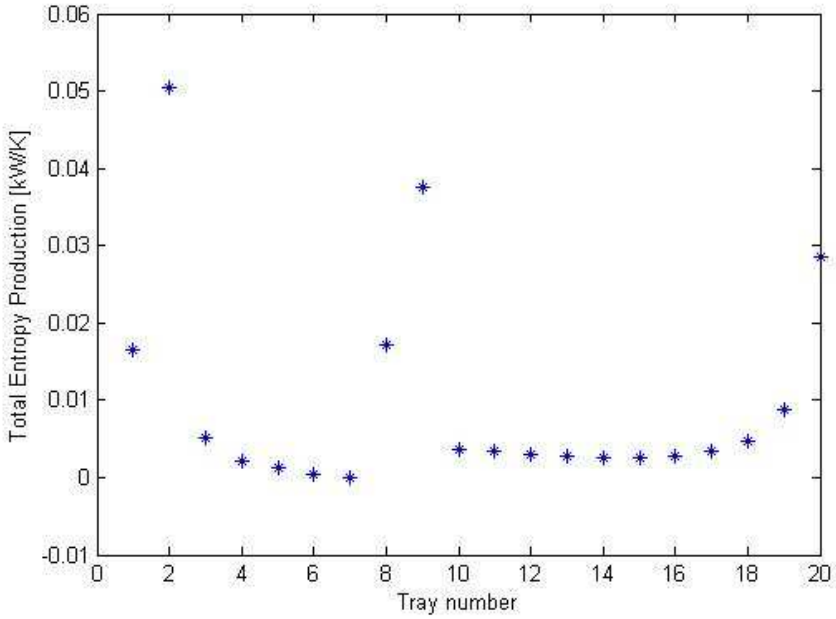

Figure 5.5 – Entropy production of the diabatic column with integrated compression resorption heat pump

Figure 5.5 is similar to figure 5.3. The high entropy production on the second tray is cause by the extra heat load coming from the external condenser, as described earlier.

Figure 5.6 shows the overall entropy production (including losses in the compressor and expansion device) as a function of the average ammonia concentration in the working fluid of the compression resorption heat pump. In figure 5.6 there is a gap in average concentration, between 30wt% and 54wt% ammonia. This is caused by the fact that the pressure lines are too steep for iteration in this region. Meaning that the enthalpy differences become very small while the compressor work is becoming larger. At some point the state points within the cycle can not be calculated anymore, due to the constraints of the compression resorption heat pump, see section 3.1.3. For this reason, there is a gap between the average ammonia concentrations of 30wt% to 54wt%.

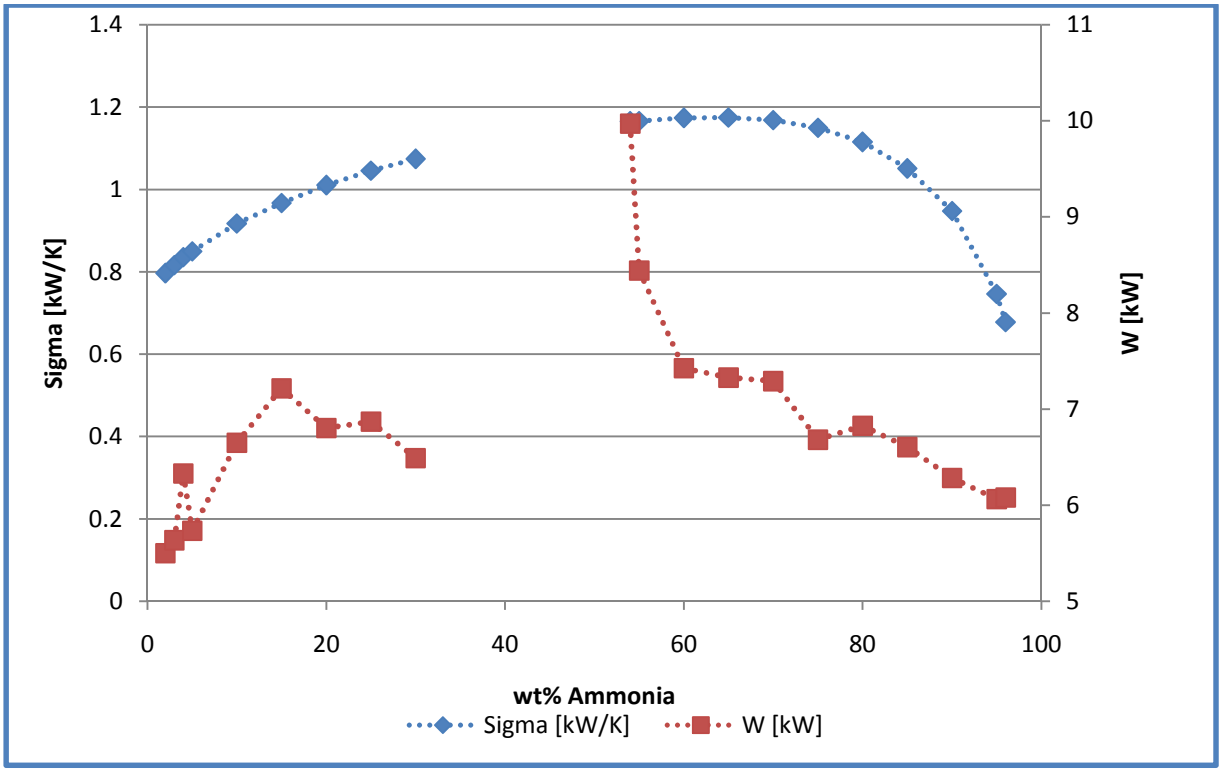

Figure 5.6 – Minimized entropy production for several average concentrations ammonia, and delivered work by the compressor

From figure 5.6, it can be seen that the lowest entropy production occurs at low average ammonia concentrations or at very high ammonia concentrations. The lowest value for the entropy production is obtained for an average concentration of 96wt%. The lowest entropy production for the low concentrations is at 2wt% ammonia.

The second part of the figure consists of the technical power required by the compressor. This work has a lowest value for the low average concentration of ammonia (2%). If the high concentrations are observed, it can be seen that the work has also a lowest value at the high average concentration of 96wt% ammonia.

This results in two interesting concentration levels, namely a high average concentration (96wt%) and a low average concentration (2%).

To operate the diabatic column heat is supplied in the stripping section of the column. This is done using the resorber. The reboiler duty is a constant value in the optimization since the results of the diabatic column are taken as a "fixed" input. Heat is removed from the column in the rectifying section. This is done using a desorber and an external condenser. Figure 5.7 presents the heat load of the resorber, which is constant, the desorber and the external condenser. The fourth line in the figure is the removed heat from the column. This value is equal to the heat removed by the desorber plus the heat removed by the external condenser:

$$\dot{Q}_{removal} = \dot{Q}_{desorber} + \dot{Q}_{ext.condenser} \qquad [5.1]$$

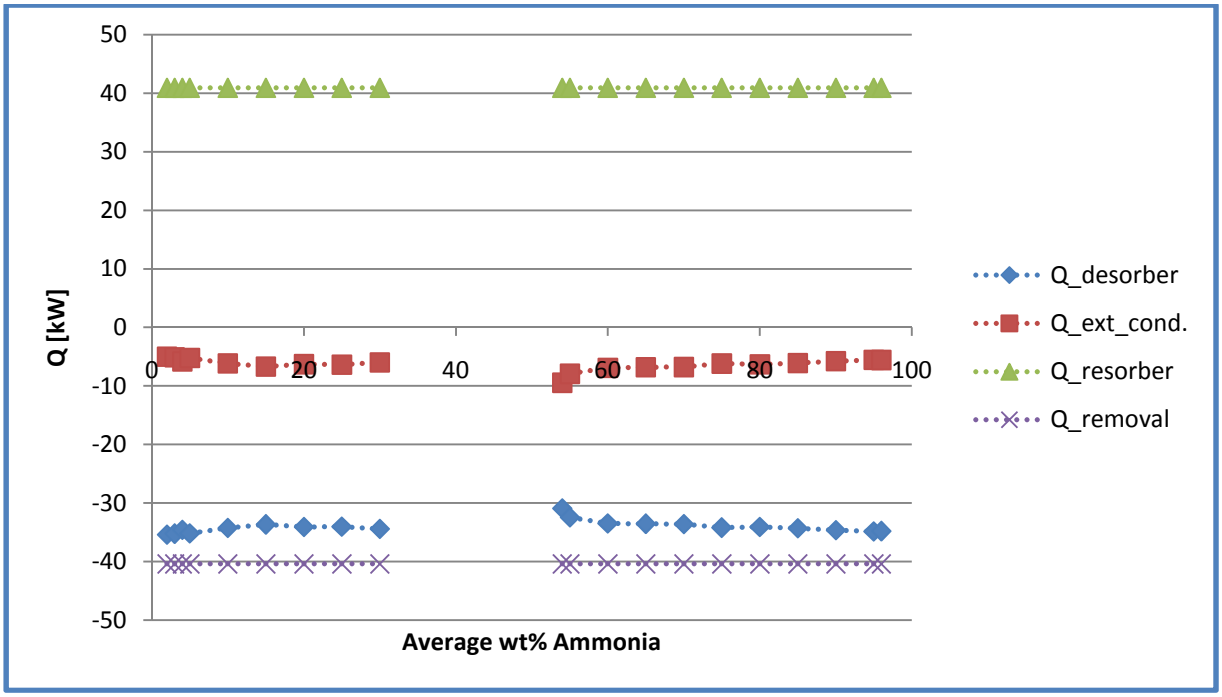

Figure 5.7 – Heat load of the desorber, resorber and external condenser

It can be seen that the absolute value for the heat load of the desorber has a maximum at the low average concentration (2wt% ammonia), and at the high average concentration (96wt% ammonia). This means that for these concentrations the external condenser is smaller compared to the other concentrations. The result of the compressor work (figure 5.6) and desorber heat load (figure 5.7) for the different average concentrations of ammonia can be used to study the performance of the compression resorption heat pump.

The energetic performance of the compression resorption heat pump can be expressed using the Coefficient Of Performance (COP). The COP is defined as the heat that is delivered by the heat pump divided by the work required by the compressor:

$$COP = \left|\frac{\dot{Q}_{desorber}}{\dot{W}}\right| \qquad [5.2]$$

Figure 5.8 presents the COP of the compression resorption heat pump as function of the average concentrations.

What can be seen from figure 5.8 is that the best performance is at an average concentration of 2wt% ammonia. For the higher concentrations the best performance is at an average concentration of 95/96wt% ammonia.

This result is consistent with the results obtained from figure 5.6 and 5.7. The entropy production, figure 5.6, was low for the average concentration of 2wt% and 95/96wt%. At these average concentrations the power required by the compressor was also low, and the desorber heat load, figure 5.7, was the highest. This explains the resulting COP values obtained from figure 5.8.

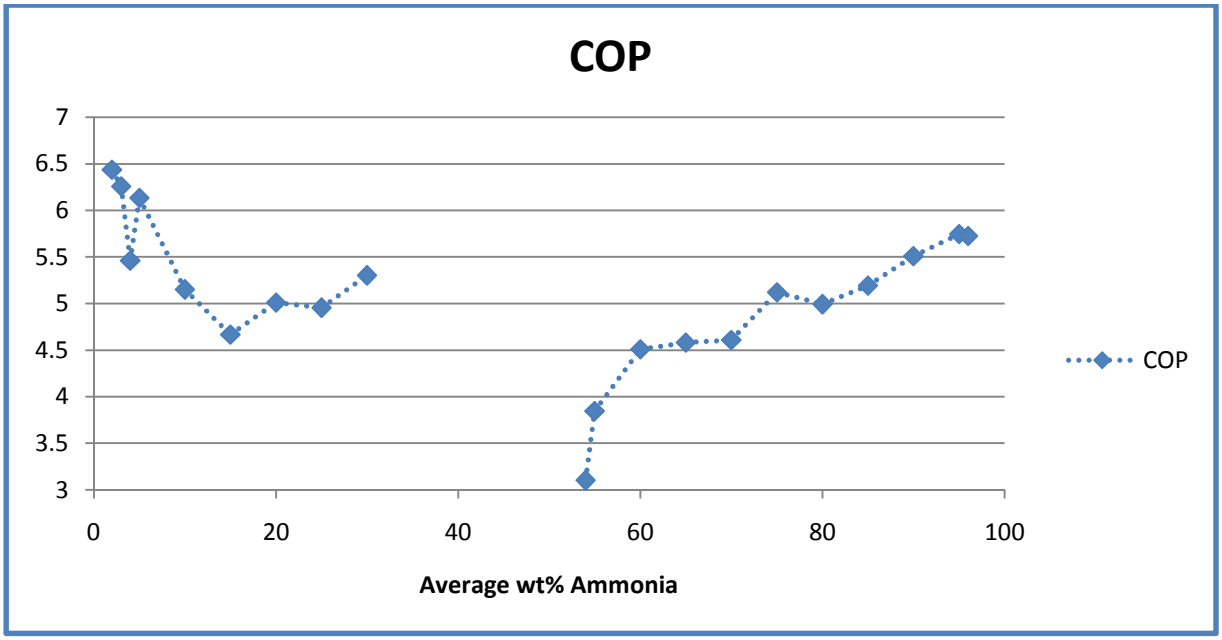

Figure 5.8 – Coefficients Of Performance (COP)

The pressure levels in the system depend on the average concentrations of ammonia. This is represented in figure 5.9. What can be seen from this figure is that the pressure ratio, i.e. the ratio between the high pressure level (resorber) and the low pressure level (desorber), decreases with rising average concentration of ammonia in the compression resorption heat pump.

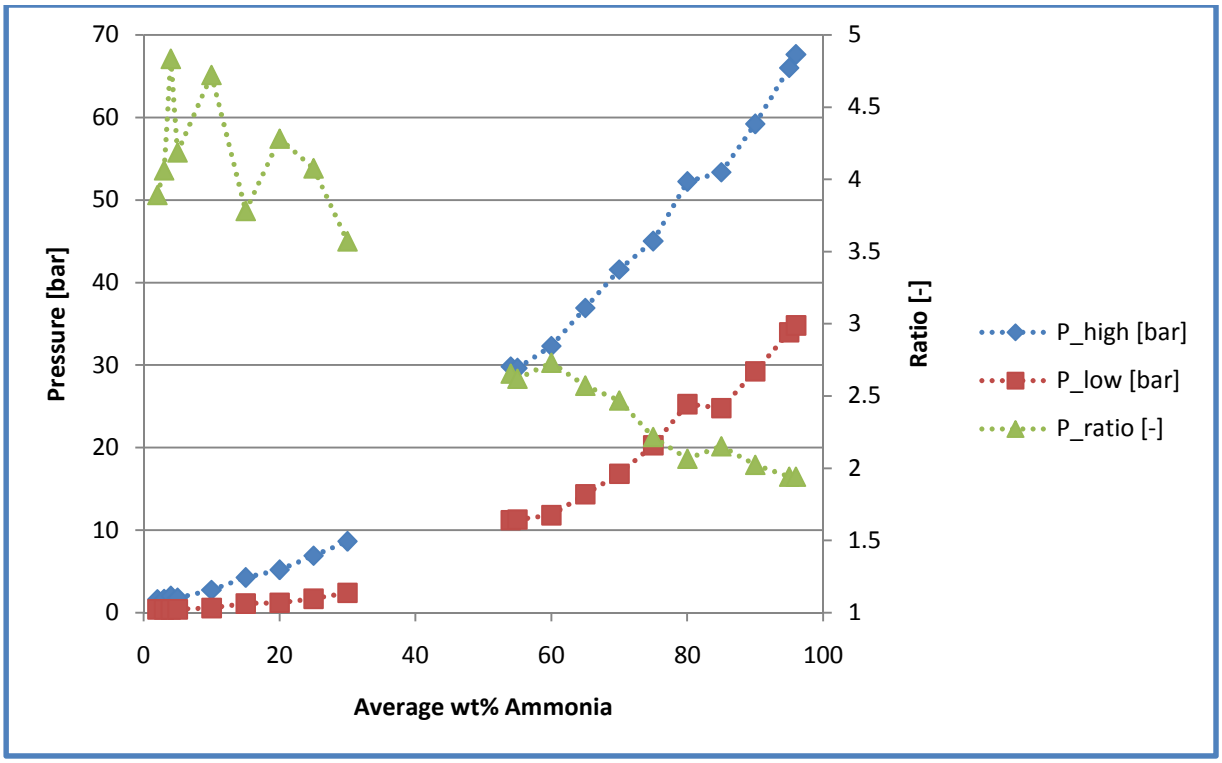

Figure 5.9 – Pressure levels and pressure ratio in the compression resorption heat pump

However, the differences between the high and low pressure levels are increasing with the average concentration of ammonia.

For the two cases, 2wt% and 96wt%, discussed above the pressure levels are widely different. In case of the average concentration of 2wt% ammonia the pressure ratio reaches a maximum, while the difference between the low and high pressure levels reach a minimum. For the second case the opposite applies: the pressure ratio has a minimum and the pressure difference has a maximum value for the average concentration of 96wt% ammonia.

The mass flow of the ammonia / water solution depends on the resorber heat load and the enthalpy difference at the in- and outlet of the resorber. This enthalpy difference is determined by the temperature driving forces between the column and the resorber, and the pressure in the resorber, see also section 3.1.3. Figure 5.10 represents the mass flow of the ammonia / water solution in the system.

For the two cases discussed above the mass flow of the solution has a minimum value. It is also interesting that the mass flow trend line has the same shape as the compressor power trend line. The explanation for this behavior is that the mass flow is a very important (coupled) variable while calculating the power required by the compressor.

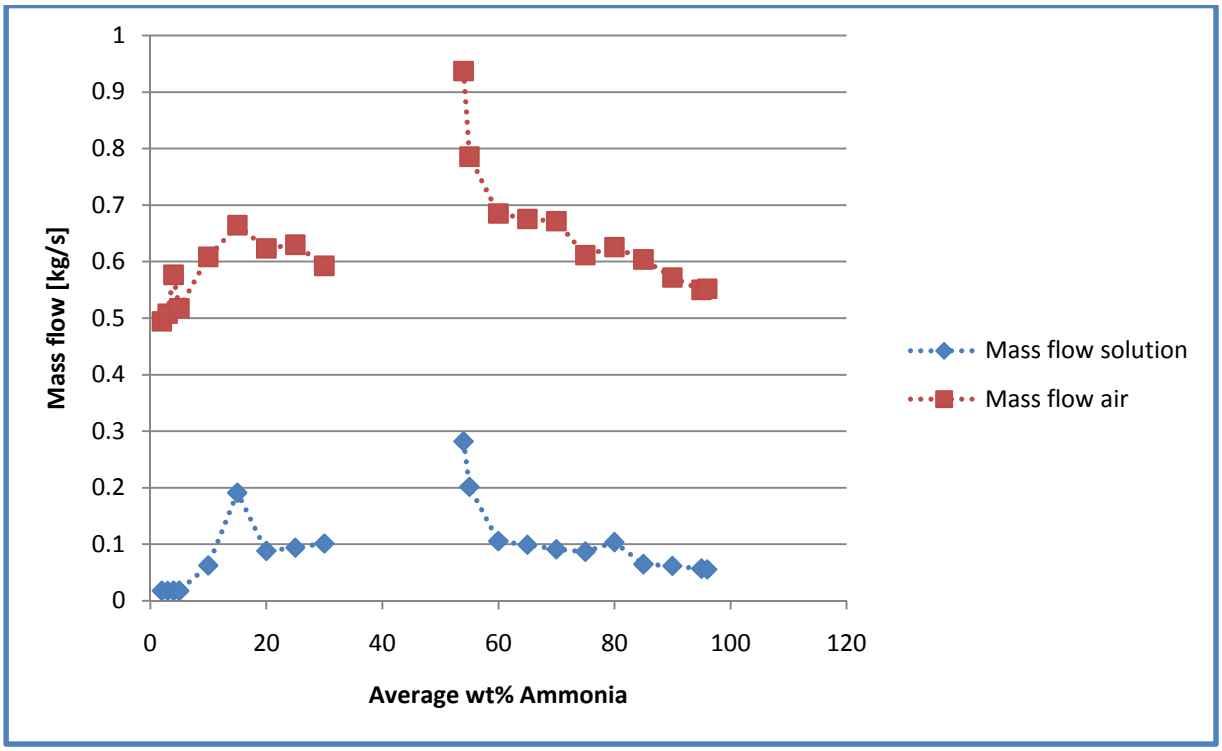

Figure 5.10 – mass flow of the solution in the compression resorption heat pump, and air mass flow of the external condenser

The second (red) line in figure 5.10 represents the mass flow of air that is required for the external condenser. This line depends on the heat load of the external condenser, because the in- and outlet temperatures of air were fixed.

The two most interesting cases, average concentration of 2wt% and 96wt% ammonia, are presented in temperature - enthalpy (T-h) diagrams, figures 5.11 and 5.12. From these figures it can be seen that the pressure lines have small gradients, in comparison with the other T-h diagrams presented in Appendix C. The red dots are the enthalpy and temperatures at the four state points, i.e. at the in- and outlet of the resorber and desorber. The resorber is operating on the high pressure line and the desorber is operating on the low pressure line.

The two dots on the left side of the figures are states 3 and 4. This is obvious because isenthalpic expansion was assumed in the expansion valve. Only the pressure and thus the temperature decreases from state 3 to state 4. The dots on the right side of the figure are states 1 and 2, i.e. at the in- and outlet of the compressor. The compression was not assumed isentropic, which explains the position of the dots. The upper right dot is shifted to the right in comparison with the lower right dot.

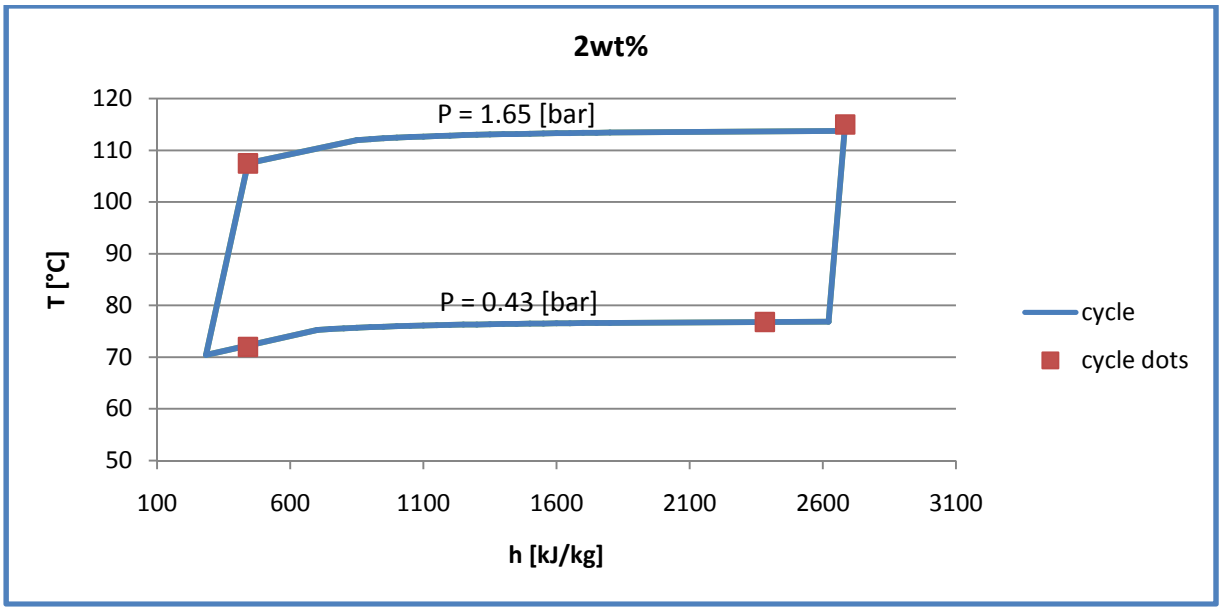

Figure 5.11 – Average concentration of 2wt% ammonia in the compression resorption heat pump

The COP for the cycle presented in figure 5.11 is high. This is because the enthalpy difference is large, i.e. the enthalpy trajectory on the high pressure line is fully utilized. The pressure difference is very small in this case, so therefore a small compressor work is required.

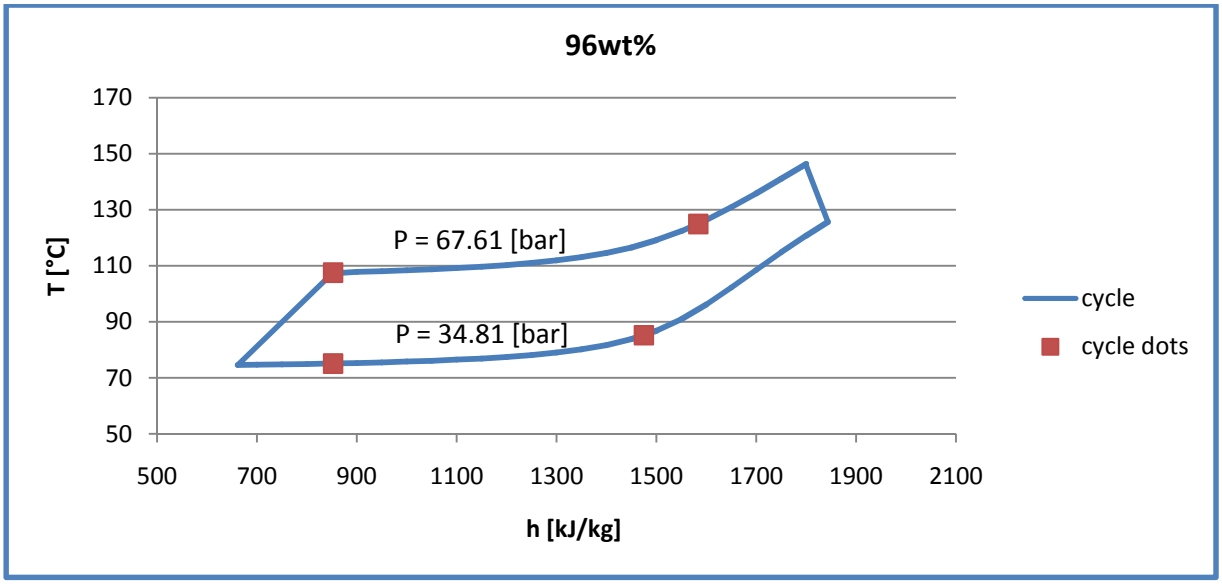

Figure 5.12 – Average concentration of 96wt% ammonia in the compression resorption heat pump

5.2 Entropy production analysis

The entropy production of the diabatic column with integrated compression resorption heat pump is compared with an adiabatic column with a conventional reboiler and condenser. The case with an average of 96wt% ammonia in the compression resorption heat pump mixture is used for the comparison. In this case the total entropy production is 0.6782 kW/K.

If an adiabatic column is used with reboiler and condenser, the entropy production 1.5679kW/K. The entropy production in the adiabatic column is caused by phase transitions on the trays and feed mixing. This entropy production is larger than the entropy production in the diabatic column with integrated compression resorption heat pump. This is due to the heat load of the column. The heat load of the diabatic column is at constant temperature gradient, while the heat is supplied to or rejected from the adiabatic column at high and low temperature respectively. This is the main reason for the larger entropy production in the adiabatic column.

Figure 5.13 presents the entropy production of the adiabatic distillation column with a conventional reboiler and condenser. From this figure it can be seen that the entropy production is the highest on the feed tray, which is comparable for the diabatic column, figure 5.5. The largest entropy production occurs in the reboiler.

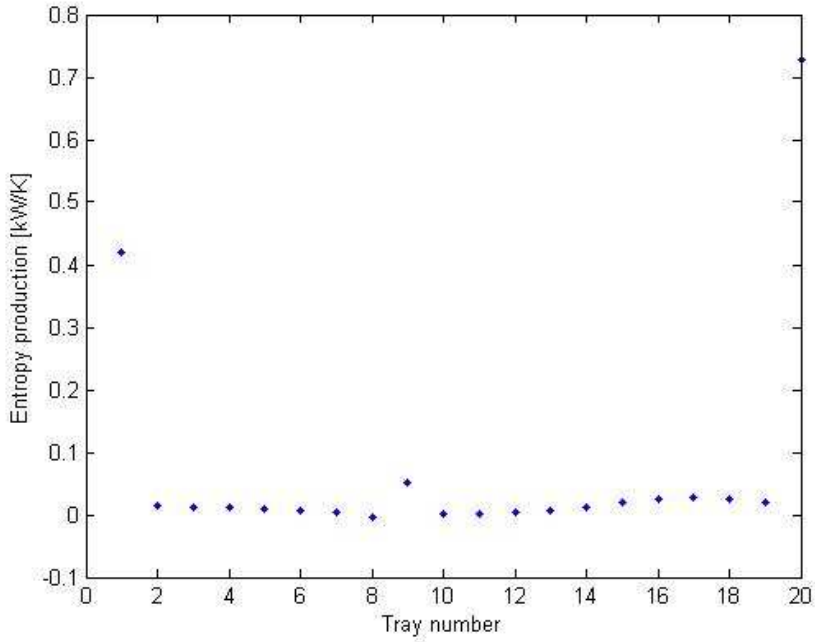

Figure 5.13 – Entropy production in an adiabatic column

5.3 Energy analysis

This section contains a energy analysis of the diabatic column with integrated compression resorption heat pump versus an adiabatic column, with conventional reboiler and condenser.

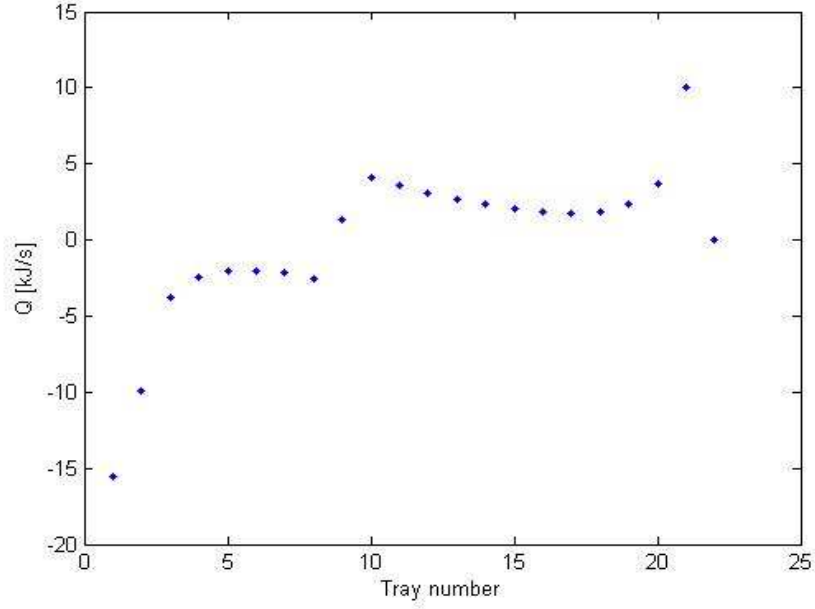

Figure 5.14 – Heat load requirements diabatic column

Figure 5.14 presents the heat load requirements of the diabatic column, see also Appendix B. The heat load requirements for the adiabatic column are represented in figure 5.15.

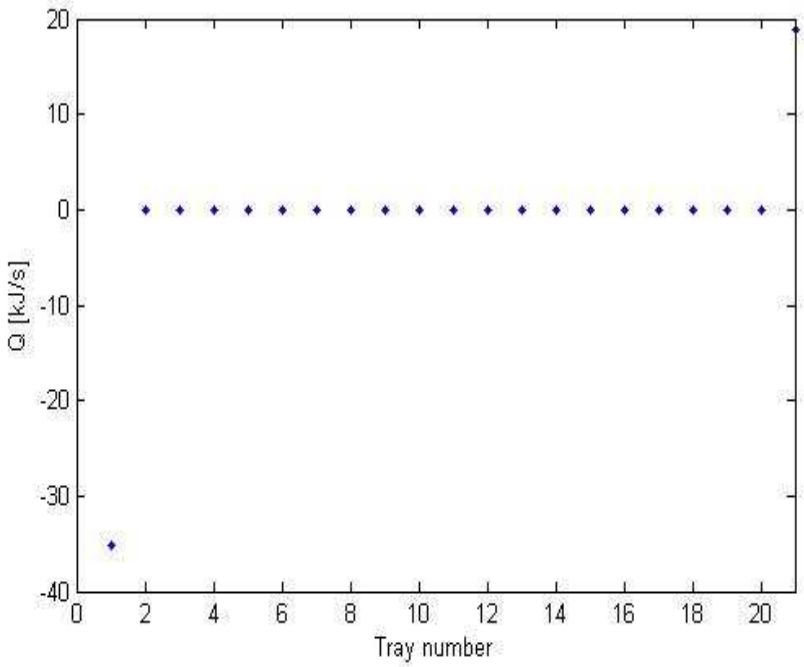

Figure 5.15 – Heat load requirements adiabatic column

Finally the energy savings between the diabatic and the adiabatic columns will be investigated. Secondly the energy costs between the two columns will be compared.

The energy input for the diabatic column is the compressor work, which is electric energy. For the adiabatic column steam is used in the reboiler, instead of electric energy for a compressor.

If only the heat loads are compared, the diabatic column has a larger heat requirement than the adiabatic column. This is because of the flows in the column. The flows in the diabatic column are very different as the flows in the adiabatic column and therefore another reflux is needed to obtain the given purities. For the diabatic column 40.9 kW is needed to operate it while the adiabatic column only needs 19.0 kW for the same operation. If a compression resorption heat pump is integrated on the diabatic column the heat load is only 5.5 kW. So the adiabatic column uses more than three times the energy that is needed for the diabatic column with integrated compression resorption heat pump. These results are presented in figure 5.10.

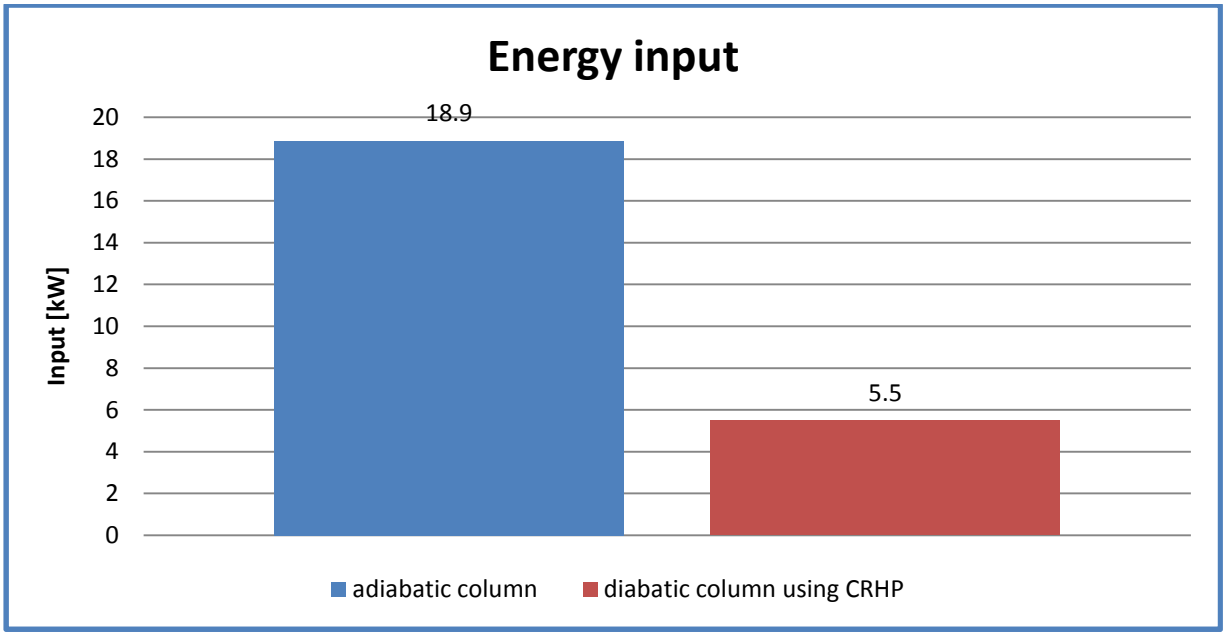

Figure 5.16 – Energy input for the adiabatic column versus the diabatic column with integrated compression resorption heat pump

This energy input can be translated to energy costs:

- Natural gas costs for large industries including taxes: 0.0279 €/kWh[5]
- Electricity prices for large industries including taxes: 0.0706 €/kWh[5]

Natural gas is needed to produce steam for the reboiler (adiabatic column). Electricity is needed for the compressor of the diabatic column with integrated compression resorption heat pump.

The costs to operate 5000h/year are then:

Cost for energy input adiabatic column: € 3102 (This includes a boiler efficiency of 85%)

Cost for energy input diabatic column with integrated compression resorption heat pump: € 1942

This is a cost saving of € 3102 - € 1942 = € 1160 per year.

The cost saving in this is very low. This is due to the fact that it concerns an extremely small column i.e. small top and bottom streams. If the column would be larger or the purities of the distillate and bottom streams would be higher, the cost savings would increase significantly.

[5] Eurostat (2007)

5.2 Detailed models

The results obtained from the two detailed models are presented in this section. First the results of model A: Heat and mass transfer models will be presented followed by the second model, model B: Irreversible thermodynamics model.

The tray with the largest entropy production is selected to implement the two models. From the results above it can be seen that the first tray produces the highest entropy production. The models for the desorber are used, because the first tray is covered by the desorber.

The heat load for the first tray of the desorber is 20.23 kW. The length of the tubes is constrained by the height of the trays which is 0.6 m. The diameter for the tubes is 30 mm. There are 20 parallel circuits on the trays. The results presented are for an average concentration of 2wt% ammonia.

The entering conditions at the inlet of the tubes are known: The inlet temperature of the liquid and vapor is 73.55°C, the inlet concentrations of ammonia are 0.0109 [kg/kg] for the solution and 0.1545 [kg/kg] for the vapor. The pressure is taken constant, which follows also from the optimization results (0.425 bar). The heat that is supplied to the desorber is homogeneous over the tube length.

The step size used to calculate the tubes is small in the first part of the tube. This is because the heat and mass transfer are playing a large role. A small step size is keeping the error as small as possible. The step size is however increasing along the tube length because the errors that are made are much smaller.

The tables below are presenting the results for model A, the heat and mass transfer model, at the outlet of the desorber tube.

Table 5.1 – Results model A

	unit	In	Out		unit	
$\dot{m}_s$	[kg/s]	8.5224e-4	8.55e-4	$d\dot{m}_s$	[kg/s]	2.3403e-6
$\dot{m}_v$	[kg/s]	5.7760e-5	5.54e-5	$d\dot{m}_v$	[kg/s]	-2.3403e-6
x_s	[kg/kg]	0.010882	0.002429	$d\dot{Q}_s$	[kW]	-0.00058
y_v	[kg/kg]	0.154541	0.0689	$d\dot{Q}_v$	[kW]	0.0060

Table 5.2 – Results model A

	unit	
T_{out}	[°C]	74.8403
T^{int}	[°C]	74.9579

Table 5.3 – Dimensions desorber (heat exchanger)

	Unit	
L	[m]	0.6
d	[mm]	30
Number of parallel circuits		20

The heat and mass transfer coefficients are presented below in table 5.4.

Table 5.4 – Heat and Mass transfer coefficients

	Unit	
α_s	[W/m^2 K]	12210.05
α_v	[W/m^2 K]	76.133
k_s	[m/s]	0.053878
k_v	[m/s]	0.002661

Results from the heat and mass transfer model, model A, are presented in the following figures. Figure 5.17 is presenting the ammonia concentrations in the solution and in the vapor versus the tube length.

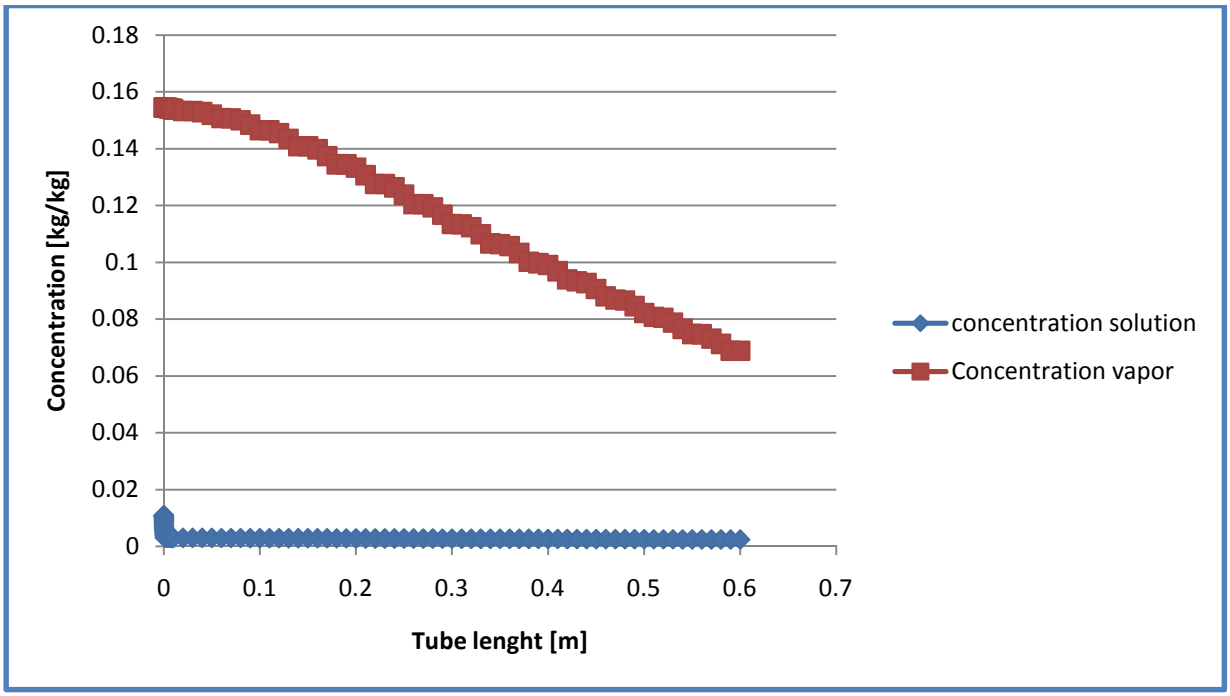

Figure 5.17 – Ammonia concentrations versus tube length

From figure 5.17 it can be seen that the concentration of ammonia is decreasing along the tube length and the concentration of the ammonia in the vapor is consequently decreasing also along the tube length.

The temperature profile obtained from the model is presented in figure 5.18. It can be seen that the temperature in the beginning of the tube is rising rapidly. This because most of the heat is supplied in the first part of the tube, by the calculation of the temperature differences between the diabatic column and the heat pump mixture, combined with the overall heat transfer coefficient.

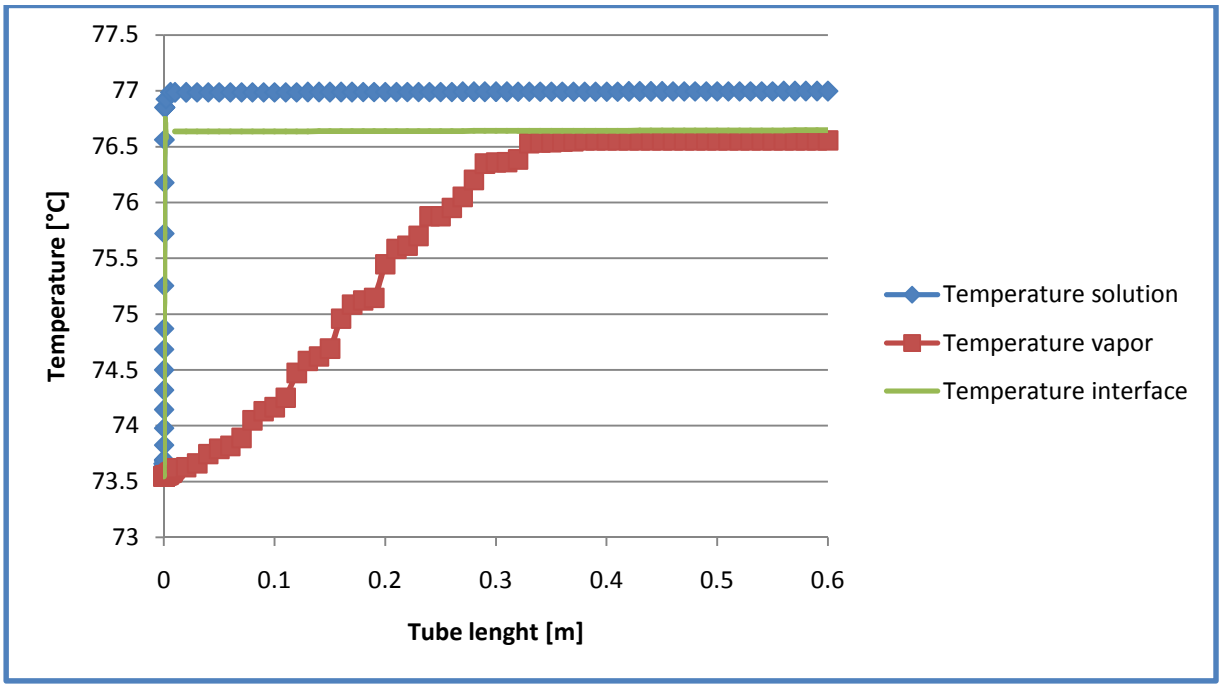

Figure 5.18 – Temperature profile in the desorber

Figure 5.19 is presenting the detailed temperature profiles in the solution, interface and vapor in the first part of the tube. What can be seen from this figure is that the interface temperature is in between the solution and vapor temperatures as expected.

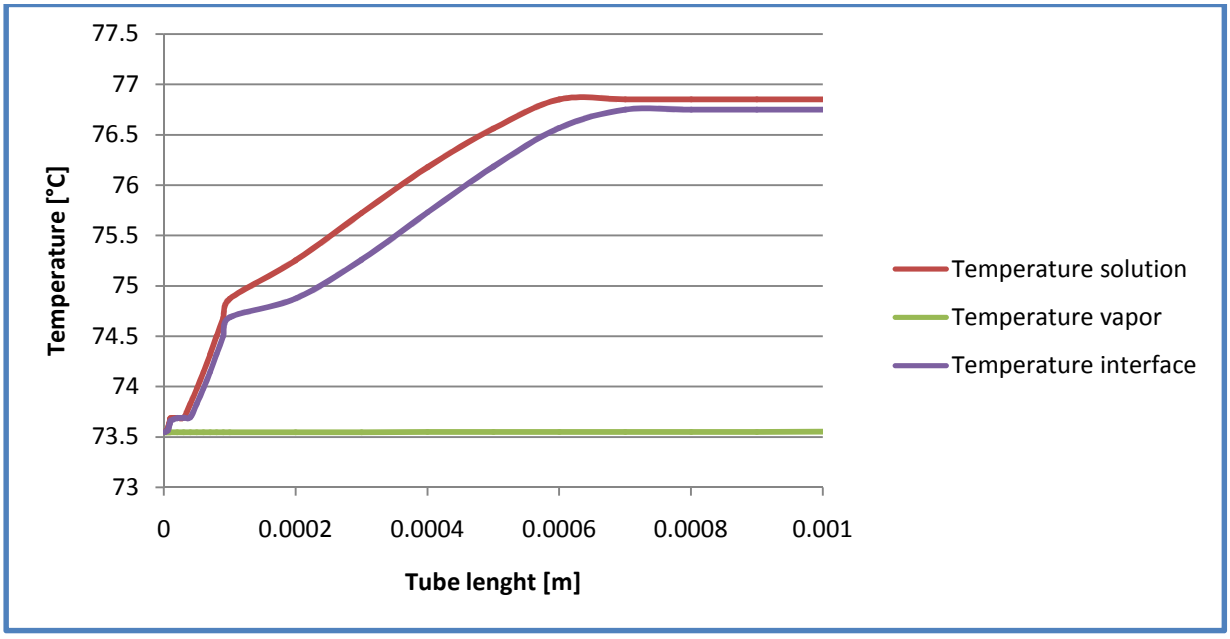

Figure 5.19 – Temperature profiles along the tube length

At last the entropy production of model A, the heat and mass transfer model, is presented, see figure 5.20. From this figure it can be seen that the entropy production is comparable with the entropy production obtained from the optimization. In the first part of the tube the entropy is increasing the most rapid because the largest part of the heat is transferred in this area.

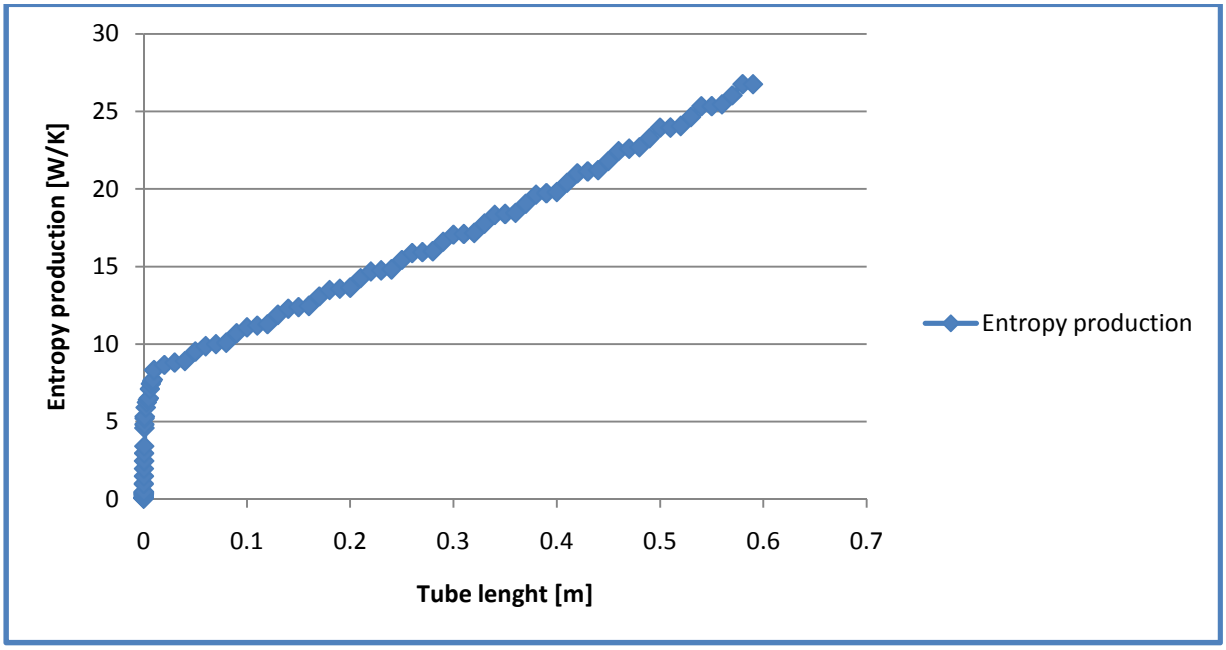

Figure 5.20 – Entropy production in the desorber

For the irreversible thermodynamics model the results are presented in Appendix D. Due to time restrictions it was not possible to evaluate the model in detail.

6. Conclusions

Several optimization studies have been performed to get a minimum of entropy production in diabatic columns with integrated compression resorption heat pumps. From the results it can be noticed that an optimal set of operating variables for the system has been identified. This includes an optimal set of operating conditions for the compression resorption heat pump. These operating conditions are identified while minimizing the entropy production of the system. There are favorable operating conditions identified both at high average concentrations of ammonia, and at low average concentrations of ammonia in the mixture. When the average ammonia concentration is low, low pressures are obtained in the resorber and desorber, but the compression ratio, however, is large. When the average ammonia concentration is high, the pressures are high in the desorber and resorber, however, the compression ratio is low.

More conclusions, regarding the compression resorption heat pump, that can be drawn from the elaboration of this thesis are:

- The compression resorption heat pump can not operate with concentrations below the 2 wt% and above the 96 wt% of ammonia, because there is no superheating assumed after the compressor, which means that the vapor quality should always be smaller than 1.
- The model chosen for the desorber is a falling film desorber. For the resorber, a bubble absorber is chosen. These models are used for the detailed evaluation of the tray in the diabatic column with the highest entropy production.
- For all cases considered, the tray with the highest entropy production is tray 1.

Two detailed models have been proposed which describe the local entropy production on the tray with the highest entropy production. The first model is based on the heat and mass transfer on the tray. The second model is based on the irreversible thermodynamics theory. The conclusions that can be drawn from these models are:

- The entropy production in the first model (heat and mass transfer model) is not constant along the tube length. It has a maximum local entropy production at the end of the tube.
- The total entropy production in the first model has a value of 0.027 kW/K, which is lower than the entropy production required from the optimization model, but order of magnitude is the same.
- The second, irreversible thermodynamics model, is not discussed in detail due to time restrictions.

7. Future research recommendations

In this study the entropy production in diabatic columns with integrated compression resorption heat pumps has been investigated. The results of the study are the operating conditions of the compression resorption heat pump for the lowest entropy production. The compression resorption heat pump operates with an ammonia water mixture. Recommendations for future research are given in this chapter.

- The proposed model should be adjusted to optimize both the column and the heat pump at the same time.
- The ammonia water mixture should be replaced by a wider range of operating mixtures, to study the influence of the several mixtures on the heat pump performance.
- It is interesting to use the compression resorption heat pump in other bulk separation processes, like for example crystallization processes, due to the similarities with distillation processes.
- The optimization model can be adjusted using the detailed models on every tray in the diabatic distillation column. However, the model will be much more complex.
- The irreversible thermodynamics model must be modeled and evaluated in more detail.

References

Auracher, H. (1984). "Fundamental aspects of exergy application to the analysis and optimization of energy processes." *Universität Stuttgart*.

Beek, W. J. (1962). “Stofoverdracht door beweeglijke grensvlakken.” Ph. D. Thesis, Delft University of Tehnology

Chesters, A. K. (1976). “Stroming- en warmteoverdracht.” Delft University of Technology, Lecturing notes bw32.

Chilton, T. H., Colburn, A. P., (1934). "Evaporation of water into a laminar stream of air and superheated steam."*Ind. Eng. Chem, 26, 373-380.*

Colonna, P., van der Stelt, T.P. (2004). " FluidProp: a program for the estimation of thermo physical properties of fluids." *Energy Technology Section, Delft University of Technology, The Netherlands (http://www.FluidProp.com)*.

de Koeijer, G., and Rivero, R. (2003). "Entropy production and exergy loss in experimental distillation columns." *Chemical Engineering Science*, 58(8), 1587-1597.

de Koeijer, G. M., Kjelstrup, S., Salamon, P., Siragusa, G., Schaller, M., and Hoffmann, K. H. (2002). "Comparison of Entropy Production Rate Minimization Methods for Binary Diabatic Distillation." *Ind. Eng. Chem. Res.*, 41(23), 5826-5834.

Edgar, T. F., Himmelblau, D. M. and Lasdon, L. S. (2001) "Optimization of chemical processes." *2nd edition. McGraw-Hill. Singapore*.

Hobler, T. (1966) “Mass transfer in absorbers.” Pergamon press.

Infante Ferreira, C. A. I., Keizer, C., and Machielsen, C. H. M. (1984). "Heat and mass transfer in vertical tubular bubble absorbers for ammonia-water absorption refrigeration systems." *International Journal of Refrigeration*, 7(6), 348-357.

Infante Ferreira, C. A. (1985). "Combined momentum, heat and mass transfer in vertical slug flow absorbers." *International Journal of Refrigeration*, 8(6), 326-334.

Islam, M. R. "Absorption process of a falling film on a tubular absorber: An experimental and numerical study." *Applied Thermal Engineering*, In Press, Corrected Proof.

Itard, L. C. M., and Machielsen, C. H. M. (1994). "Considerations when modelling compression/resorption heat pumps." *International Journal of Refrigeration*, 17(7), 453-460.

Kang, Y. T., Nagano, T., and Kashiwagi, T. (2002). "Visualization of bubble behavior and bubble diameter correlation for NH3-H2O bubble absorption." *International Journal of Refrigeration*, 25(1), 127-135.

Kaynakli, O. and Yamankaradeniz, R. (2007). "Thermodynamic analysis of absorption refrigeration system based on entropy generation." *Current science* 92(4): 472-479.

Kilic, M., and Kaynakli, O. (2007). "Second law-based thermodynamic analysis of water-lithium bromide absorption refrigeration system." *Energy*, 32(8), 1505-1512.

Kim, D. S. (2007). **"** Solar absorption cooling**."** Mechanical *Maritime and Materials Engineering, Delft.* ISBN 978-90-9022181-6

Kjelstrup, S. and Bedeaux, D. (2001). "Elements of irreversible thermodynamics for engineers.", *International centre for applied thermodynamics, Istanbul*

Kjelstrup, S., Bedeaux, D. (2008). "Non equilibrium thermodynamics of heterogeneous systems." *World scientific, Singapore*.

Kjelstrup, S. and de Koeijer, G. (2003) "Transport equations for distillation of ethanol and water from the entropy production rate." *Chem. Eng. Science*, 58:1147-1161.

Labidi, J., Boulet, E., and Paris, J. (2000). "On Intrinsic Exergy Efficiency and Heat Pumps." *Chemical Engineering Research and Design*, 78(2), 180-183.

Medrano, M., Bourouis, M., Perez-Blanco, H., and Coronas, A. (2003). "A simple model for falling film absorption on vertical tubes in the presence of non-absorbables." *International Journal of Refrigeration*, 26(1), 108-116.

Nusselt W. (1923). "Der Wärmteaustausch am Berieselungskühler." *ZVDI 67 Nr.9*, pp. 206-210.

Peters, M. S. and Timmerhaus, K. D. (1991) "Plant design and economics for chemical engineers." *McGraw-Hill. Singapore.*

Rao, S. S. (1996) "Engineering optimization: Theory and practice." *John Wiley and Sons. New York*.

Rivero, R. (2002). "Application of the exergy concept in the petroleum refining and petrochemical industry." *Energy Conversion and Management*, 43(9-12), 1199-1220.

Røsjorde, A. (2004) "Minimization of entropy production in separate and connected process units." *Norwegian University of Science and Technology.*

Satapathy, P. K., Ram Gopal, M., Arora, R. C. (2004). "Studies on a compression-absorption heat pump for simultaneous cooling and heating." *International Journal of Energy Research* **28**(7): 567-580.

Sencan, A., Yakut, K. A., and Kalogirou, S. A. (2005). "Exergy analysis of lithium bromide/water absorption systems." *Renewable Energy*, 30(5), 645-657.

Taboada Rilo, R. (2007). "Applications of compression-resorption heat pumps in bulk separation processes." *Delft University of Technology.*

Wilke, W. (1962) "Warmeubergang an Rieselfilme", VDI – Forschungsheft 490, Ausgabe B, Vol. 28

Xiaofeng, N., Kai, D., and Shunxiang, D. (2007). "Numerical analysis of falling film absorption with ammonia-water in magnetic field." *Applied Thermal Engineering*, 27(11-12), 2059-2065.

Zamfirescu C., Nannan N., Marin M., Infante Ferreira C.A. (2004) " Oil Free Two Phase Ammonia (Water) Compressor." *Final Report Novem Contract BSE-NEO 0268.02.03.03.0002, Report K-336*, Faculty of Desig, Costruction and Production, Delft University of Technology, The Netherlands.

Appendix A – Correlations for falling film flows

Dimensionless numbers:

Reynolds number: $Re = \frac{\Gamma}{\mu}$ (Wilke 1962) [A.1]

Schmidt number: $Sc = \frac{\nu}{D_{AB}}$ [A.2]

Sherwood number: $Sh = \frac{k\delta}{D_{AB}}$ [A.3]

Nusselt number: $Nu = \frac{\alpha\delta}{\lambda}$ [A.4]

The mass flow rate per wetted perimeter is represented by: $\Gamma = \frac{4\dot{m}}{\pi D_i}$ [A.5]

Mass and heat transfer coefficients liquid-vapor interface *resorber*:

Mass transfer: $Sh = 0.04 Re^{0.75} Sc^{1/3}$ [A.6]

Heat transfer: $Nu_L = 0.0942 Re_L Pr_L \frac{\delta}{z} + 1.88$ [A.7]

Film thickness: $\delta^3 = \frac{3\eta_L D(u_G - u_L)}{2g(\rho_L - \rho_G)}$ [A.8]

Note that eq. A.12 is only valid for minimal pressure drop and smooth laminar films (Reynolds smaller then 200), proposed by Chesters (1976). Beek (1962) proposed a relation for film thickness by continuity:

Film thickness: $\delta^3 = \frac{3}{4}\frac{\eta_L D u_G}{\rho_L g}$ [A.9]

Mass and heat transfer coefficients liquid-vapor interface *desorber*:

Mass transfer liquid side: $Sh_L = 2 + 1.13 Re_L^{0.50} Sc_L^{0.5}$ [A.10]

Mass transfer vapor side: $Sh_G = 3.66$ [A.11]

Heat transfer liquid side $Nu_L = 0.0323 Re_L^{0.2} Pr_L^{0.344}$ [A.12]

Heat transfer vapor side $Nu_G = 3.66$ [A.13]

Film thickness: $\delta = \left(\frac{\mu^2}{\rho^2 g}\right)^{1/3}$ [A.14]

Appendix B – Results optimization diabatic column

The entropy production in the diabatic column is optimized using the model of Røsjorde (2004). Results are presented below.

Note that the temperature profile, heat load and vapor flow figures are plotted with Matlab. This program does not recognize tray 0. Therefore tray 2 in the figure corresponds with tray 1 of the real system, tray 3 in the figure corresponds with tray 2 in the real system, etc. Tray 1 is used to plot the external condenser.

The temperature profile of the column is presented in figure B.1:

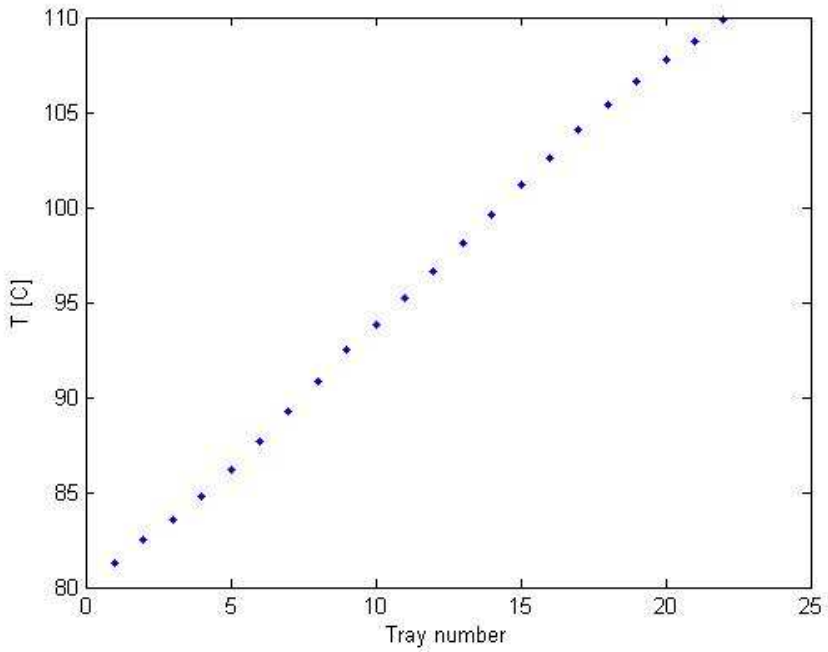

Figure B.1 – Temperature profile diabatic column

The heat load supplied of rejected to or from the column is presented per tray of the column in figure B.2:

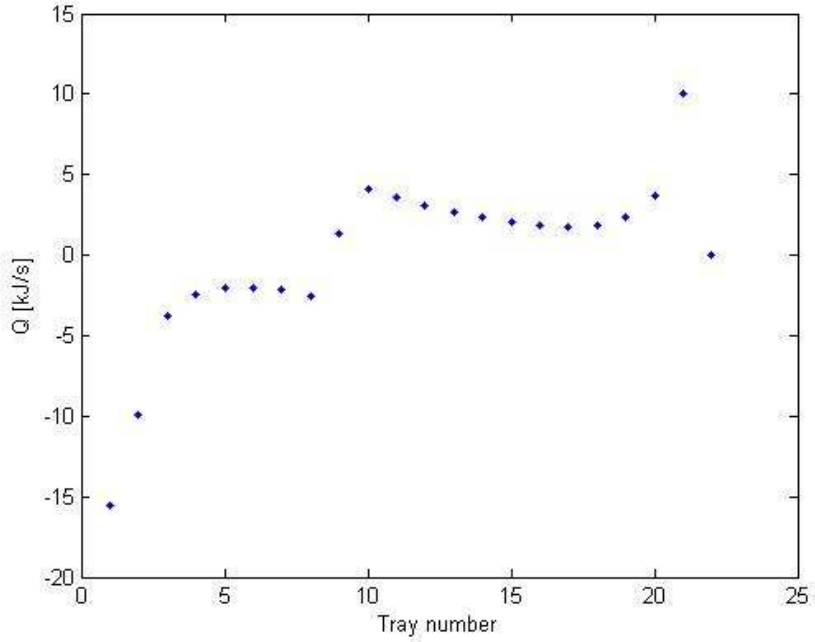

Figure B.2 – Temperature profile diabatic column

The vapor flow in the column is presented in figure B.3:

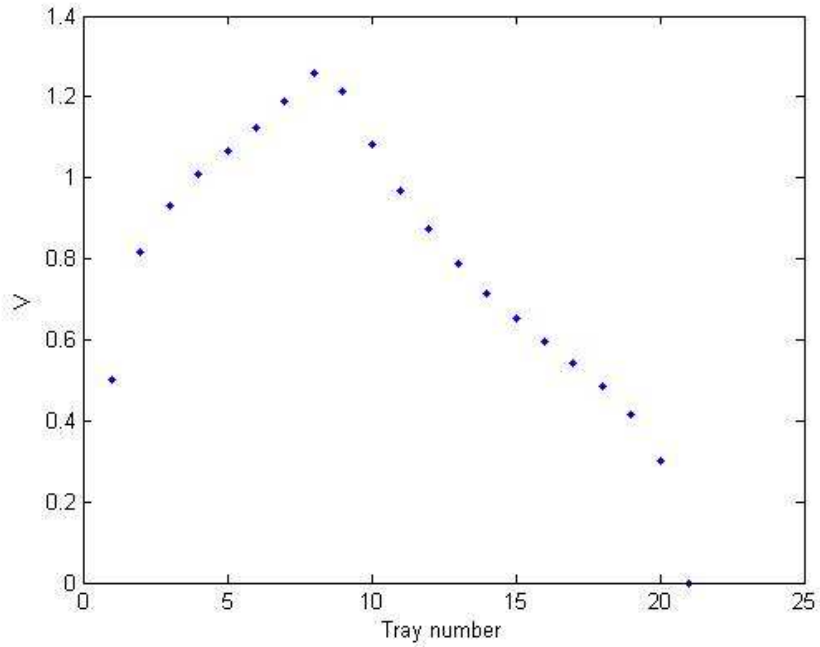

Figure B.3 – Temperature profile diabatic column

Appendix C – Results optimization compression resorption heat pump

Results of the optimization which minimize the entropy production of a diabatic column with integrated compression resorption heat pump are presented in the following sections. The average weight percentage of ammonia is varied from 2 – 96 percent.

The state points are depicted in figure C.1:

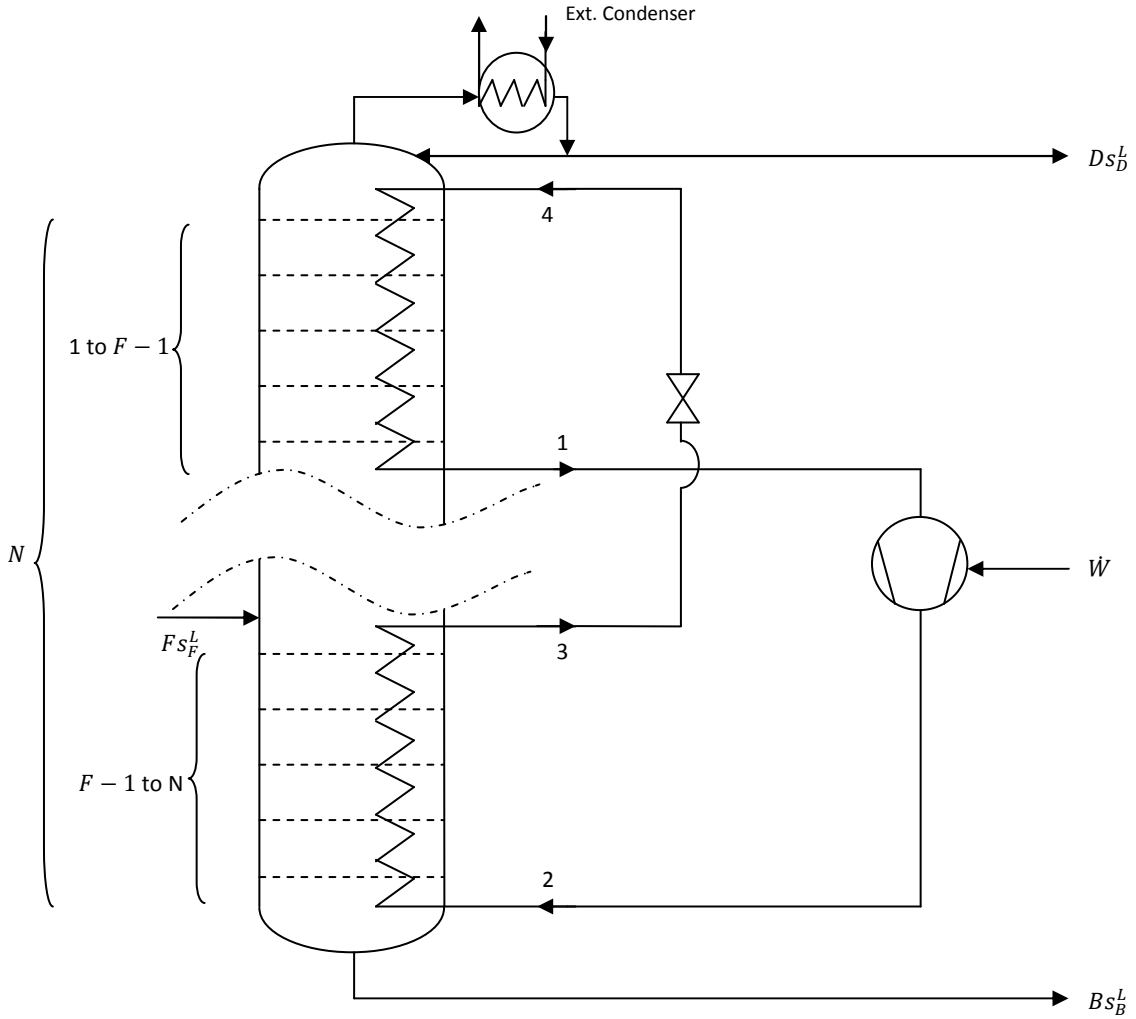

Figure C.1 – State points of the compression resorption heat pump

Note that the temperature profile, and entropy production figures are plotted with Matlab. This program does not recognize tray 0. Therefore tray 2 in the figure corresponds with tray 1 of the real system, tray 3 in the figure corresponds with tray 2 in the real system, etc. Tray 1 is used to plot the external condenser.

Appendix C.1 – Average ammonia concentration of 2 wt%

Thermodynamic states of the compression resorption heat pump cycle:

Table C.1.1 – Thermodynamic states of the heat pump cycle

State	Temperature [°C]	Pressure [bar]	Enthalpy [kJ/kg]	Entropy [kJ/kg K]	P_{high}/P_{low}
1	76.81343487	0.425	2382.1	7.009840617	3.89
2s	113.7148775	1.6542	2593.3	7.009929958	
2	114.9778109	1.6542	2683.8	7.243845315	
3	107.4568972	1.6542	440.58623	1.430308273	
4	73.54516535	0.425	440.58623	1.451291445	

Using the data given in table C.1.1, a T-h diagram can be presented in figure C.1.1:

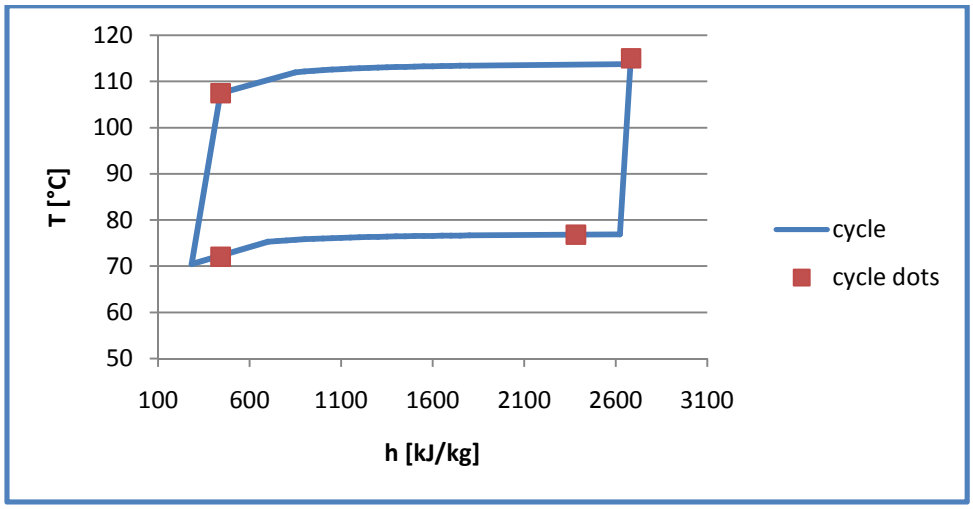

Figure C.1.1 – T-h diagram of the compression resorption heat pump

The heat loads and mass flows for the heat pump are represented in table C.1.2:

Table C.1.2 – Heat loads and mass flows compression resorption heat pump

$Q_{removed}$ [kW]	$Q_{desorber}$ [kW]	$Q_{external\_cond.}$ [kW]	$Q_{resorber}$ [kW]	W [kW]	$\dot{m}_{solution}$ [kg/s]	$\dot{m}_{air}$ [kg/s]
-40.3911	-35.3998	-4.9912	40.9	5.5001	0.0182	0.4942

The coefficient of performance (COP) for the heat pump is equal to:

$$COP = \frac{Q_{des}}{W} = 6.21$$

The temperature profile of the diabatic column (blue dots), desorber and resorber (green dots) are presented in figure C.1.2:

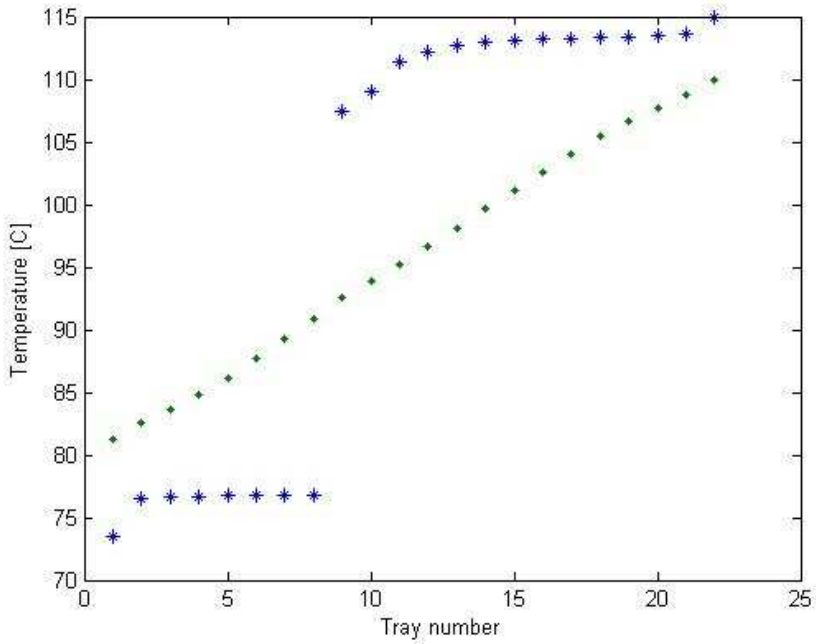

Figure C.1.2 – Temperature profile diabatic column, desorber and resorber

The minimized entropy production in the compression resorption heat pump heat pump is presented in figure C.1.3:

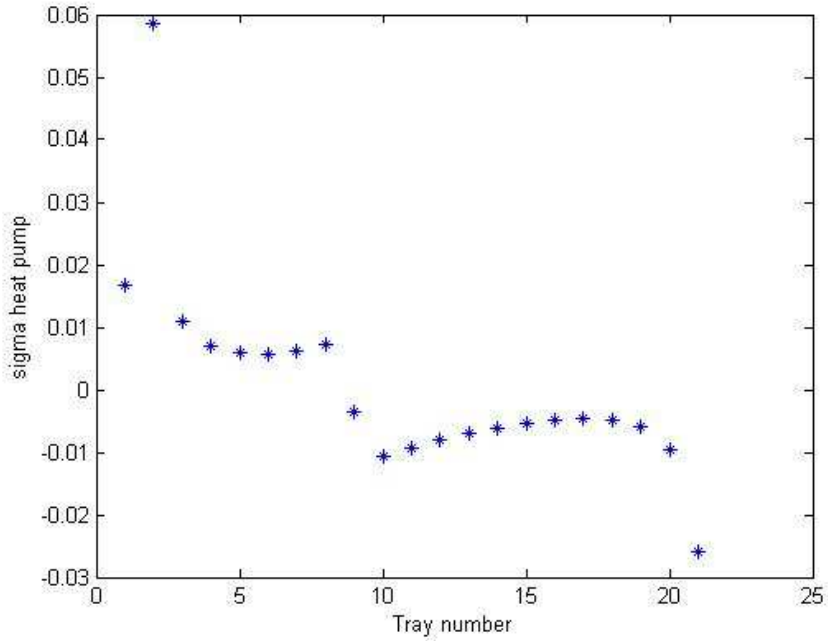

Figure C.1.3 – Minimized entropy production in the compression resorption heat pump

The entropy production for the diabatic column with integrated compression resorption heat pump is 0.7965[kW/K].

Appendix C.2 – Average ammonia concentration of 3 wt%

Thermodynamic states of the compression resorption heat pump cycle:

Table C.2.1 – Thermodynamic states of the heat pump cycle

State	Temperature [°C]	Pressure [bar]	Enthalpy [kJ/kg]	Entropy [kJ/kg K]	P_{high}/P_{low}
1	75.8865365	0.4133	2383.4	7.066153962	4.06
2s	113.8731058	1.6791	2602.5	7.065982048	
2	124.6629198	1.6791	2696.4	7.307791324	
3	104.7187709	1.6791	424.35731	1.414762963	
4	70.92594245	0.4133	424.35731	1.436634475	

Using the data given in table C.2.1, a T-h diagram can be presented in figure C.2.1:

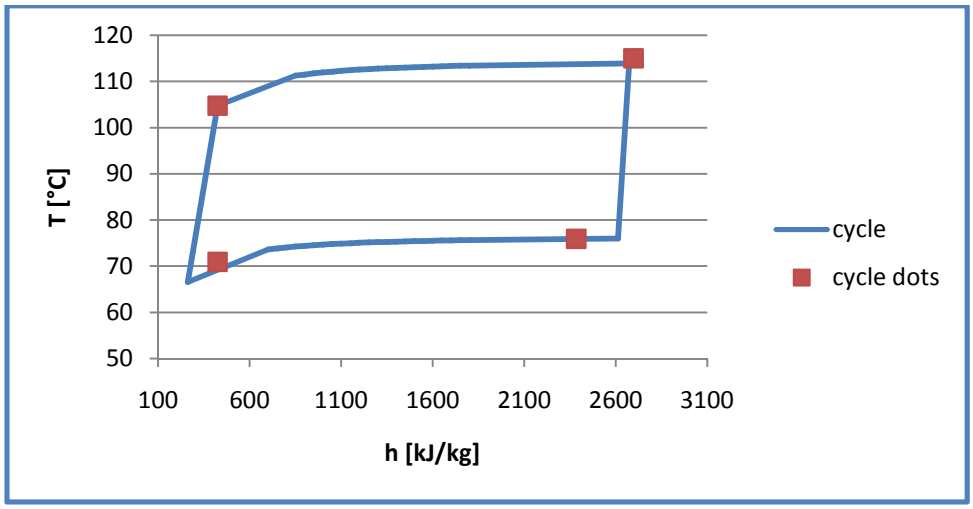

Figure C.2.1 – T-h diagram of the compression resorption heat pump

The heat loads and mass flows for the heat pump are represented in table C.2.2:

Table C.2.2 – Heat loads and mass flows compression resorption heat pump

$Q_{removed}$ [kW]	$Q_{desorber}$ [kW]	$Q_{external\_cond.}$ [kW]	$Q_{resorber}$ [kW]	W [kW]	$\dot{m}_{solution}$ [kg/s]	$\dot{m}_{air}$ [kg/s]
-40.3911	-35.2645	-5.1266	40.9	5.6355	0.018	0.5076

The coefficient of performance (COP) for the heat pump is equal to:

$$COP = \frac{Q_{des}}{W} = 6.27$$

The temperature profile of the diabatic column (blue dots), desorber and resorber (green dots) are presented in figure C.2.2:

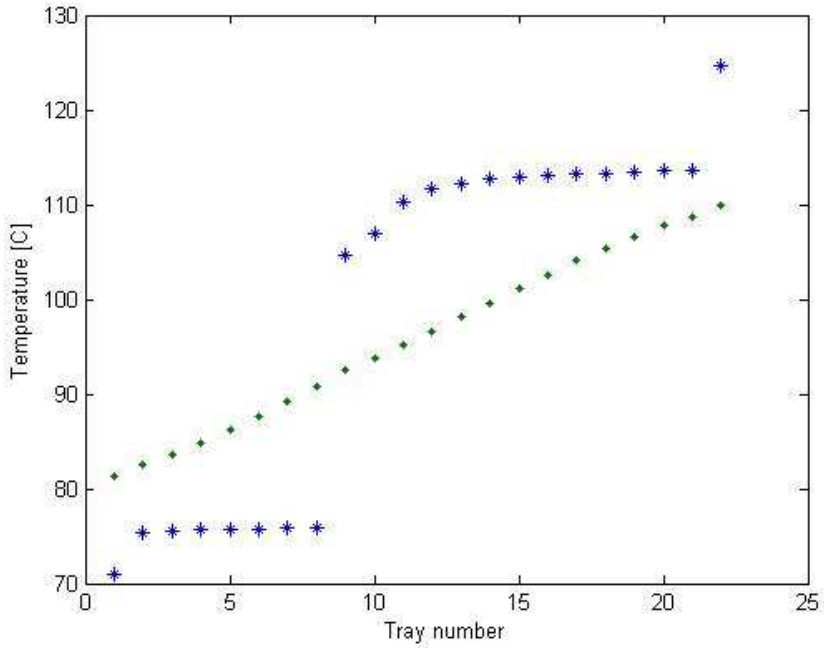

Figure C.2.2 – Temperature profile diabatic column, desorber and resorber

The minimized entropy production in the compression resorption heat pump heat pump is presented in figure C.2.3:

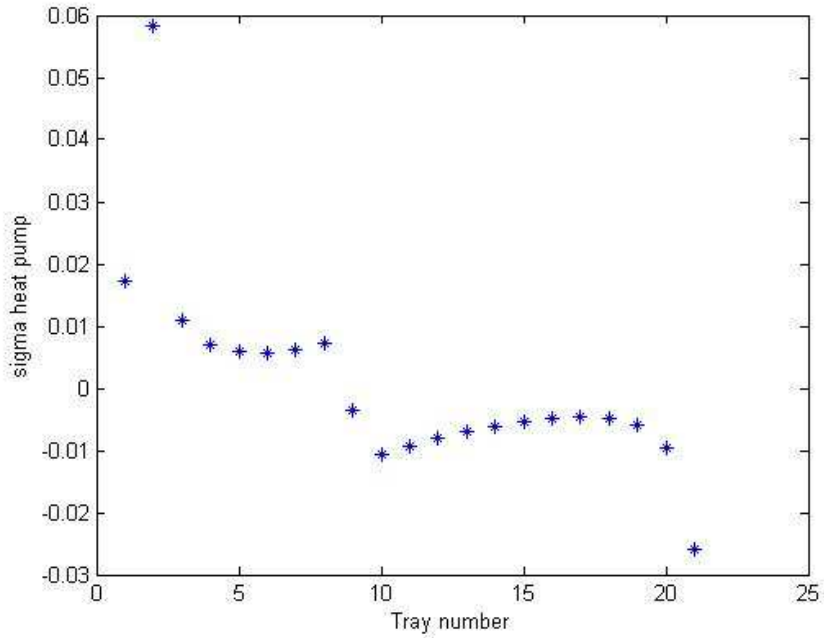

Figure C.2.3 – Minimized entropy production in the compression resorption heat pump

The entropy production for the diabatic column with integrated compression resorption heat pump is 0.8162 [kW/K].

Appendix C.3 – Average ammonia concentration of 4 wt%

Thermodynamic states of the compression resorption heat pump cycle:

Table C.3.1 – Thermodynamic states of the heat pump cycle

State	Temperature [°C]	Pressure [bar]	Enthalpy [kJ/kg]	Entropy [kJ/kg K]	P_{high}/P_{low}
1	75.87432001	0.4179	2332.8	6.956090284	4.83
2s	119.2588588	2.0193	2576.5	6.956075017	
2	122.6228154	2.0193	2681	7.22228475	
3	107.4575814	2.0193	431.79364	1.459860983	
4	69.63800087	0.4179	431.79364	1.487996467	

Using the data given in table C.3.1, a T-h diagram can be presented in figure C.3.1:

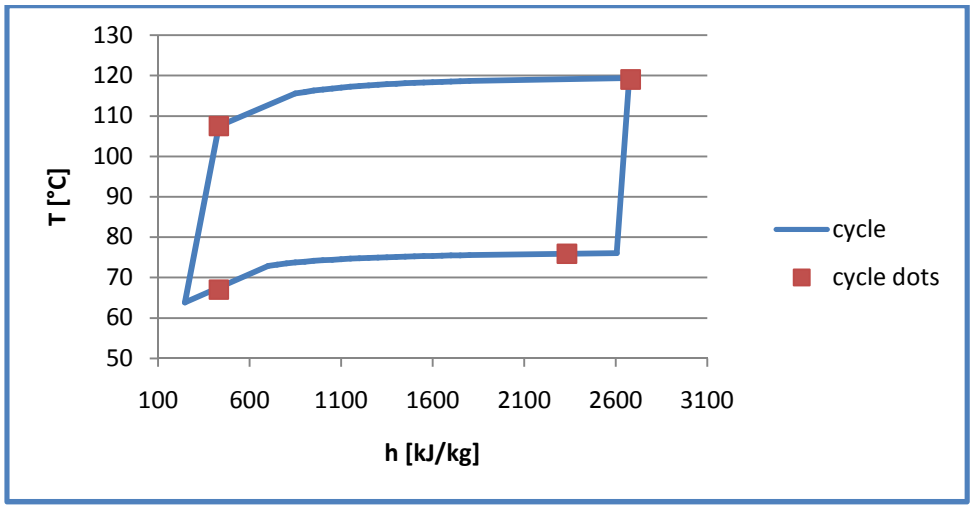

Figure C.3.1 – T-h diagram of the compression resorption heat pump

The heat loads and mass flows for the heat pump are represented in table C.3.2:

Table C.3.2 – Heat loads and mass flows compression resorption heat pump

$Q_{removed}$ [kW]	$Q_{desorber}$ [kW]	$Q_{external\_cond.}$ [kW]	$Q_{resorber}$ [kW]	W [kW]	$\dot{m}_{solution}$ [kg/s]	$\dot{m}_{air}$ [kg/s]
-40.3911	-34.5687	-5.8224	40.9	6.3313	0.0182	0.5765

The coefficient of performance (COP) for the heat pump is equal to:

$$COP = \frac{Q_{des}}{W} = 6.23$$

The temperature profile of the diabatic column (blue dots), desorber and resorber (green dots) are presented in figure C.3.2:

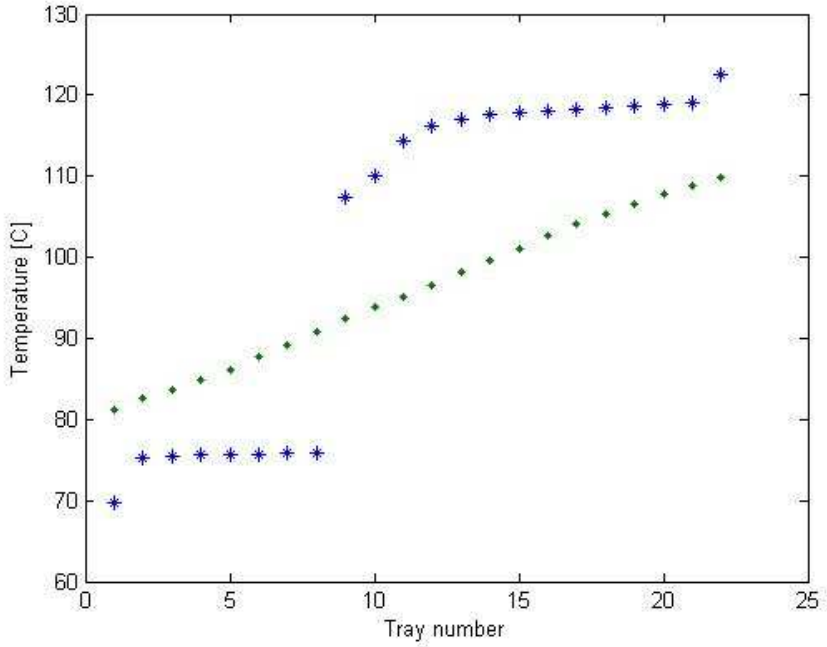

Figure C.3.2 – Temperature profile diabatic column, desorber and resorber

The minimized entropy production in the compression resorption heat pump heat pump is presented in figure C.3.3:

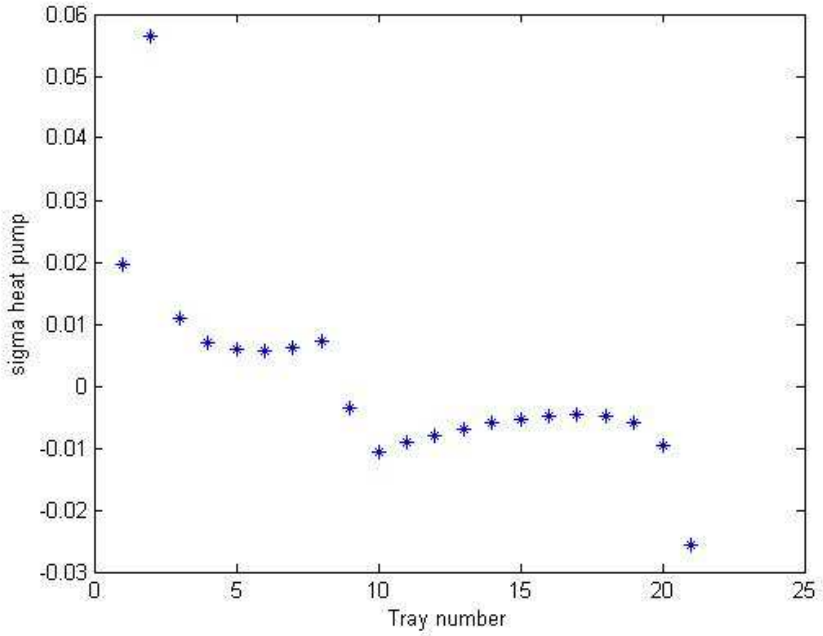

Figure C.3.3 – Minimized entropy production in the compression resorption heat pump

The entropy production for the diabatic column with integrated compression resorption heat pump is 0.8357 [kW/K].

Appendix C.4 – Average ammonia concentration of 5 wt%

Thermodynamic states of the compression resorption heat pump cycle:

Table C.4.1 – Thermodynamic states of the heat pump cycle

State	Temperature [°C]	Pressure [bar]	Enthalpy [kJ/kg]	Entropy [kJ/kg K]	P_{high}/P_{low}
1	76.11834456	0.4267	2341.1	7.009675454	4.19
2s	115.1370524	1.7865	2562.8	7.009708087	
2	115.1986459	1.7865	2657.8	7.254353153	
3	100.7351941	1.7865	398.69077	1.39655906	
4	67.69740417	0.4267	398.69077	1.419267637	

Using the data given in table C.4.1, a T-h diagram can be presented in figure C.4.1:

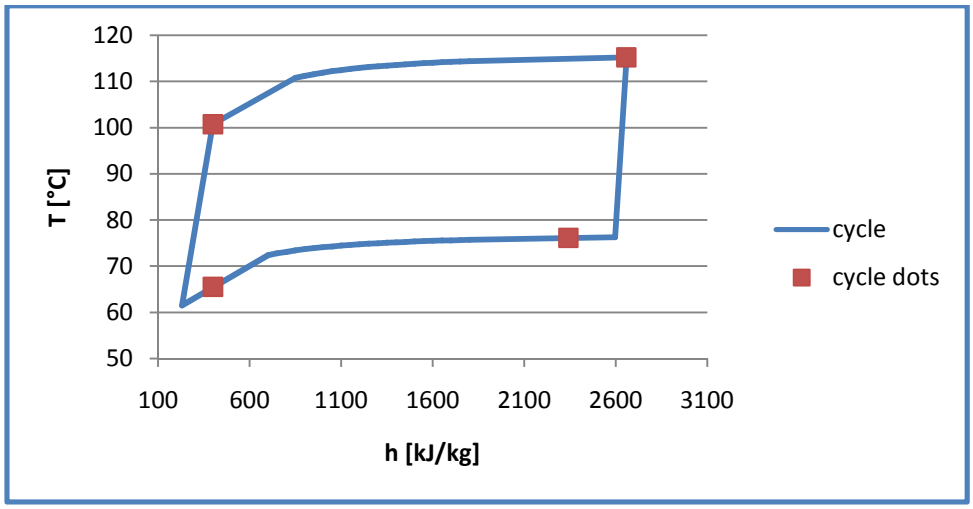

Figure C.4.1 – T-h diagram of the compression resorption heat pump

The heat loads and mass flows for the heat pump are represented in table C.4.2:

Table C.4.2 – Heat loads and mass flows compression resorption heat pump

$Q_{removed}$ [kW]	$Q_{desorber}$ [kW]	$Q_{external\_cond.}$ [kW]	$Q_{resorber}$ [kW]	W [kW]	$\dot{m}_{solution}$ [kg/s]	$\dot{m}_{air}$ [kg/s]
-40.3911	-35.1663	-5.2247	40.9	5.7336	0.0181	0.5173

The coefficient of performance (COP) for the heat pump is equal to:

$$COP = \frac{Q_{des}}{W} = 6.13$$

The temperature profile of the diabatic column (blue dots), desorber and resorber (green dots) are presented in figure C.4.2:

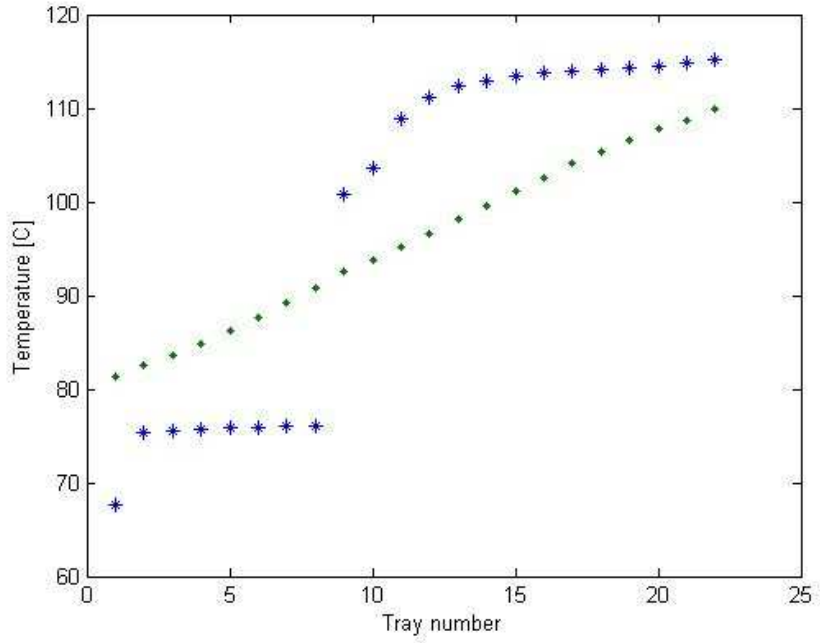

Figure C.4.2 – Temperature profile diabatic column, desorber and resorber

The minimized entropy production in the compression resorption heat pump heat pump is presented in figure C.4.3:

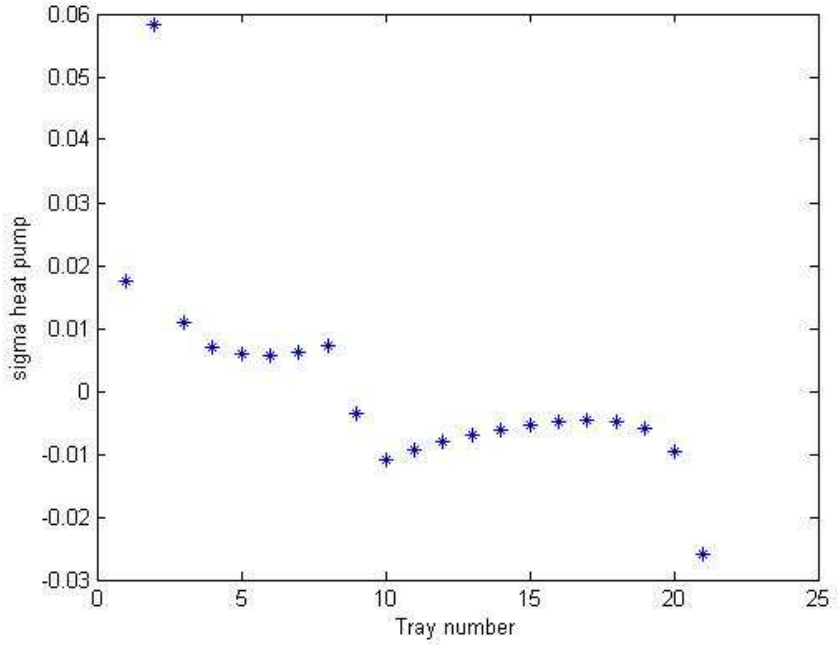

Figure C.4.3 – Minimized entropy production in the compression resorption heat pump

The entropy production for the diabatic column with integrated compression resorption heat pump is 0.8499 [kW/K].

Appendix C.5 – Average ammonia concentration of 10 wt%

Thermodynamic states of the compression resorption heat pump cycle:

Table C.5.1 – Thermodynamic states of the heat pump cycle

State	Temperature [°C]	Pressure [bar]	Enthalpy [kJ/kg]	Entropy [kJ/kg K]	P_{high}/P_{low}
1	77.55336878	0.5859	929.1	3.069138496	4.72
2s	120.2636703	2.7673	1003.1	3.069227971	
2	120.6671941	2.7673	1034.8	3.149766805	
3	101.8837097	2.7673	385.0086	1.469093026	
4	66.24987719	0.5859	385.0086	1.498247849	

Using the data given in table C.5.1, a T-h diagram can be presented in figure C.5.1:

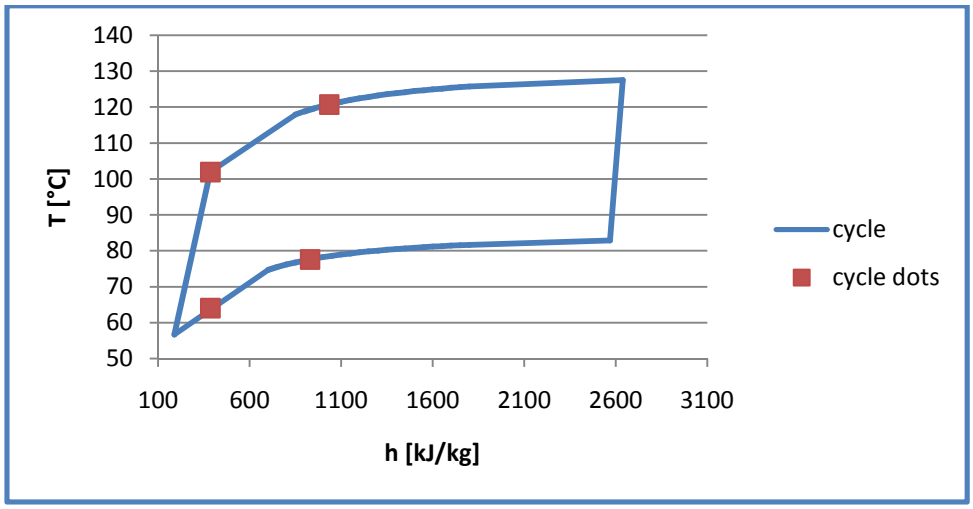

Figure C.5.1 – T-h diagram of the compression resorption heat pump

The heat loads and mass flows for the heat pump are represented in table C.5.2:

Table C.5.2 – Heat loads and mass flows compression resorption heat pump

$Q_{removed}$ [kW]	$Q_{desorber}$ [kW]	$Q_{external\_cond.}$ [kW]	$Q_{resorber}$ [kW]	W [kW]	$\dot{m}_{solution}$ [kg/s]	$\dot{m}_{air}$ [kg/s]
-40.3911	-34.249	-6.1421	40.9	6.651	0.0629	0.6082

The coefficient of performance (COP) for the heat pump is equal to:

$$COP = \frac{Q_{des}}{W} = 5.15$$

The temperature profile of the diabatic column (blue dots), desorber and resorber (green dots) are presented in figure C.5.2:

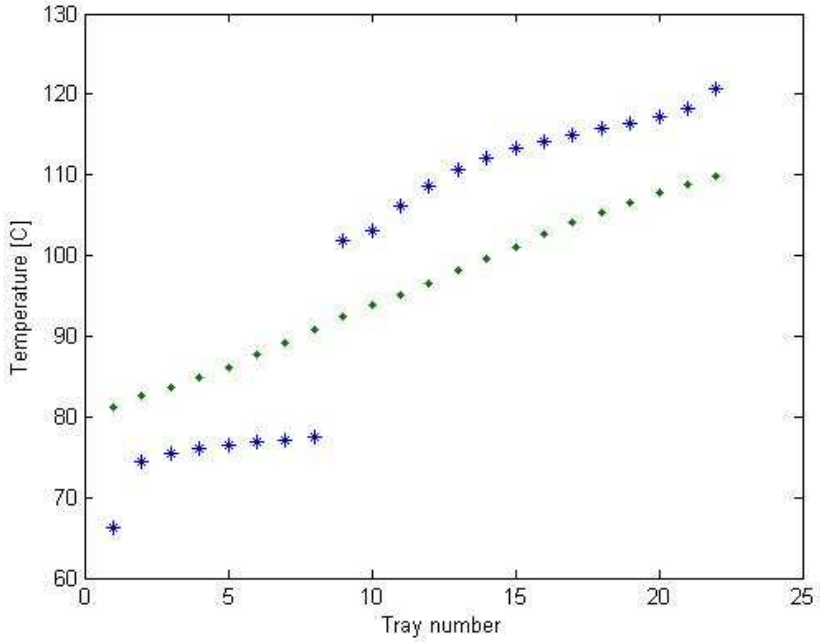

Figure C.5.2 – Temperature profile diabatic column, desorber and resorber

The minimized entropy production in the compression resorption heat pump heat pump is presented in figure C.5.3:

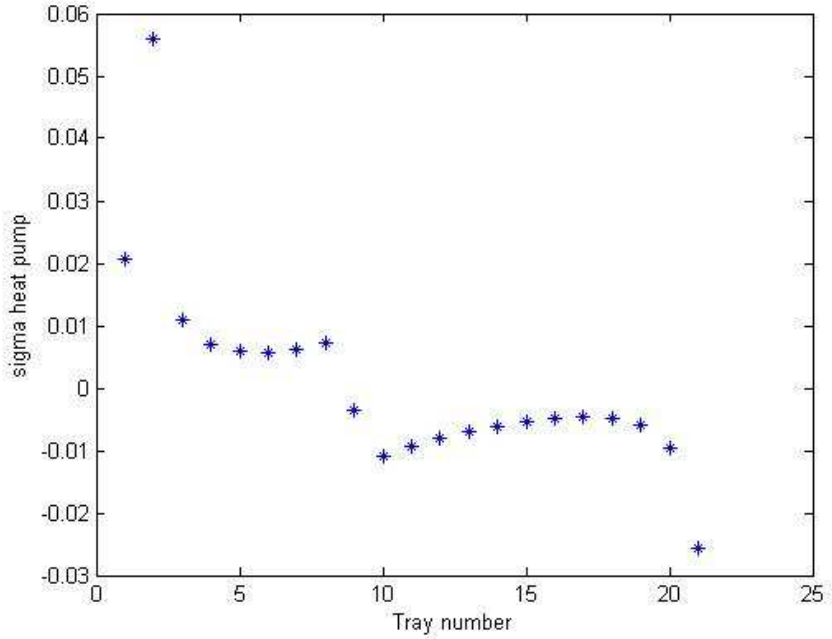

Figure C.5.3 – Minimized entropy production in the compression resorption heat pump

The entropy production for the diabatic column with integrated compression resorption heat pump is 0.9173 [kW/K].

Appendix C.6 – Average ammonia concentration of 15 wt%

Thermodynamic states of the compression resorption heat pump cycle:

Table C.6.1 – Thermodynamic states of the heat pump cycle

State	Temperature [°C]	Pressure [bar]	Enthalpy [kJ/kg]	Entropy [kJ/kg K]	P_{high}/P_{low}
1	80.52718214	1.1288	560.4768	2.088559049	3.78
2s	115.614181	4.2664	586.8757	2.088591364	
2	116.1161484	4.2664	598.1896	2.117674772	
3	105.1286512	4.2664	384.60207	1.561462834	
4	73.06733336	1.1288	384.60207	1.586224272	

Using the data given in table C.6.1, a T-h diagram can be presented in figure C.6.1:

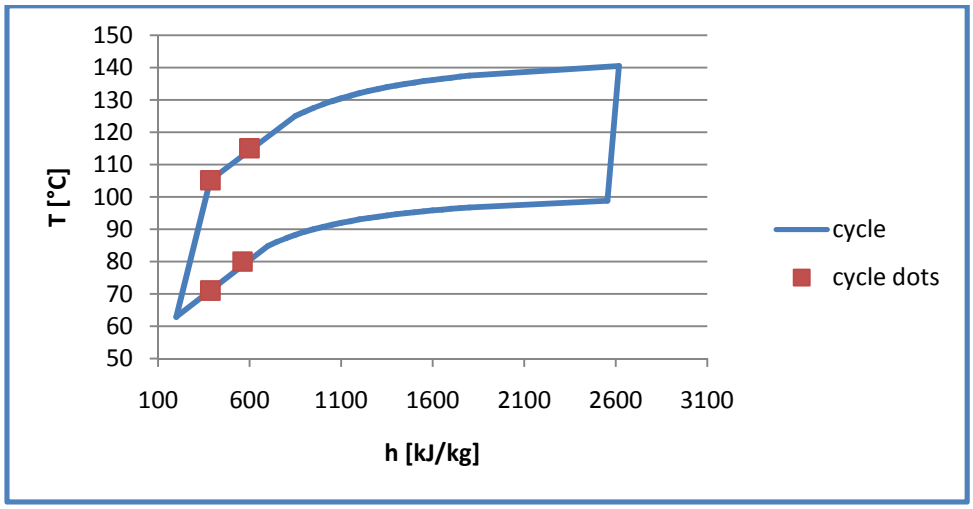

Figure C.6.1 – T-h diagram of the compression resorption heat pump

The heat loads and mass flows for the heat pump are represented in table C.6.2:

Table C.6.2 – Heat loads and mass flows compression resorption heat pump

$Q_{removed}$ [kW]	$Q_{desorber}$ [kW]	$Q_{external\_cond.}$ [kW]	$Q_{resorber}$ [kW]	W [kW]	$\dot{m}_{solution}$ [kg/s]	$\dot{m}_{air}$ [kg/s]
-40.3911	-33.6827	-6.7084	40.9	7.2173	0.1914	0.6642

The coefficient of performance (COP) for the heat pump is equal to:

$$COP = \frac{Q_{des}}{W} = 4.67$$

The temperature profile of the diabatic column (blue dots), desorber and resorber (green dots) are presented in figure C.6.2:

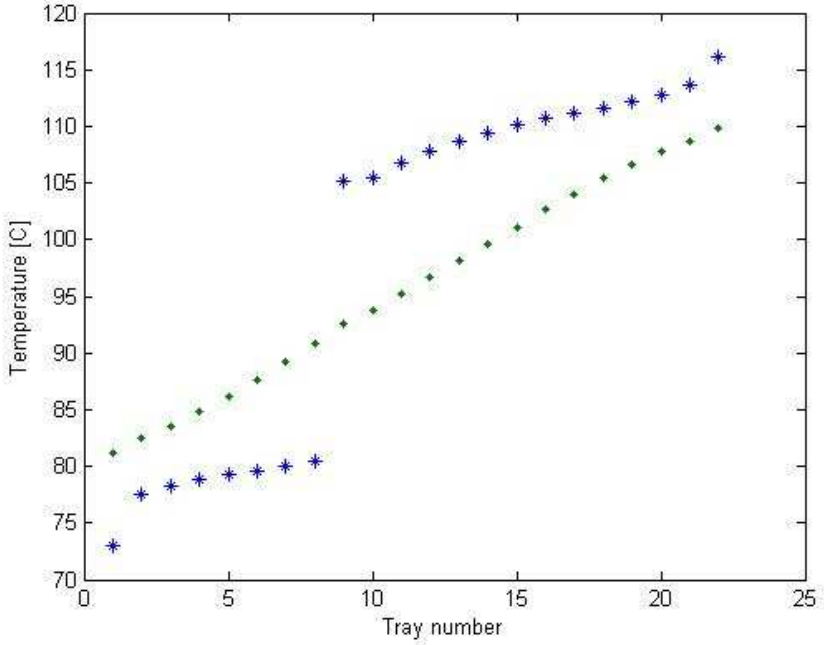

Figure C.6.2 – Temperature profile diabatic column, desorber and resorber

The minimized entropy production in the compression resorption heat pump heat pump is presented in figure C.6.3:

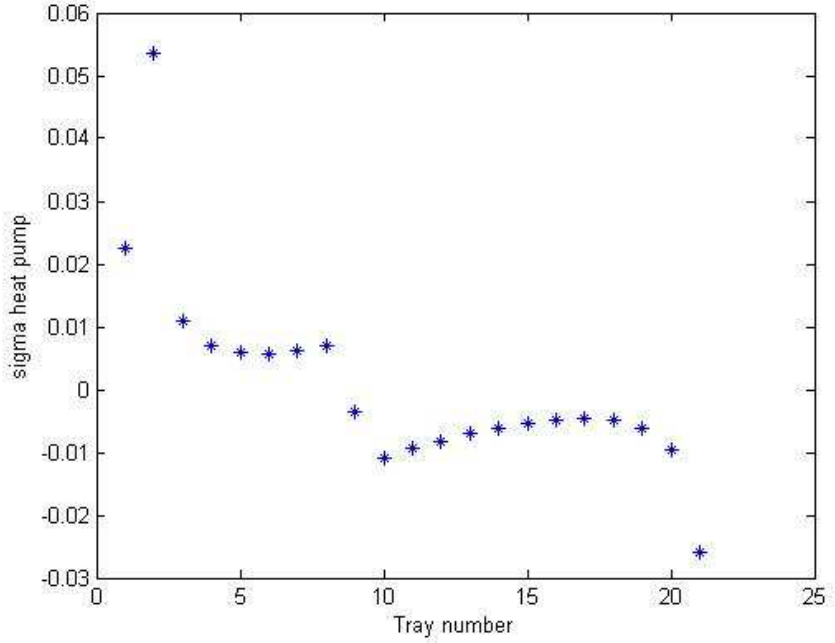

Figure C.6.3 – Minimized entropy production in the compression resorption heat pump

The entropy production for the diabatic column with integrated compression resorption heat pump is 0.967 [kW/K].

Appendix C.7 – Average ammonia concentration of 20 wt%

Thermodynamic states of the compression resorption heat pump cycle:

Table C.7.1 – Thermodynamic states of the heat pump cycle

State	Temperature [°C]	Pressure [bar]	Enthalpy [kJ/kg]	Entropy [kJ/kg K]	P_{high}/P_{low}
1	82.43116189	1.2142	739.3531	2.699664749	4.28
2s	123.0593824	5.1979	793.0549	2.699661871	
2	123.8984965	5.1979	816.0701	2.757691635	
3	100.9474976	5.1979	354.91445	1.564521273	
4	66.28110054	1.2142	354.91445	1.595762258	

Using the data given in table C.7.1, a T-h diagram can be presented in figure C.7.1:

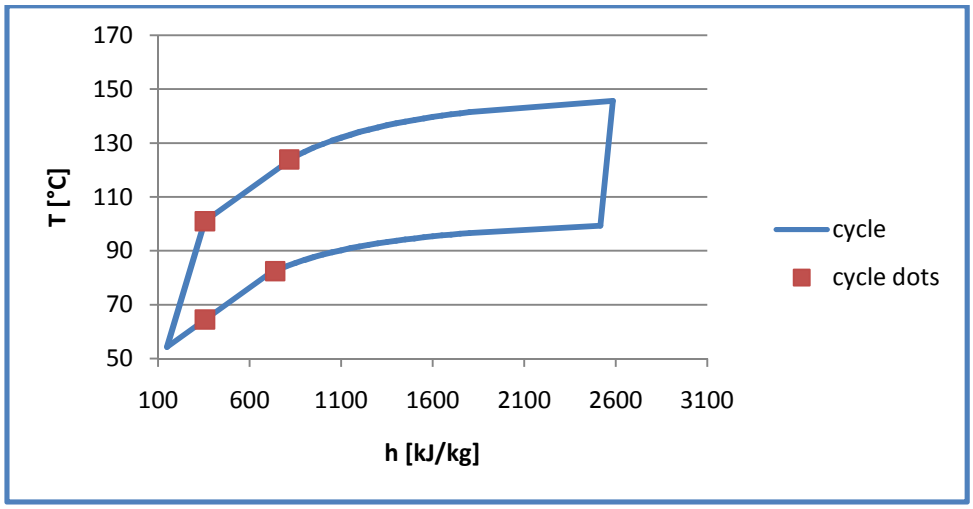

Figure C.7.1 – T-h diagram of the compression resorption heat pump

The heat loads and mass flows for the heat pump are represented in table C.7.2:

Table C.7.2 – Heat loads and mass flows compression resorption heat pump

$Q_{removed}$ [kW]	$Q_{desorber}$ [kW]	$Q_{external\_cond.}$ [kW]	$Q_{resorber}$ [kW]	W [kW]	$\dot{m}_{solution}$ [kg/s]	$\dot{m}_{air}$ [kg/s]
-40.3911	-34.0959	-6.2952	40.9	6.8041	0.0887	0.6233

The coefficient of performance (COP) for the heat pump is equal to:

$$COP = \frac{Q_{des}}{W} = 5.01$$

The temperature profile of the diabatic column (blue dots), desorber and resorber (green dots) are presented in figure C.7.2:

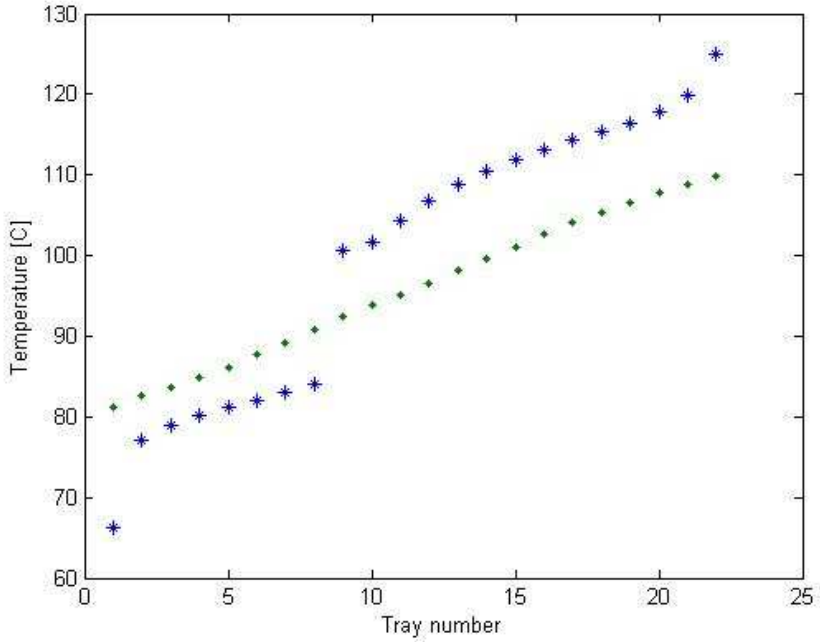

Figure C.7.2 – Temperature profile diabatic column, desorber and resorber

The minimized entropy production in the compression resorption heat pump heat pump is presented in figure C.7.3:

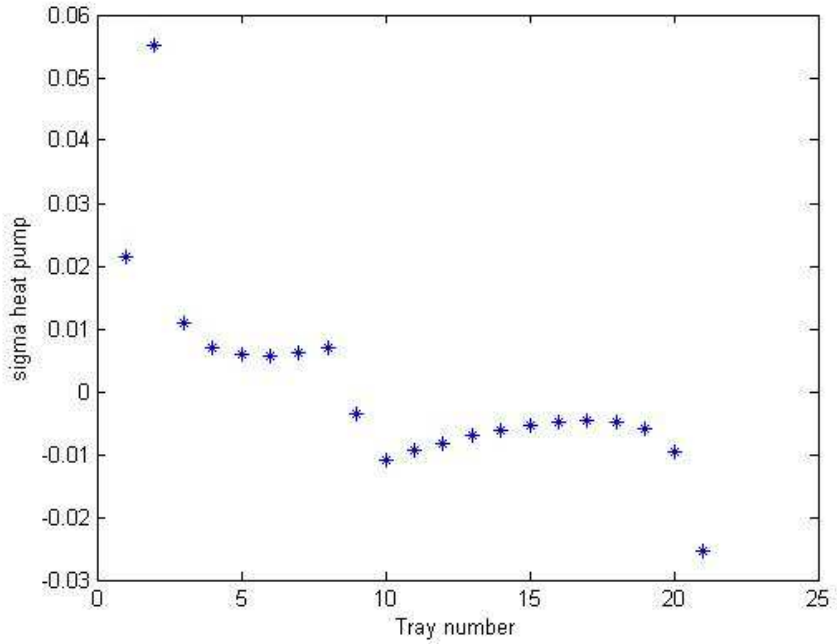

Figure C.7.3– Minimized entropy production in the compression resorption heat pump

The entropy production for the diabatic column with integrated compression resorption heat pump is 1.0104 [kW/K].

Appendix C.8 – Average ammonia concentration of 25 wt%

Thermodynamic states of the compression resorption heat pump cycle:

Table C.8.1 – Thermodynamic states of the heat pump cycle

State	Temperature [°C]	Pressure [bar]	Enthalpy [kJ/kg]	Entropy [kJ/kg K]	P_{high}/P_{low}
1	84.00031364	1.7007	707.5242	2.680969804	4.07
2s	123.9052969	6.9294	758.474	2.680968795	
2	124.8908429	6.9294	780.3095	2.735894013	
3	100.6970815	6.9294	346.95155	1.614766933	
4	66.24034762	1.7007	346.95155	1.647240874	

Using the data given in table C.8.1, a T-h diagram can be presented in figure C.8.1:

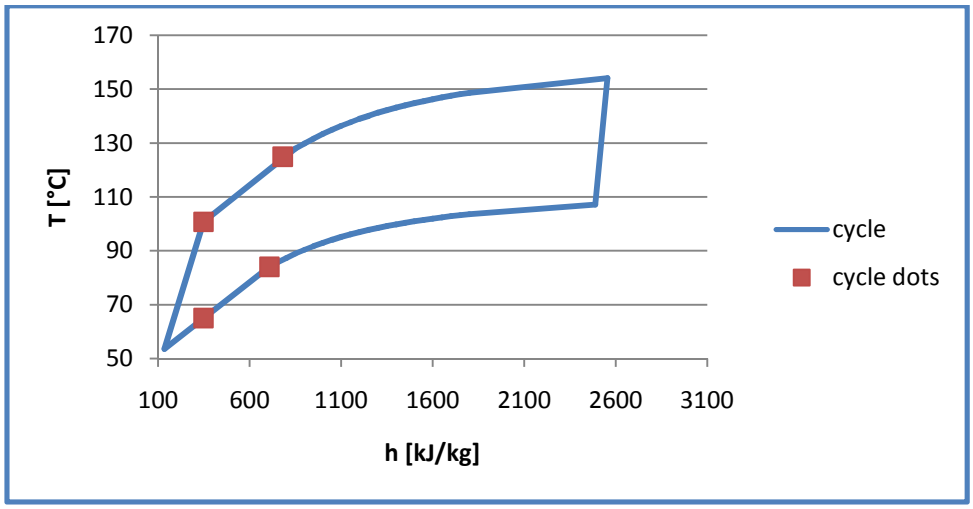

Figure C.8.1 – T-h diagram of the compression resorption heat pump

The heat loads and mass flows for the heat pump are represented in table C.8.2:

Table C.8.2 – Heat loads and mass flows compression resorption heat pump

$Q_{removed}$ [kW]	$Q_{desorber}$ [kW]	$Q_{external\_cond.}$ [kW]	$Q_{resorber}$ [kW]	W [kW]	$\dot{m}_{solution}$ [kg/s]	$\dot{m}_{air}$ [kg/s]
-40.3911	-34.0305	-6.3605	40.9	6.8694	0.0944	0.6298

The coefficient of performance (COP) for the heat pump is equal to:

$$COP = \frac{Q_{des}}{W} = 4.95$$

The temperature profile of the diabatic column (blue dots), desorber and resorber (green dots) are presented in figure C.8.2:

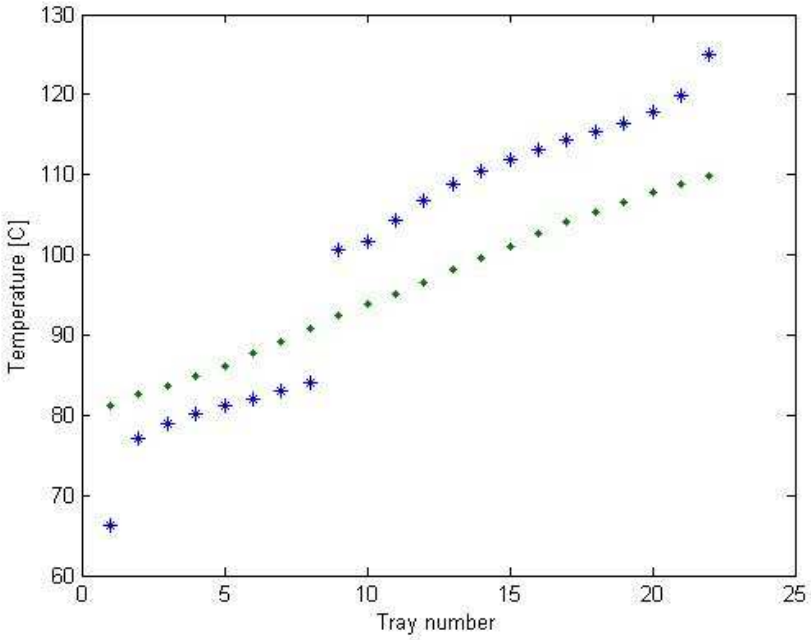

Figure C.8.2 – Temperature profile diabatic column, desorber and resorber

The minimized entropy production in the compression resorption heat pump heat pump is presented in figure C.8.3:

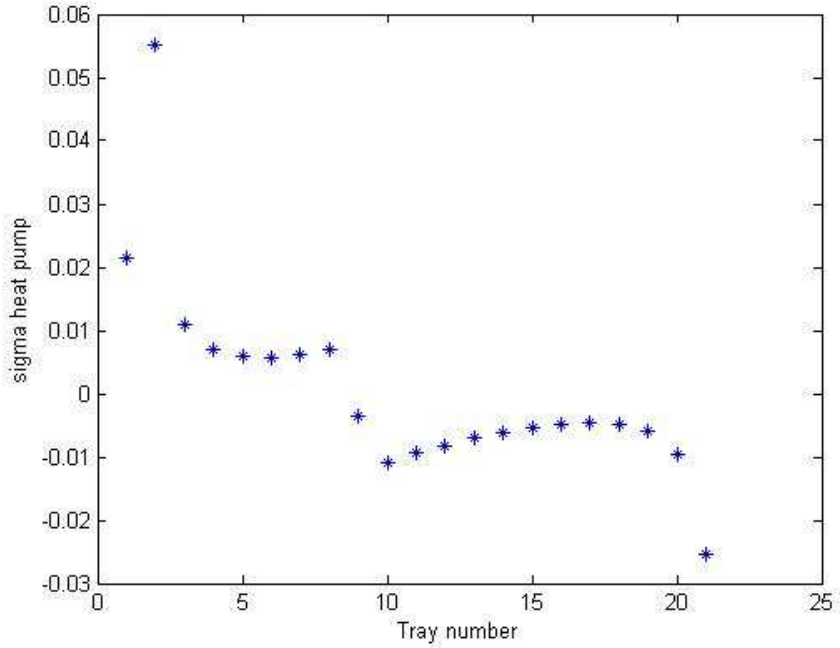

Figure C.8.3 – Minimized entropy production in the compression resorption heat pump

The entropy production for the diabatic column with integrated compression resorption heat pump is 1.0455 [kW/K].

Appendix C.9 – Average ammonia concentration of 30 wt%

Thermodynamic states of the compression resorption heat pump cycle:

Table C.9.1 – Thermodynamic states of the heat pump cycle

State	Temperature [°C]	Pressure [bar]	Enthalpy [kJ/kg]	Entropy [kJ/kg K]	P_{high}/P_{low}
1	85.14258521	2.4221	672.8277	2.642107348	3.57
2s	121.7801707	8.6448	717.5531	2.642105504	
2	122.7993243	8.6448	736.7212	2.690578202	
3	98.42369107	8.6448	334.14756	1.642297793	
4	66.242058	2.4221	334.14756	1.672122631	

Using the data given in table C.9.1, a T-h diagram can be presented in figure C.9.1:

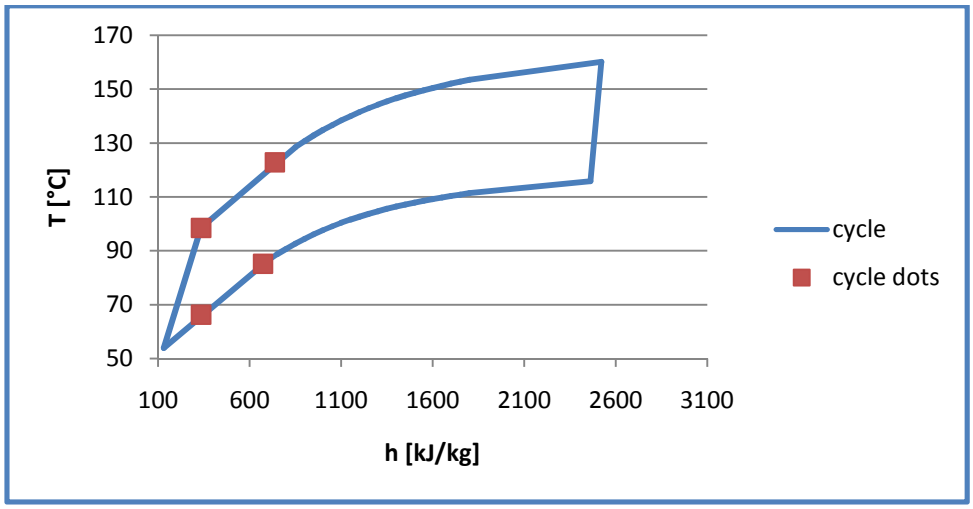

Figure C.9.1 – T-h diagram of the compression resorption heat pump

The heat loads and mass flows for the heat pump are represented in table C.9.2:

Table C.9.2 – Heat loads and mass flows compression resorption heat pump

$Q_{removed}$ [kW]	$Q_{desorber}$ [kW]	$Q_{external\_cond.}$ [kW]	$Q_{resorber}$ [kW]	W [kW]	$\dot{m}_{solution}$ [kg/s]	$\dot{m}_{air}$ [kg/s]
-40.3911	-34.4086	-5.9824	40.9	6.4913	0.1016	0.5924

The coefficient of performance (COP) for the heat pump is equal to:

$$COP = \frac{Q_{des}}{W} = 5.30$$

The temperature profile of the diabatic column (blue dots), desorber and resorber (green dots) are presented in figure C.9.2:

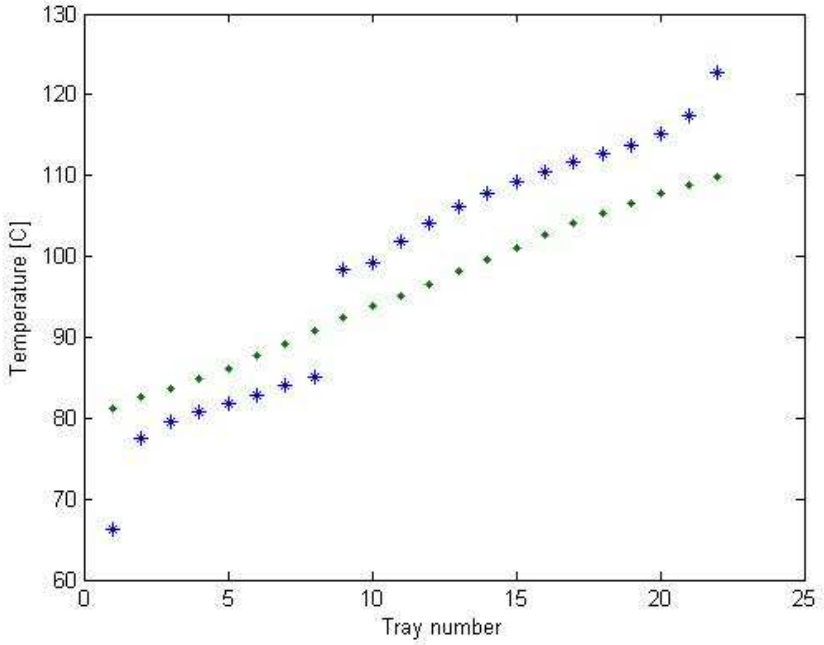

Figure C.9.2 – Temperature profile diabatic column, desorber and resorber

The minimized entropy production in the compression resorption heat pump heat pump is presented in figure C.9.3:

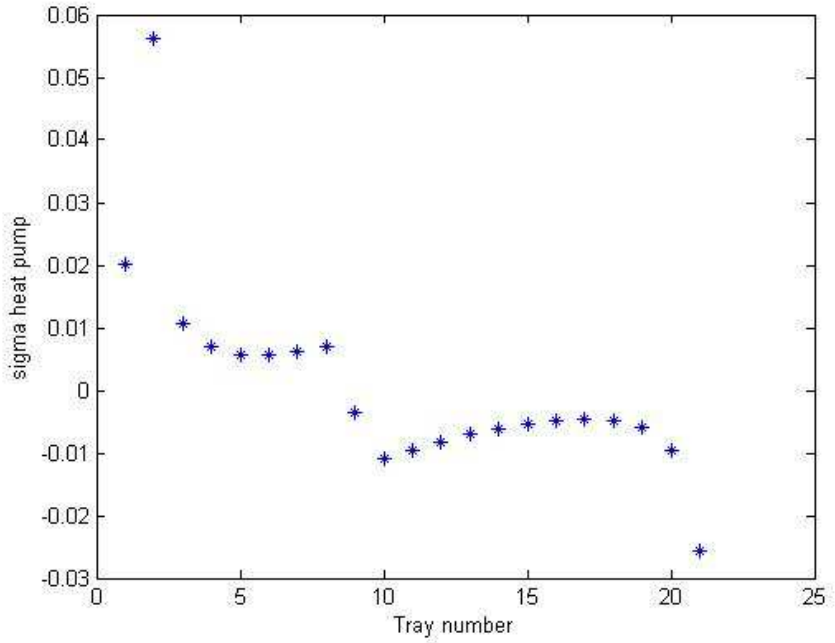

Figure C.9.3 – Minimized entropy production in the compression resorption heat pump

The entropy production for the diabatic column with integrated compression resorption heat pump is 1.074 [kW/K].

Appendix C.10 – Average ammonia concentration of 54 wt%

Thermodynamic states of the compression resorption heat pump cycle:

Table C.10.1 – Thermodynamic states of the heat pump cycle

State	Temperature [°C]	Pressure [bar]	Enthalpy [kJ/kg]	Entropy [kJ/kg K]	P_{high}/P_{low}
1	80.84921116	11.231	553.0153	2.452844155	2.66
2s	114.9954433	29.8213	577.759	2.45284456	
2	115.633321	29.8213	588.3635	2.480143093	
3	107.4873261	29.8213	443.36116	2.103111986	
4	74.16735445	11.231	443.36116	2.140073325	

Using the data given in table C.10.1, a T-h diagram can be presented in figure C.10.1:

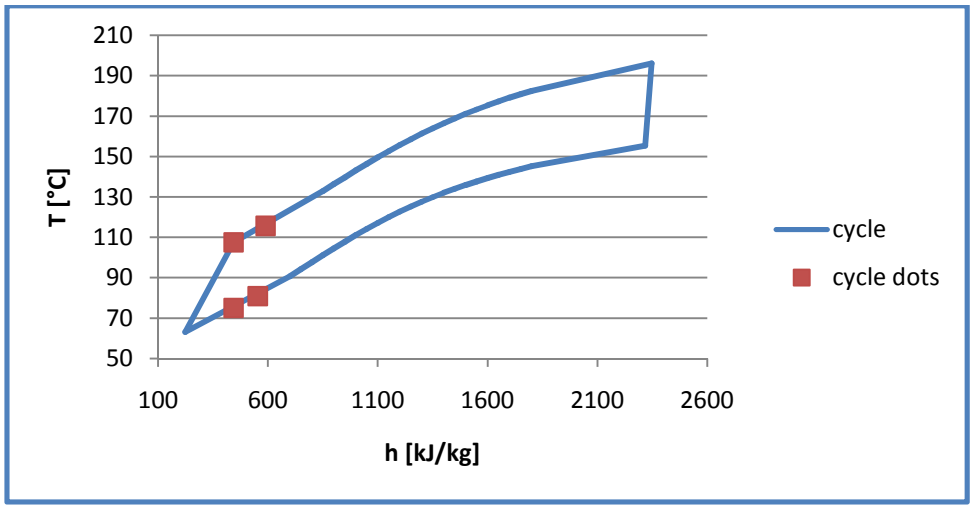

Figure C.10.1 – T-h diagram of the compression resorption heat pump

The heat loads and mass flows for the heat pump are represented in table C.10.2:

Table C.10.2 – Heat loads and mass flows compression resorption heat pump

$Q_{removed}$ [kW]	$Q_{desorber}$ [kW]	$Q_{external\_cond.}$ [kW]	$Q_{resorber}$ [kW]	W [kW]	$\dot{m}_{solution}$ [kg/s]	$\dot{m}_{air}$ [kg/s]
-40.3911	-30.9295	-9.4615	40.9	9.9704	0.2821	0.9368

The coefficient of performance (COP) for the heat pump is equal to:

$$COP = \frac{Q_{des}}{W} = 3.10$$

The temperature profile of the diabatic column (blue dots), desorber and resorber (green dots) are presented in figure C.10.2:

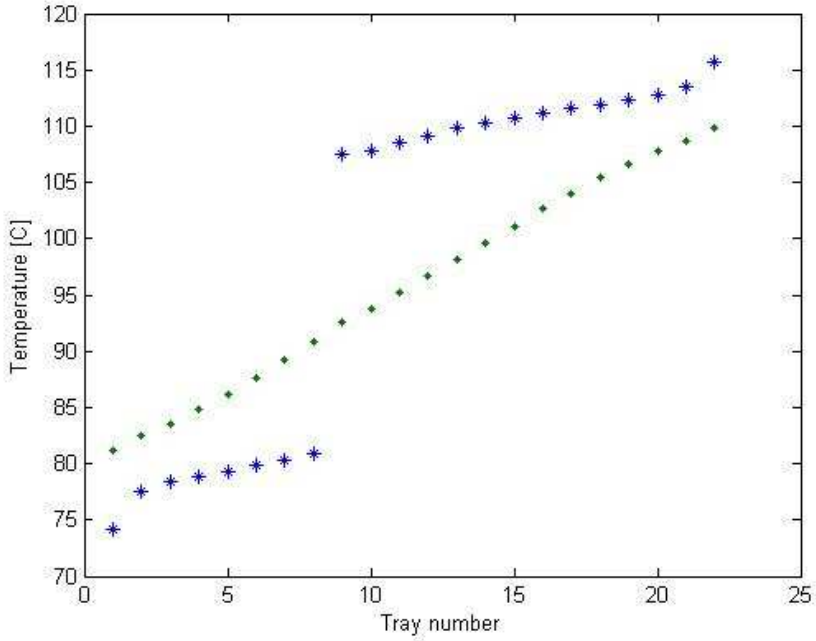

Figure C.10.2 – Temperature profile diabatic column, desorber and resorber

The minimized entropy production in the compression resorption heat pump heat pump is presented in figure C.10.3:

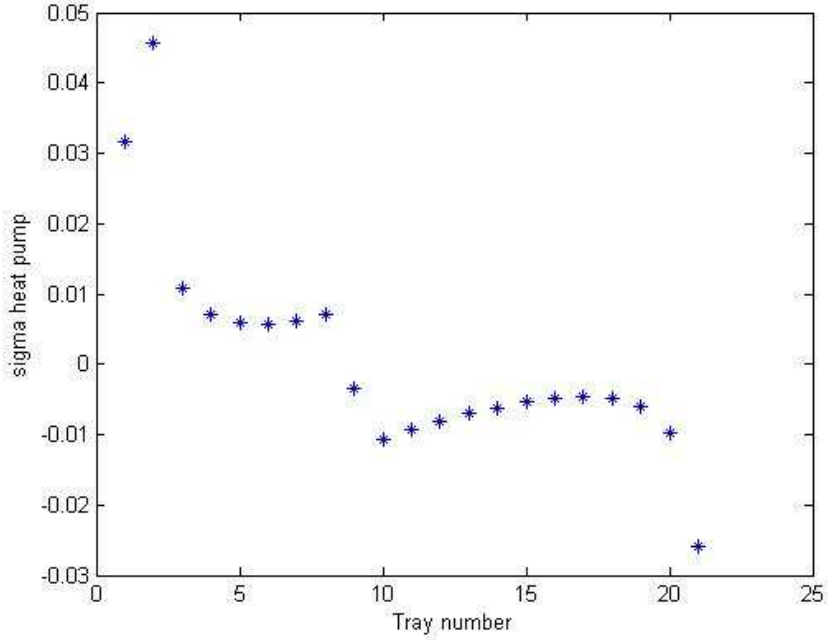

Figure C.10.3 – Minimized entropy production in the compression resorption heat pump

The entropy production for the diabatic column with integrated compression resorption heat pump is 1.1649 [kW/K].

Appendix C.11 – Average ammonia concentration of 55 wt%

Thermodynamic states of the compression resorption heat pump cycle:

Table C.11.1 – Thermodynamic states of the heat pump cycle

State	Temperature [°C]	Pressure [bar]	Enthalpy [kJ/kg]	Entropy [kJ/kg K]	P_{high}/P_{low}
1	82.25609327	11.3032	599.2506	2.589136087	2.62
2s	116.1075934	29.6152	628.5213	2.58913588	
2	116.8870296	29.6152	641.066	2.621330897	
3	105.4272575	29.6152	438.46276	2.093813455	
4	72.41338223	11.3032	438.46276	2.130183264	

Using the data given in table C.11.1, a T-h diagram can be presented in figure C.11.1:

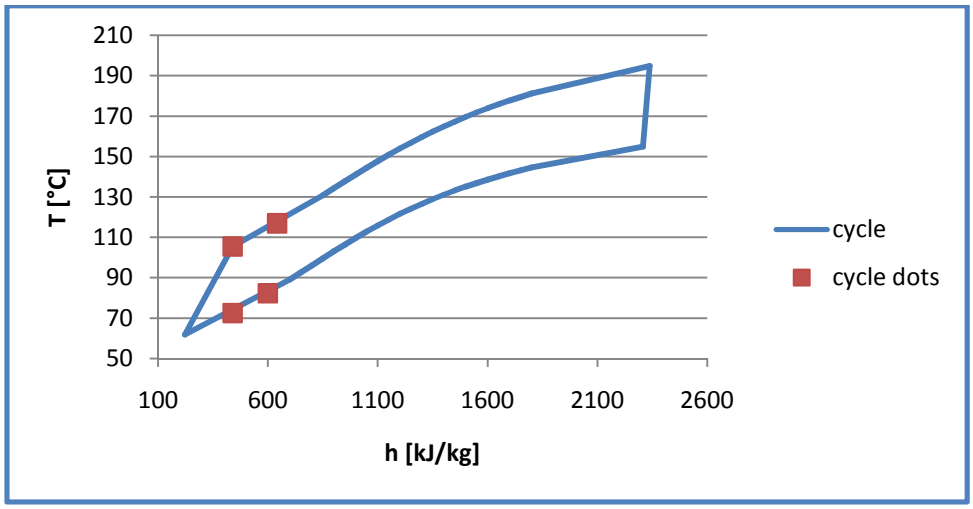

Figure C.11.1 – T-h diagram of the compression resorption heat pump

The heat loads and mass flows for the heat pump are represented in table C.11.2:

Table C.11.2 – Heat loads and mass flows compression resorption heat pump

$Q_{removed}$ [kW]	$Q_{desorber}$ [kW]	$Q_{external\_cond.}$ [kW]	$Q_{resorber}$ [kW]	W [kW]	$\dot{m}_{solution}$ [kg/s]	$\dot{m}_{air}$ [kg/s]
-40.3911	-32.4586	-7.9325	40.9	8.4414	0.2019	0.7854

The coefficient of performance (COP) for the heat pump is equal to:

$$COP = \frac{Q_{des}}{W} = 3.85$$

The temperature profile of the diabatic column (blue dots), desorber and resorber (green dots) are presented in figure C.11.2:

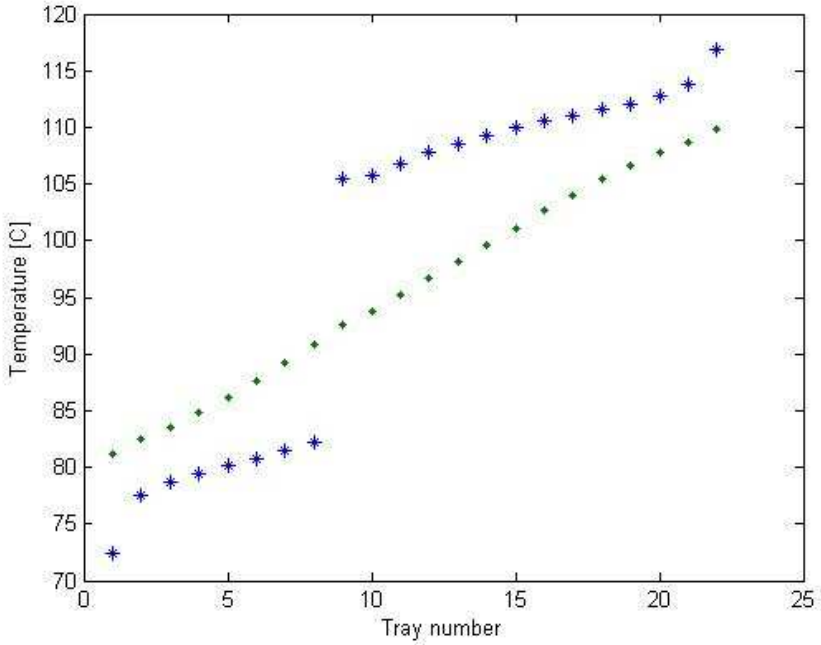

Figure C.11.2 – Temperature profile diabatic column, desorber and resorber

The minimized entropy production in the compression resorption heat pump heat pump is presented in figure C.11.3:

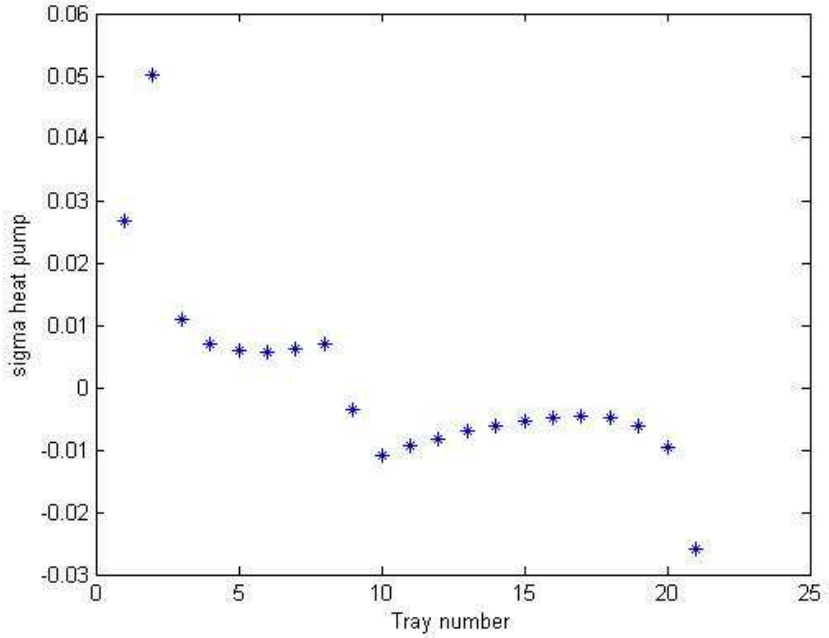

Figure C.11.3– Minimized entropy production in the compression resorption heat pump

The entropy production for the diabatic column with integrated compression resorption heat pump is 1.1661[kW/K].

Appendix C.12 – Average ammonia concentration of 60 wt%

Thermodynamic states of the compression resorption heat pump cycle:

Table C.12.1 – Thermodynamic states of the heat pump cycle

State	Temperature [°C]	Pressure [bar]	Enthalpy [kJ/kg]	Entropy [kJ/kg K]	P_{high}/P_{low}
1	85.87169244	11.8287	768.9314	3.093035799	2.73
2s	122.6059256	32.2978	818.0015	3.093035561	
2	124.0236415	32.2978	839.0316	3.146079863	
3	102.1643383	32.2978	452.91859	2.144027253	
4	66.33658487	11.8287	452.91859	2.186567515	

Using the data given in table C.12.1, a T-h diagram can be presented in figure C.12.1:

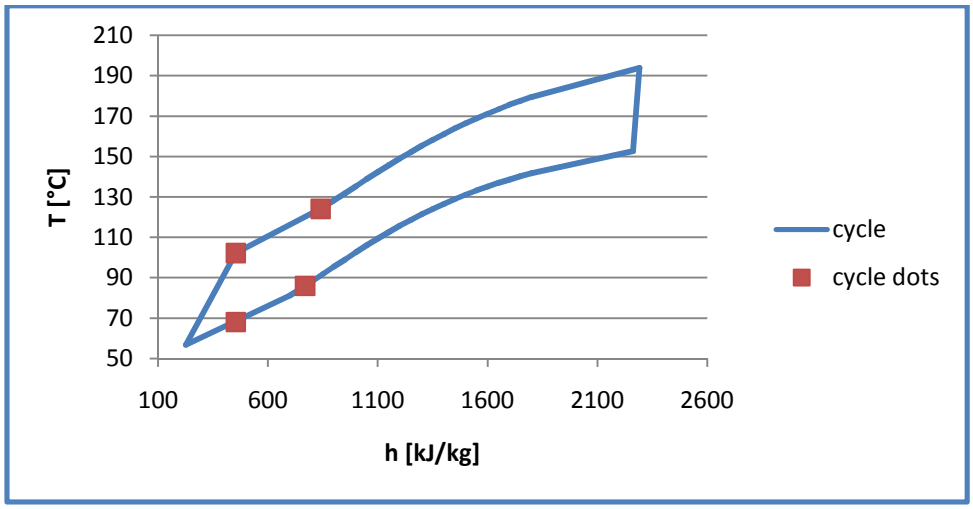

Figure C.12.1– T-h diagram of the compression resorption heat pump

The heat loads and mass flows for the heat pump are represented in table C.12.2:

Table C.12.2 – Heat loads and mass flows compression resorption heat pump

$Q_{removed}$ [kW]	$Q_{desorber}$ [kW]	$Q_{external\_cond.}$ [kW]	$Q_{resorber}$ [kW]	W [kW]	$\dot{m}_{solution}$ [kg/s]	$\dot{m}_{air}$ [kg/s]
-40.3911	-33.4744	-6.9166	40.9	7.4255	0.1059	0.6849

The coefficient of performance (COP) for the heat pump is equal to:

$$COP = \frac{Q_{des}}{W} = 4.51$$

The temperature profile of the diabatic column (blue dots), desorber and resorber (green dots) are presented in figure C.12.2:

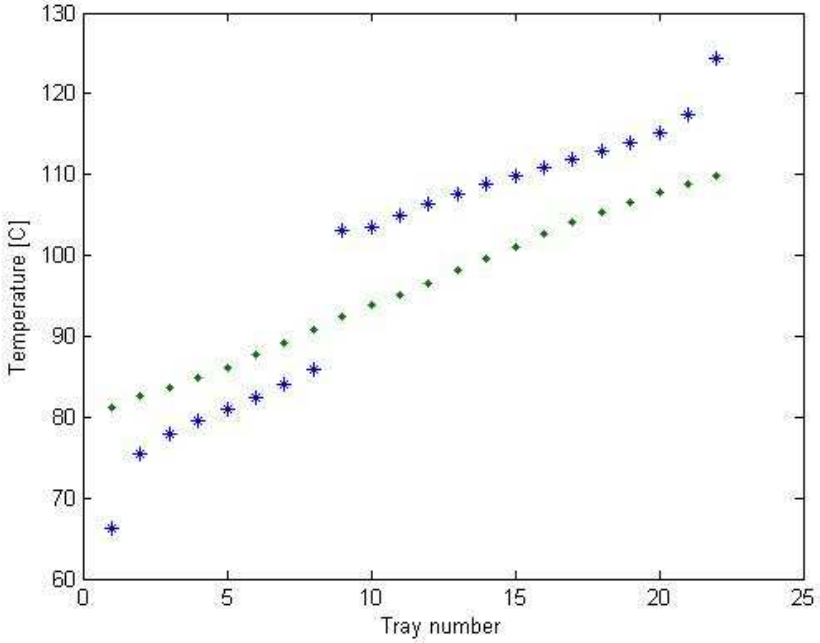

Figure C.12.2 – Temperature profile diabatic column, desorber and resorber

The minimized entropy production in the compression resorption heat pump heat pump is presented in figure C.12.3:

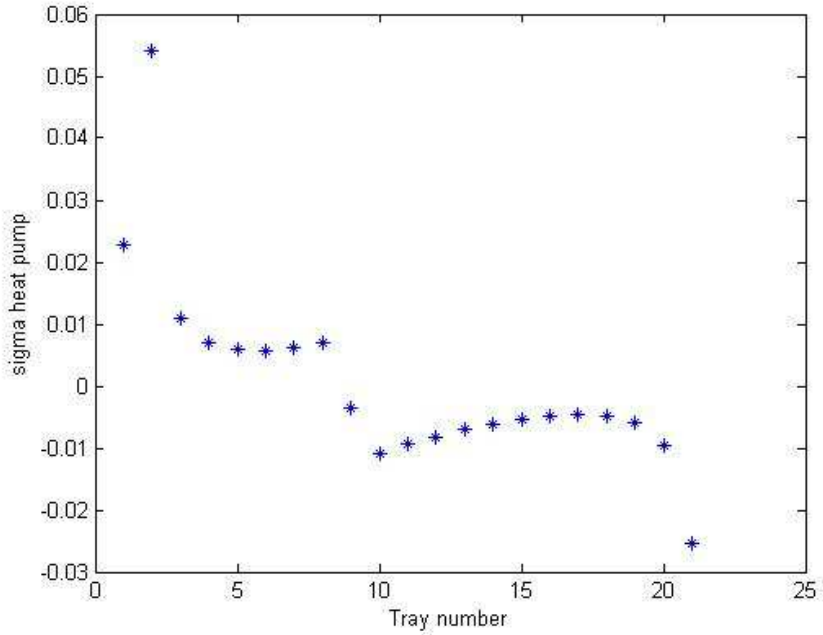

Figure C.12.3 – Minimized entropy production in the compression resorption heat pump

The entropy production for the diabatic column with integrated compression resorption heat pump is 1.1736 [kW/K].

Appendix C.13 – Average ammonia concentration of 65 wt%

Thermodynamic states of the compression resorption heat pump cycle:

Table C.13.1 – Thermodynamic states of the heat pump cycle

State	Temperature [°C]	Pressure [bar]	Enthalpy [kJ/kg]	Entropy [kJ/kg K]	P_{high}/P_{low}
1	85.86502185	14.361	826.375	3.254872917	2.57
2s	122.3168782	36.9136	877.6187	3.254872467	
2	123.7723288	36.9136	899.5803	3.310304158	
3	102.4736081	36.9136	491.01155	2.249363543	
4	66.41126802	14.361	491.01155	2.292357166	

Using the data given in table C.13.1, a T-h diagram can be presented in figure C.13.1:

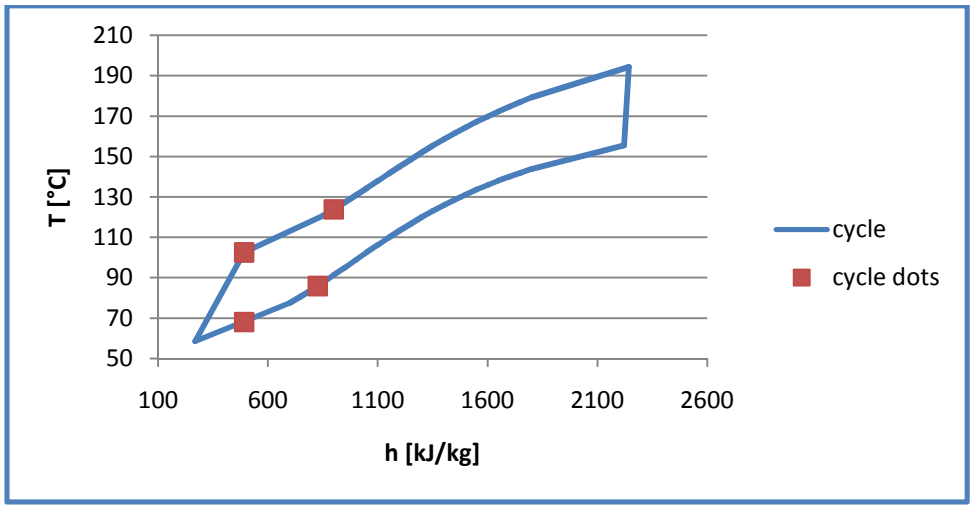

Figure C.13.1 – T-h diagram of the compression resorption heat pump

The heat loads and mass flows for the heat pump are represented in table C.13.2:

Table C.13.2 – Heat loads and mass flows compression resorption heat pump

$Q_{removed}$ [kW]	$Q_{desorber}$ [kW]	$Q_{external\_cond.}$ [kW]	$Q_{resorber}$ [kW]	W [kW]	$\dot{m}_{solution}$ [kg/s]	$\dot{m}_{air}$ [kg/s]
-40.3911	-33.5717	-6.8194	40.9	7.3283	0.0993	0.6752

The coefficient of performance (COP) for the heat pump is equal to:

$$COP = \frac{Q_{des}}{W} = 4.58$$

The temperature profile of the diabatic column (blue dots), desorber and resorber (green dots) are presented in figure C.13.2:

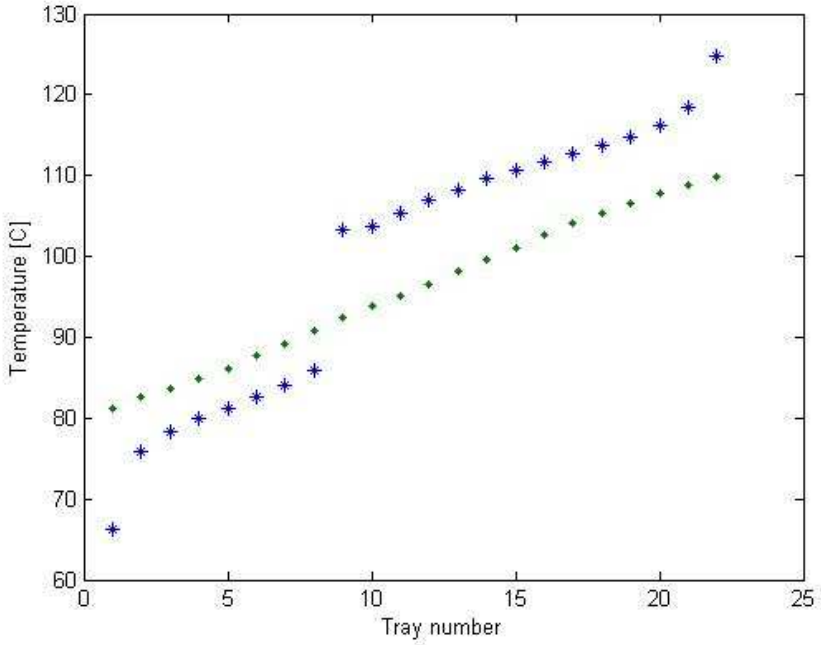

Figure C.13.2– Temperature profile diabatic column, desorber and resorber

The minimized entropy production in the compression resorption heat pump heat pump is presented in figure C.13.3:

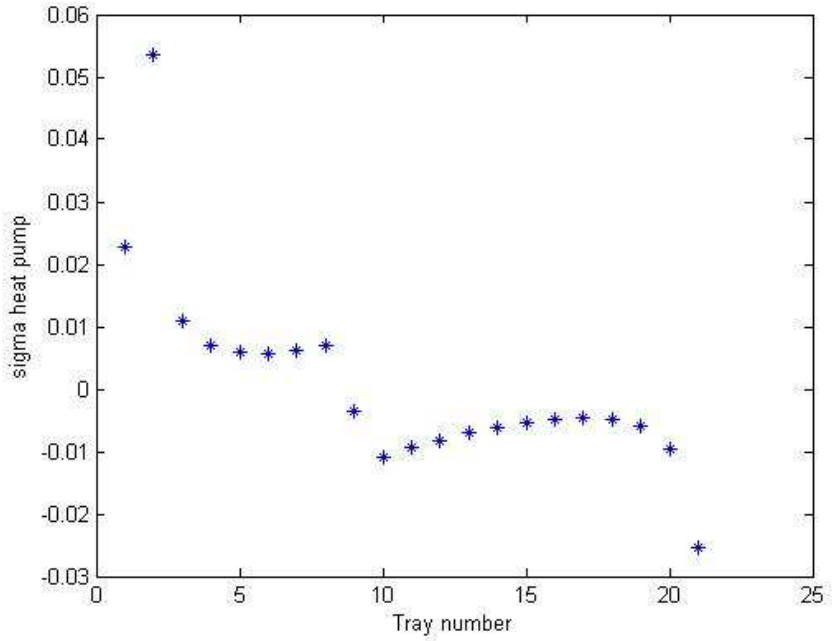

Figure C.13.3 – Minimized entropy production in the compression resorption heat pump

The entropy production for the diabatic column with integrated compression resorption heat pump is 1.1748 [kW/K].

Appendix C.14 – Average ammonia concentration of 70 wt%

Thermodynamic states of the compression resorption heat pump cycle:

Table C.14.1 – Thermodynamic states of the heat pump cycle

State	Temperature [°C]	Pressure [bar]	Enthalpy [kJ/kg]	Entropy [kJ/kg K]	P_{high}/P_{low}
1	85.87177189	16.8318	903.082	3.465761878	2.47
2s	122.7504983	41.5728	958.8938	3.46576173	
2	124.3180688	41.5728	982.8131	3.526060401	
3	103.03122	41.5728	535.55177	2.365266118	
4	66.24275684	16.8318	535.55177	2.409698281	

Using the data given in table C.14.1, a T-h diagram can be presented in figure C.14.1:

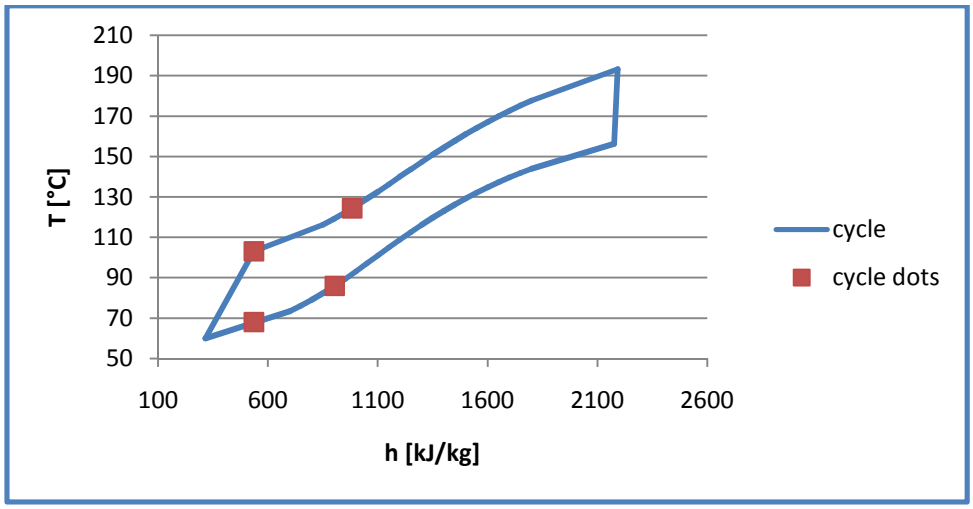

Figure C.14.1 – T-h diagram of the compression resorption heat pump

The heat loads and mass flows for the heat pump are represented in table C.14.2:

Table C.14.2 – Heat loads and mass flows compression resorption heat pump

$Q_{removed}$ [kW]	$Q_{desorber}$ [kW]	$Q_{external\_cond.}$ [kW]	$Q_{resorber}$ [kW]	W [kW]	$\dot{m}_{solution}$ [kg/s]	$\dot{m}_{air}$ [kg/s]
-40.3911	-33.609	-6.7821	40.9	7.291	0.0914	0.6715

The coefficient of performance (COP) for the heat pump is equal to:

$$COP = \frac{Q_{des}}{W} = 4.61$$

The temperature profile of the diabatic column (blue dots), desorber and resorber (green dots) are presented in figure C.14.2:

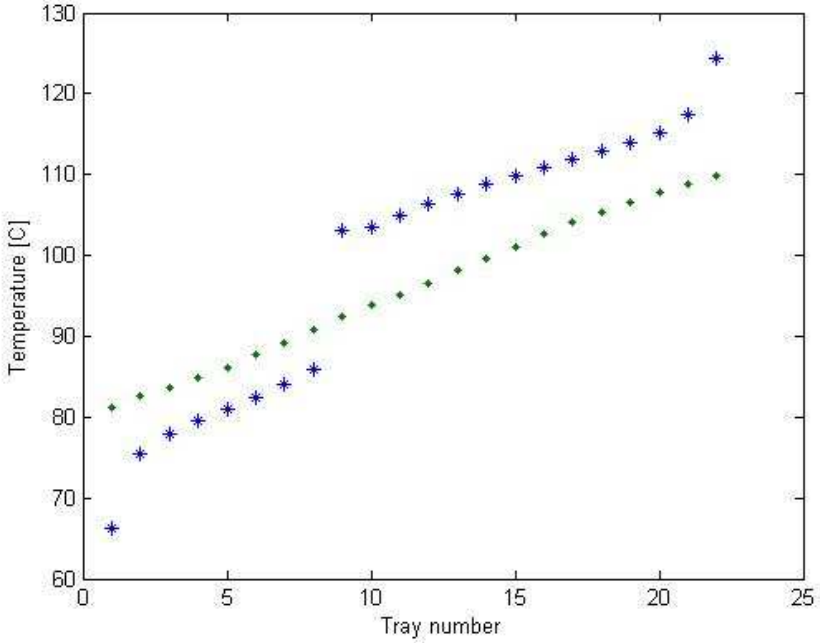

Figure C.14.2 – Temperature profile diabatic column, desorber and resorber

The minimized entropy production in the compression resorption heat pump heat pump is presented in figure C.14.3:

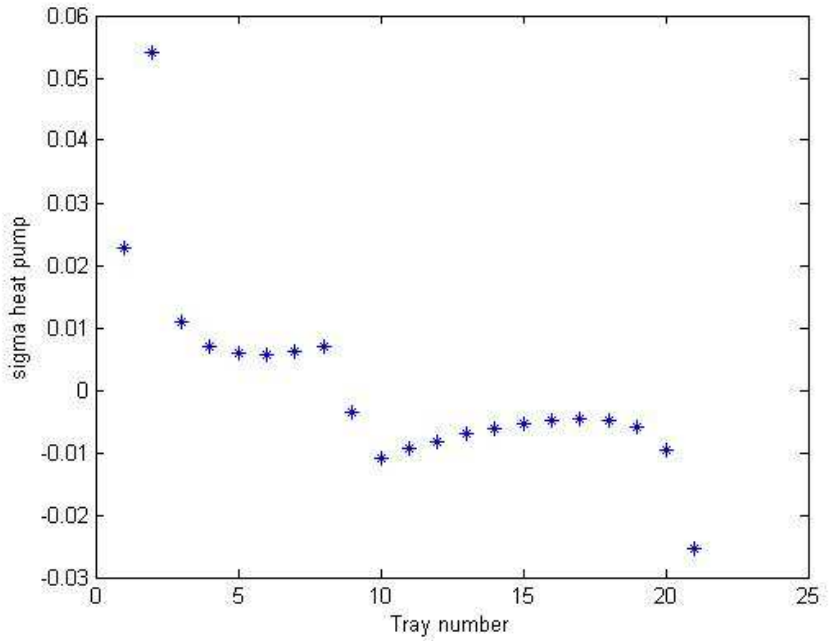

Figure C.14.3 – Minimized entropy production in the compression resorption heat pump

The entropy production for the diabatic column with integrated compression resorption heat pump is 1.1684 [kW/K].

Appendix C.15 – Average ammonia concentration of 75 wt%

Thermodynamic states of the compression resorption heat pump cycle:

Table C.15.1 – Thermodynamic states of the heat pump cycle

State	Temperature [°C]	Pressure [bar]	Enthalpy [kJ/kg]	Entropy [kJ/kg K]	P_{high}/P_{low}
1	85.87051011	20.2942	970.2	3.634191748	2.22
2s	120.2847248	45.0061	1023.9	3.634316998	
2	121.7285645	45.0061	1046.9	3.692670132	
3	102.2641357	45.0061	577.6751	2.468914966	
4	67.90874341	20.2942	577.6751	2.508187008	

Using the data given in table C.15.1, a T-h diagram can be presented in figure C.15.1:

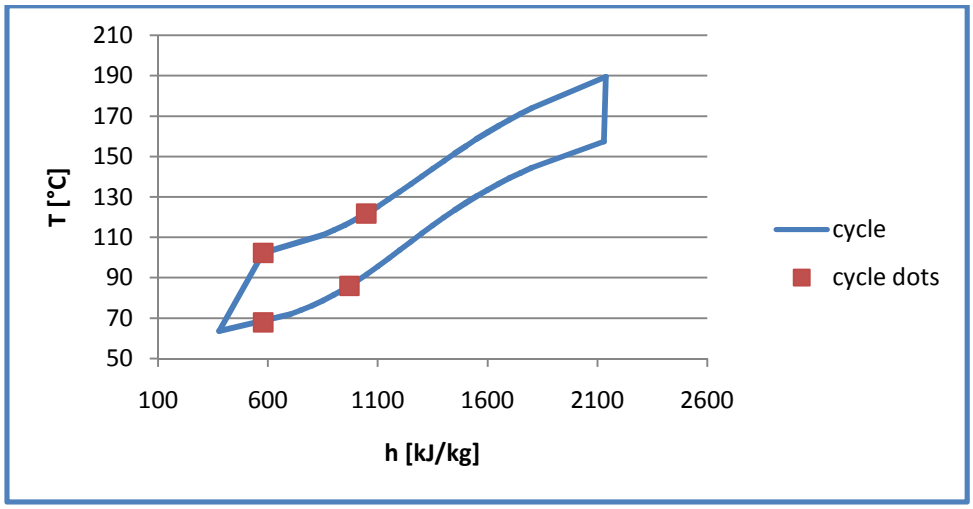

Figure C.15.1 – T-h diagram of the compression resorption heat pump

The heat loads and mass flows for the heat pump are represented in table C.15.2:

Table C.15.2 – Heat loads and mass flows compression resorption heat pump

$Q_{removed}$ [kW]	$Q_{desorber}$ [kW]	$Q_{external\_cond.}$ [kW]	$Q_{resorber}$ [kW]	W [kW]	$\dot{m}_{solution}$ [kg/s]	$\dot{m}_{air}$ [kg/s]
-40.3911	-34.2186	-6.1725	40.9	6.6814	0.0872	0.6112

The coefficient of performance (COP) for the heat pump is equal to:

$$COP = \frac{Q_{des}}{W} = 5.12$$

The temperature profile of the diabatic column (blue dots), desorber and resorber (green dots) are presented in figure C.15.2:

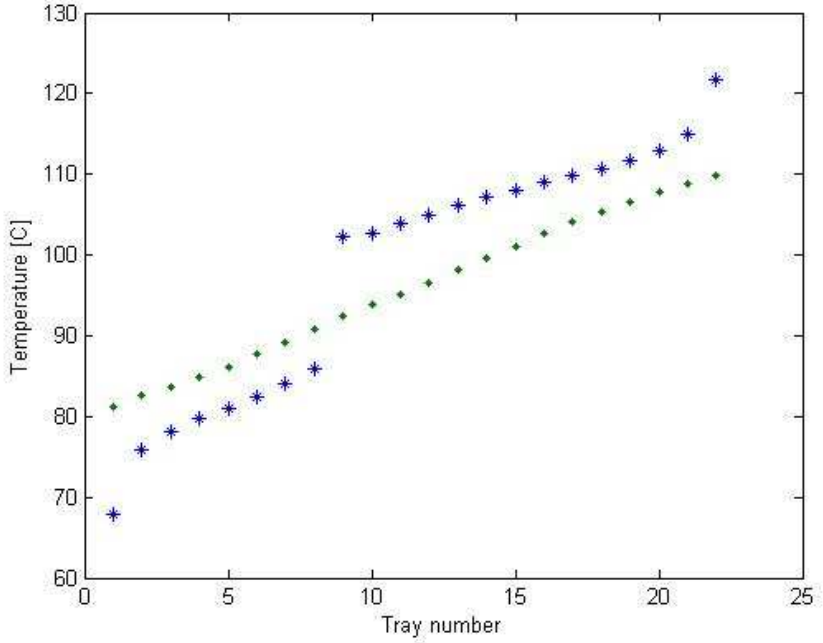

Figure C.15.2 – Temperature profile diabatic column, desorber and resorber

The minimized entropy production in the compression resorption heat pump heat pump is presented in figure C.15.3:

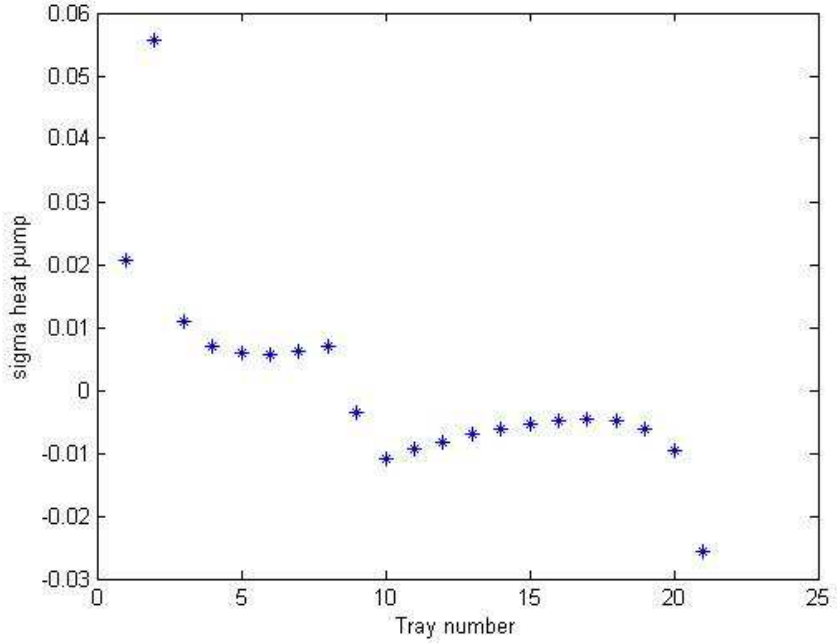

Figure C.15.3 – Minimized entropy production in the compression resorption heat pump

The entropy production for the diabatic column with integrated compression resorption heat pump is 1.1496 [kW/K].

Appendix C.16 – Average ammonia concentration of 80 wt%

Thermodynamic states of the compression resorption heat pump cycle:

Table C.16.1 – Thermodynamic states of the heat pump cycle

State	Temperature [°C]	Pressure [bar]	Enthalpy [kJ/kg]	Entropy [kJ/kg K]	P_{high}/P_{low}
1	83.63086193	25.2742	975.6	3.612174793	2.07
2s	117.3917061	52.216	1021.5	3.612188317	
2	118.3454056	52.216	1041.2	3.662570062	
3	105.9861595	52.216	648.31813	2.640165451	
4	72.67133791	25.2742	648.31813	2.678203458	

Using the data given in table C.16.1, a T-h diagram can be presented in figure C.16.1:

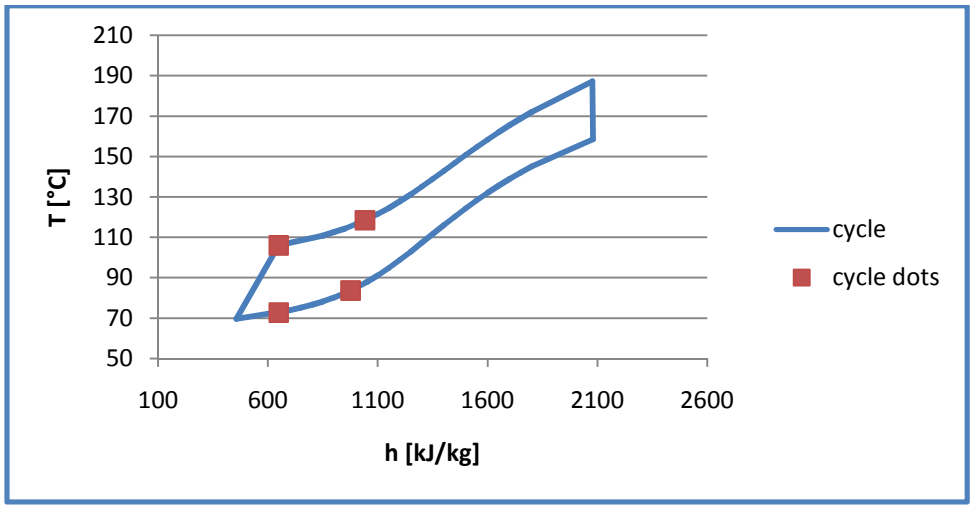

Figure C.16.1 – T-h diagram of the compression resorption heat pump

The heat loads and mass flows for the heat pump are represented in table C.16.2:

Table C.16.2 – Heat loads and mass flows compression resorption heat pump

$Q_{removed}$ [kW]	$Q_{desorber}$ [kW]	$Q_{external\_cond.}$ [kW]	$Q_{resorber}$ [kW]	W [kW]	$\dot{m}_{solution}$ [kg/s]	$\dot{m}_{air}$ [kg/s]
-40.3911	-34.074	-6.317	40.9	6.8259	0.1041	0.6255

The coefficient of performance (COP) for the heat pump is equal to:

$$COP = \frac{Q_{des}}{W} = 4.99$$

The temperature profile of the diabatic column (blue dots), desorber and resorber (green dots) are presented in figure C.16.2:

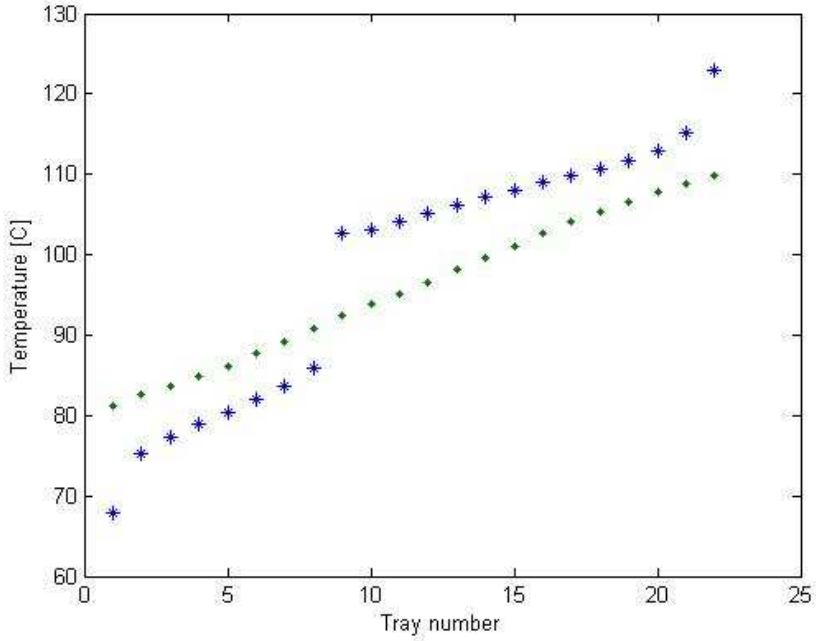

Figure C.16.2 – Temperature profile diabatic column, desorber and resorber

The minimized entropy production in the compression resorption heat pump heat pump is presented in figure C.16.3:

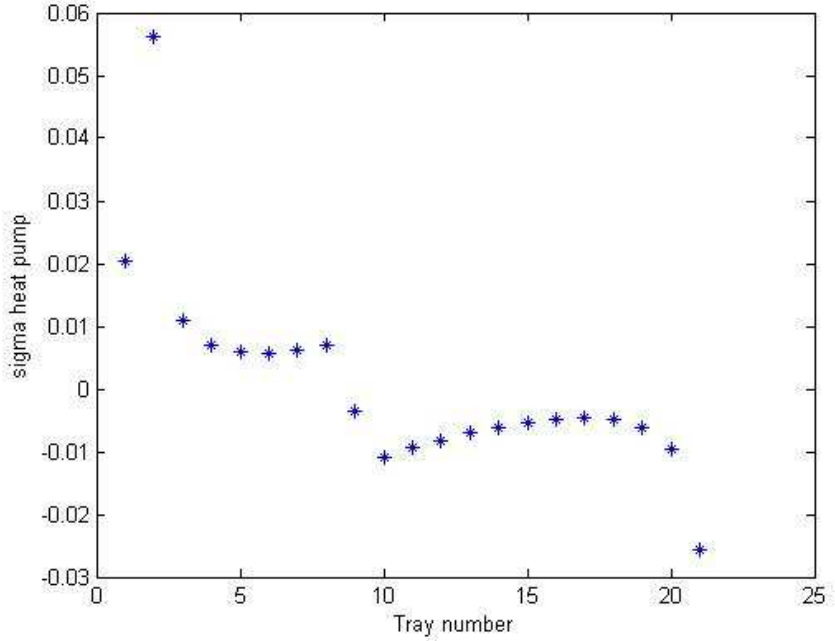

Figure C.16.3 – Minimized entropy production in the compression resorption heat pump

The entropy production for the diabatic column with integrated compression resorption heat pump is 1.1153 [kW/K].

Appendix C.17 – Average ammonia concentration of 85 wt%

Thermodynamic states of the compression resorption heat pump cycle:

Table C.17.1 – Thermodynamic states of the heat pump cycle

State	Temperature [°C]	Pressure [bar]	Enthalpy [kJ/kg]	Entropy [kJ/kg K]	P_{high}/P_{low}
1	85.87586143	24.7799	1212.3	4.277847936	2.15
2s	122.7894141	53.3579	1283.1	4.277679695	
2	124.8847944	53.3579	1313.5	4.354258749	
3	103.0608367	53.3579	686.6057	2.721603864	
4	67.66866914	24.7799	686.6057	2.764218349	

Using the data given in table C.17.1, a T-h diagram can be presented in figure C.17.1:

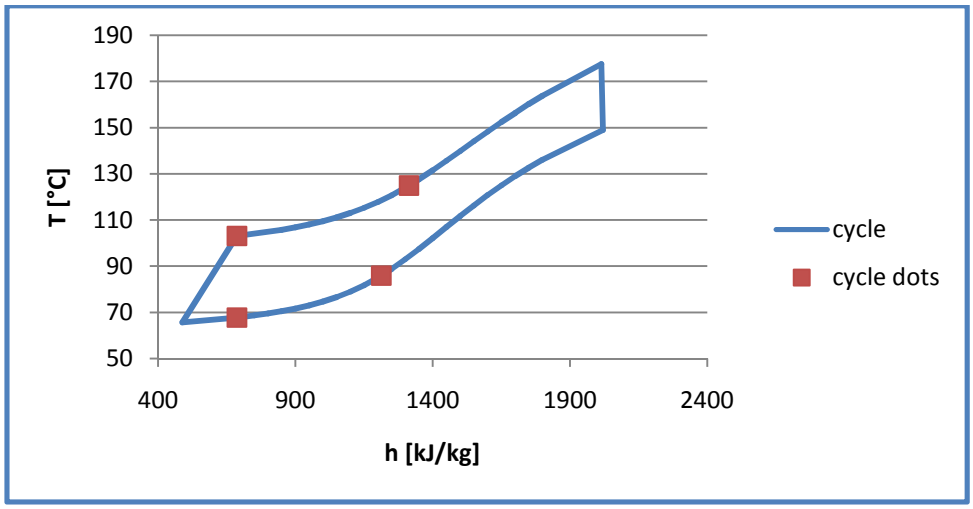

Figure C.17.1 – T-h diagram of the compression resorption heat pump

The heat loads and mass flows for the heat pump are represented in table C.17.2:

Table C.17.2 – Heat loads and mass flows compression resorption heat pump

$Q_{removed}$ [kW]	$Q_{desorber}$ [kW]	$Q_{external\_cond.}$ [kW]	$Q_{resorber}$ [kW]	W [kW]	$\dot{m}_{solution}$ [kg/s]	$\dot{m}_{air}$ [kg/s]
-40.3908	-34.295	-6.0958	40.9	6.6047	0.0652	0.6036

The coefficient of performance (COP) for the heat pump is equal to:

$$COP = \frac{Q_{des}}{W} = 5.19$$

The temperature profile of the diabatic column (blue dots), desorber and resorber (green dots) are presented in figure C.17.2:

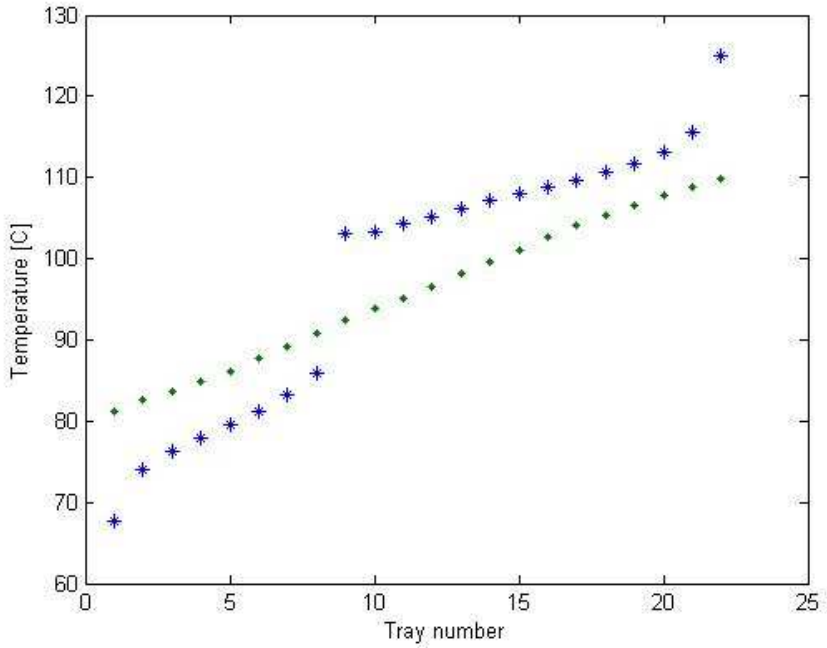

Figure C.17.2 – Temperature profile diabatic column, desorber and resorber

The minimized entropy production in the compression resorption heat pump heat pump is presented in figure C.17.3:

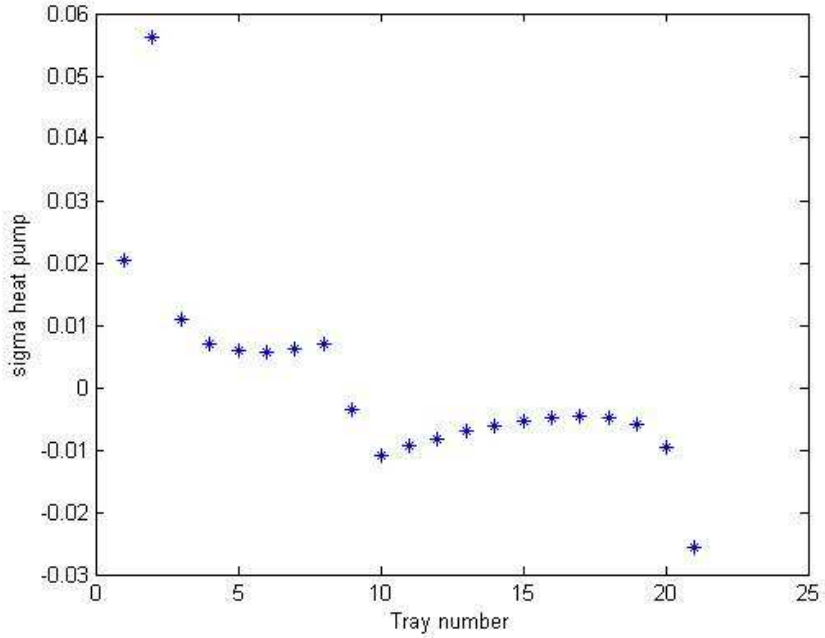

Figure C.17.3 – Minimized entropy production in the compression resorption heat pump

The entropy production for the diabatic column with integrated compression resorption heat pump is 1.0507 [kW/K].

Appendix C.18 – Average ammonia concentration of 90 wt%

Thermodynamic states of the compression resorption heat pump cycle:

Table C.18.1 – Thermodynamic states of the heat pump cycle

State	Temperature [°C]	Pressure [bar]	Enthalpy [kJ/kg]	Entropy [kJ/kg K]	P_{high}/P_{low}
1	85.87371398	29.2518	1315	4.516349948	2.02
2	122.1583705	59.1982	1386	4.516351372	
2s	124.2243637	59.1982	1416.4	4.593056036	
3	104.9566447	59.1982	756.23871	2.875754306	
4	71.36092013	29.2518	756.23871	2.916643553	

Using the data given in table C.18.1, a T-h diagram can be presented in figure C.18.1:

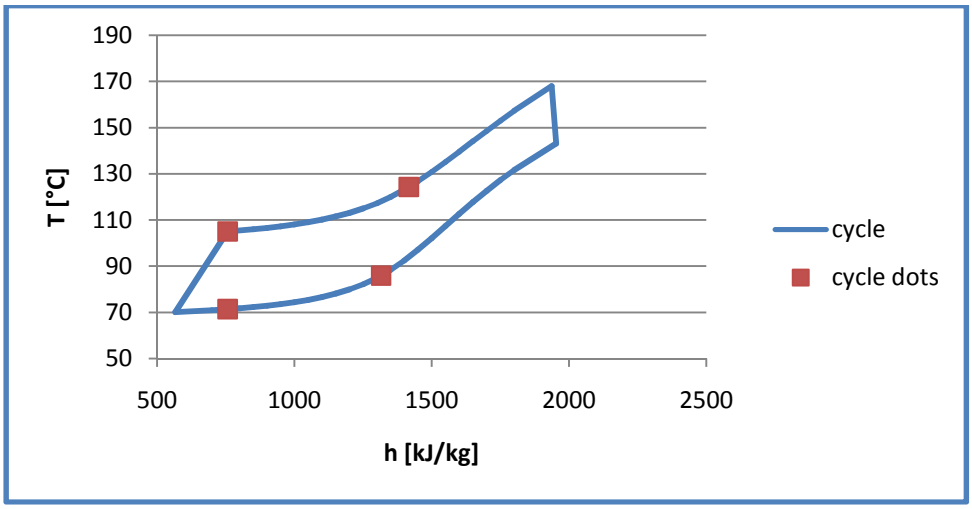

Figure C.18.1 – T-h diagram of the compression resorption heat pump

The heat loads and mass flows for the heat pump are represented in table C.18.2:

Table C.18.2 – Heat loads and mass flows compression resorption heat pump

$Q_{removed}$ [kW]	$Q_{desorber}$ [kW]	$Q_{external\_cond.}$ [kW]	$Q_{resorber}$ [kW]	W [kW]	$\dot{m}_{solution}$ [kg/s]	$\dot{m}_{air}$ [kg/s]
-40.3908	-34.616	-5.7747	40.9	6.2836	0.062	0.5718

The coefficient of performance (COP) for the heat pump is equal to:

$$COP = \frac{Q_{des}}{W} = 5.51$$

The temperature profile of the diabatic column (blue dots), desorber and resorber (green dots) are presented in figure C.18.2:

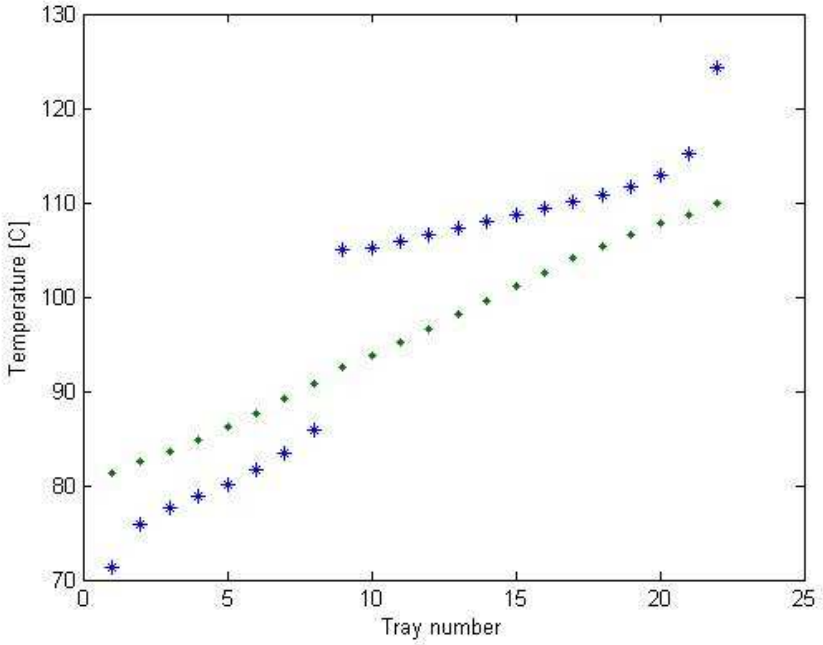

Figure C.18.2 – Temperature profile diabatic column, desorber and resorber

The minimized entropy production in the compression resorption heat pump heat pump is presented in figure C.18.3:

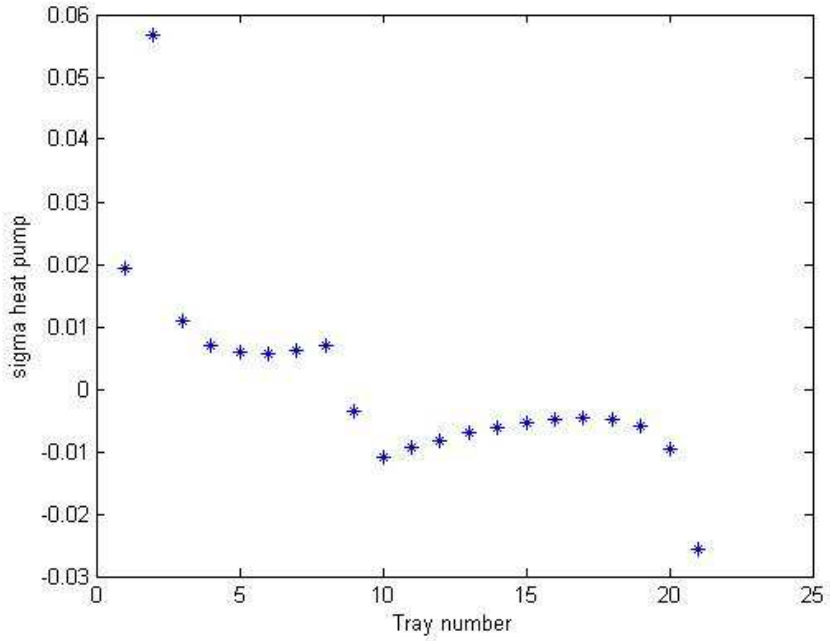

Figure C.18.3 – Minimized entropy production in the compression resorption heat pump

The entropy production for the diabatic column with integrated compression resorption heat pump is 0.9475 [kW/K].

Appendix C.19 – Average ammonia concentration of 95 wt%

Thermodynamic states of the compression resorption heat pump cycle:

Table C.19.1 – Thermodynamic states of the heat pump cycle

State	Temperature [°C]	Pressure [bar]	Enthalpy [kJ/kg]	Entropy [kJ/kg K]	P_{high}/P_{low}
1	85.5787486	33.979	1444	4.818416121	1.94
2s	122.1838422	65.993	1518.3	4.818556401	
2	124.5202634	65.993	1550.1	4.898761349	
3	107.0576179	65.993	834.56973	3.040688991	
4	74.70531636	33.979	834.56973	3.082185833	

Using the data given in table C.19.1, a T-h diagram can be presented in figure C.19.1:

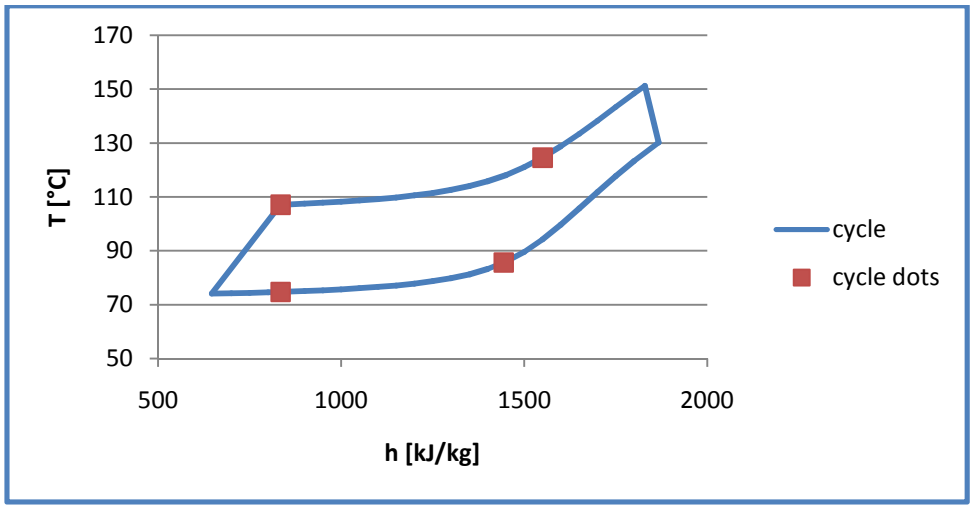

Figure C.19.1 – T-h diagram of the compression resorption heat pump

The heat loads and mass flows for the heat pump are represented in table C.19.2:

Table C.19.2 – Heat loads and mass flows compression resorption heat pump

$Q_{removed}$ [kW]	$Q_{desorber}$ [kW]	$Q_{external\_cond.}$ [kW]	$Q_{resorber}$ [kW]	W [kW]	$\dot{m}_{solution}$ [kg/s]	$\dot{m}_{air}$ [kg/s]
-40.3908	-34.8368	-5.5539	40.9	6.0628	0.0572	0.5499

The coefficient of performance (COP) for the heat pump is equal to:

$$COP = \frac{Q_{des}}{W} = 5.75$$

The temperature profile of the diabatic column (blue dots), desorber and resorber (green dots) are presented in figure C.19.2:

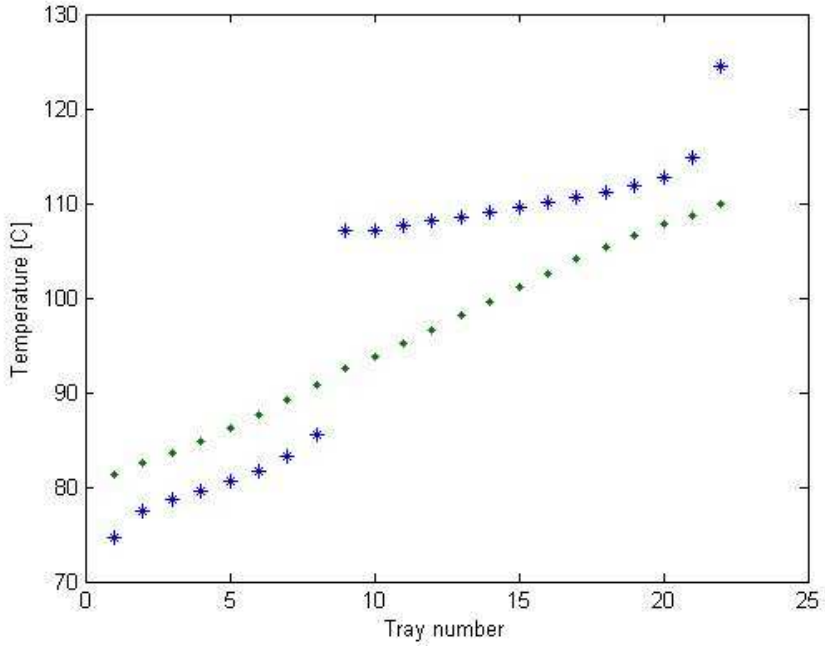

Figure C.19.2 – Temperature profile diabatic column, desorber and resorber

The minimized entropy production in the compression resorption heat pump heat pump is presented in figure C.19.3:

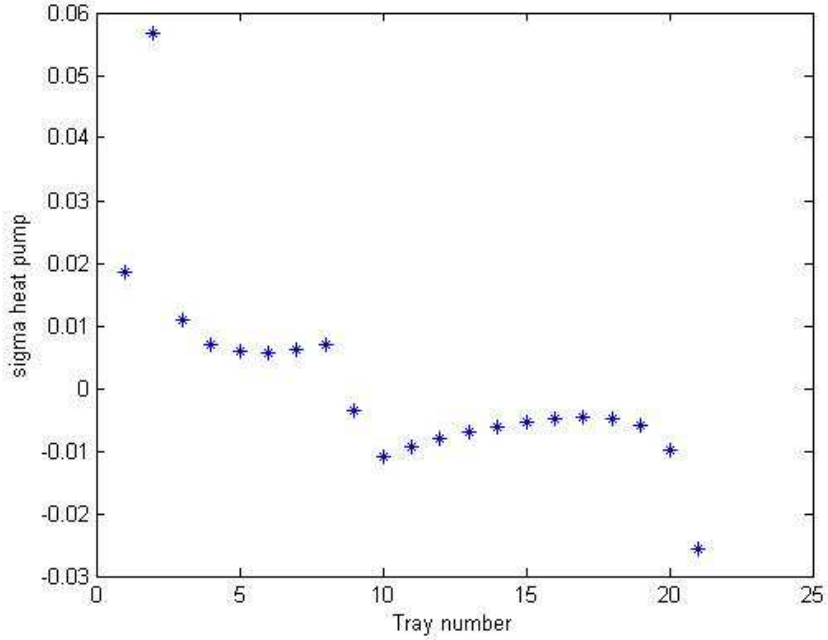

Figure C.19.3 – Minimized entropy production in the compression resorption heat pump

The entropy production for the diabatic column with integrated compression resorption heat pump is 0.7462 [kW/K].

Appendix C.20 – Average ammonia concentration of 96 wt%

Thermodynamic states of the compression resorption heat pump cycle:

Table C.20.1 – Thermodynamic states of the heat pump cycle

State	Temperature [°C]	Pressure [bar]	Enthalpy [kJ/kg]	Entropy [kJ/kg K]	P_{high}/P_{low}
1	85.19546695	34.8137	1474.8	4.892570635	1.94
2s	122.3920566	67.6061	1551	4.892722331	
2	124.9074081	67.6061	1583.6	4.97488441	
3	107.5541693	67.6061	852.05119	3.076155231	
4	75.11786306	34.8137	852.05119	3.118662135	

Using the data given in table C.20.1, a T-h diagram can be presented in figure C.20.1:

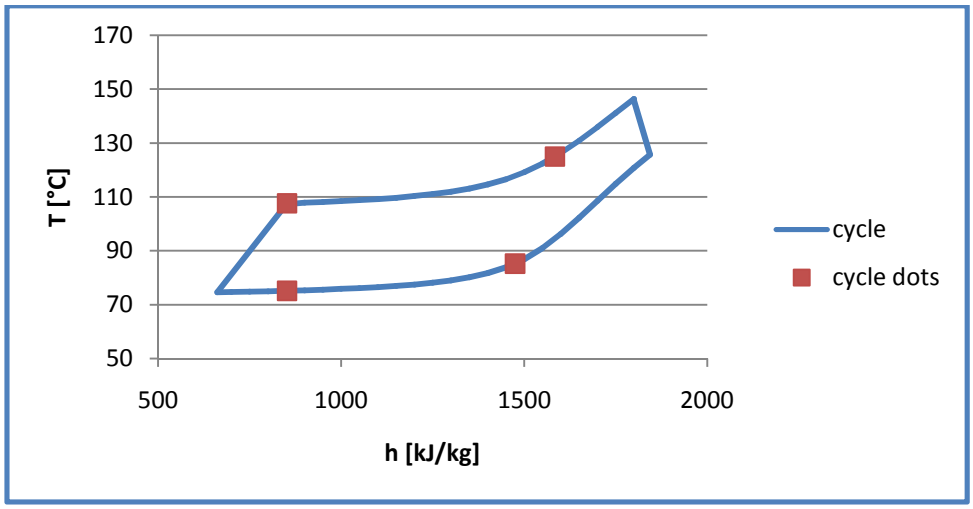

Figure C.20.1 – T-h diagram of the compression resorption heat pump

The heat loads and mass flows for the heat pump are represented in table C.20.2:

Table C.20.2 – Heat loads and mass flows compression resorption heat pump

$Q_{removed}$ [kW]	$Q_{desorber}$ [kW]	$Q_{external\_cond.}$ [kW]	$Q_{resorber}$ [kW]	W [kW]	$\dot{m}_{solution}$ [kg/s]	$\dot{m}_{air}$ [kg/s]
-40.3908	-34.8182	-5.5725	40.9	6.0814	0.0559	0.5518

The coefficient of performance (COP) for the heat pump is equal to:

$$COP = \frac{Q_{des}}{W} = 5.73$$

The temperature profile of the diabatic column (blue dots), desorber and resorber (green dots) are presented in figure C.20.2:

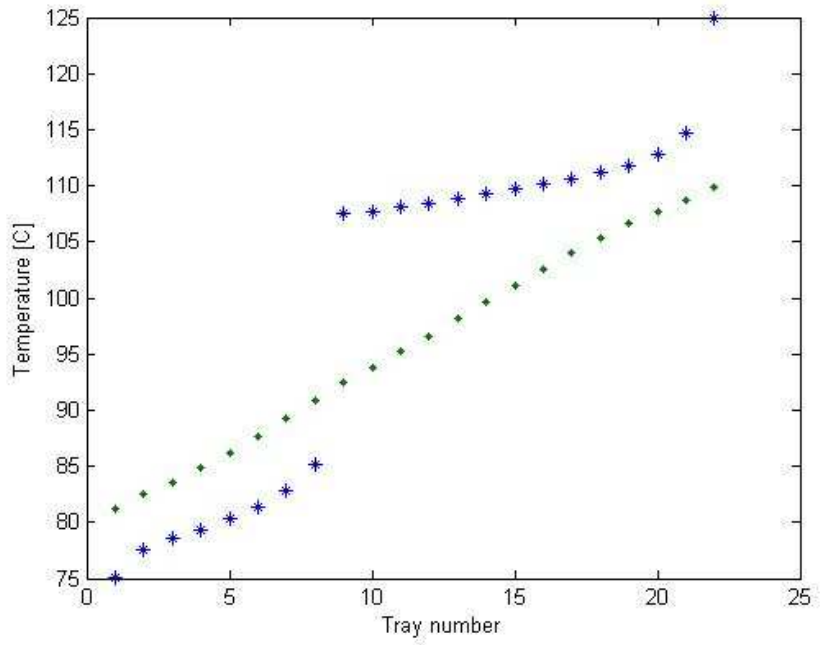

Figure C.20.2 – Temperature profile diabatic column, desorber and resorber

The minimized entropy production in the compression resorption heat pump heat pump is presented in figure C.20.3:

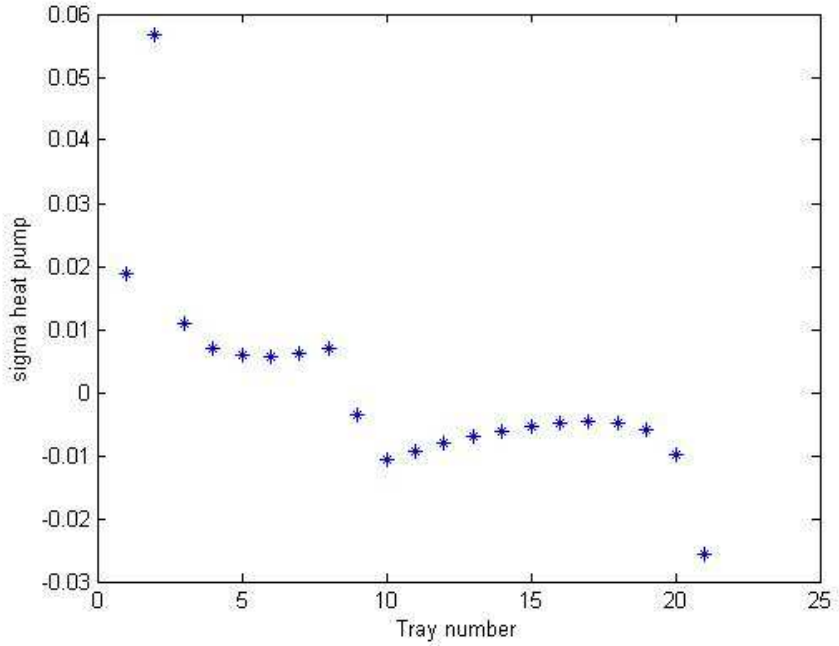

Figure C.20.3 – Minimized entropy production in the compression resorption heat pump

The entropy production for the diabatic column with integrated compression resorption heat pump is 0.6782 [kW/K].

Appendix D - Results detailed models

The second model, the irreversible thermodynamics model gives quite different local entropy production results. For the first model, heat and mass transfer model, a total entropy production of 0.031 kW/K was found, which is consistent with the optimization model. The optimization does not take into account that there is entropy production due to heat and mass transfer in the model.

The result for the second model (B) is a total entropy production of 0.18 kW/K as can be seen from figure 5.21. The reason for this high entropy production is the assumption made in section 3.3.2.2: *the vapor phase is pure ammonia*. From the heat and mass transfer model it can be seen that there is water in the vapor phase, so this assumption is not valid.

The second figure, 5.22, presents the resistivity coefficients that were used for this model. Figure 5.23 presents the heat and mass fluxes along the tube length.

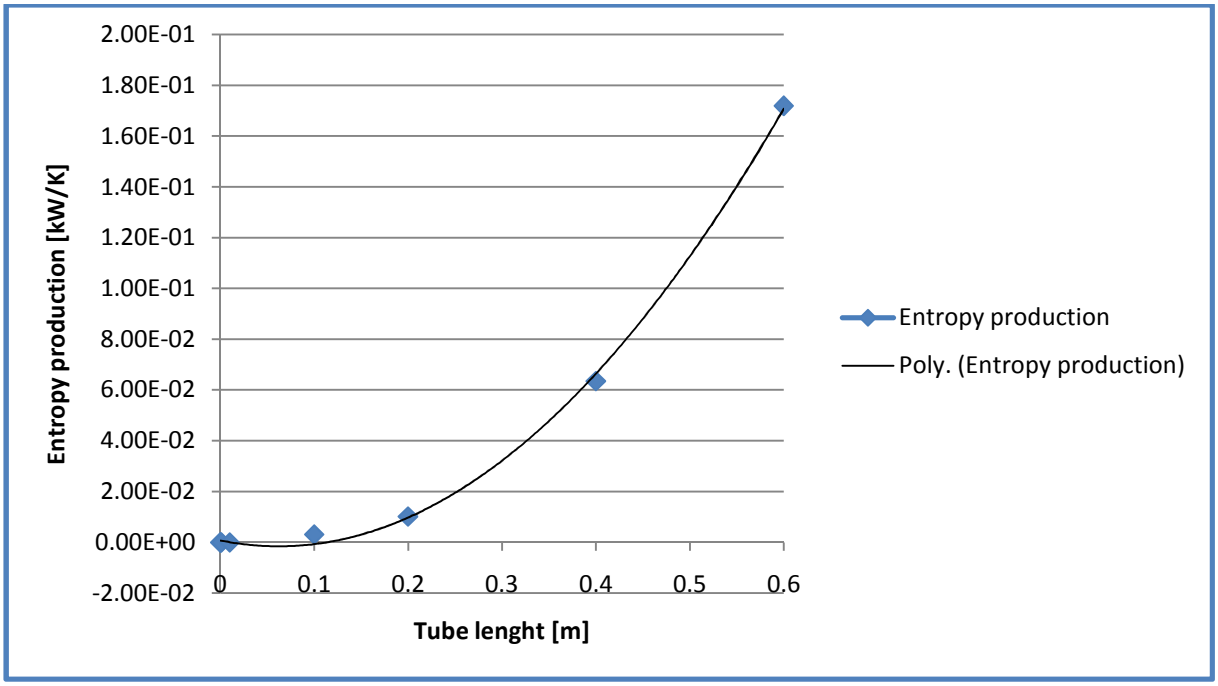

Figure 5.21 – Entropy production versus tube length

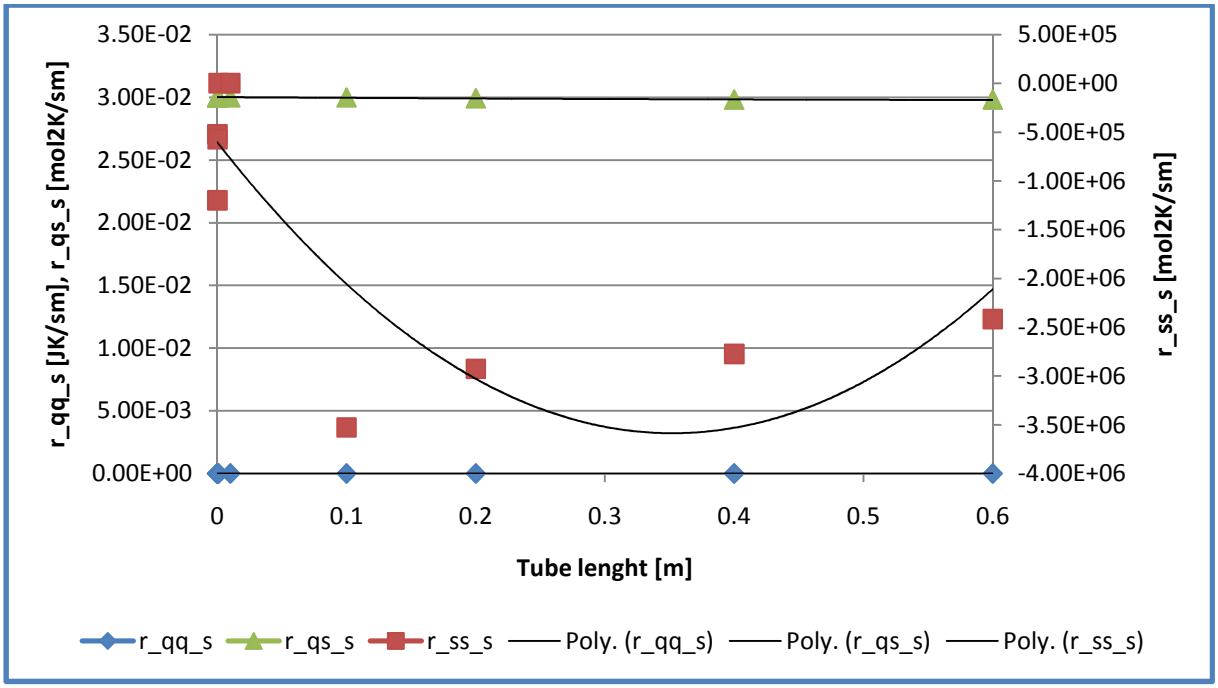

Figure 5.22 – Resistivity coefficients for bulk transport

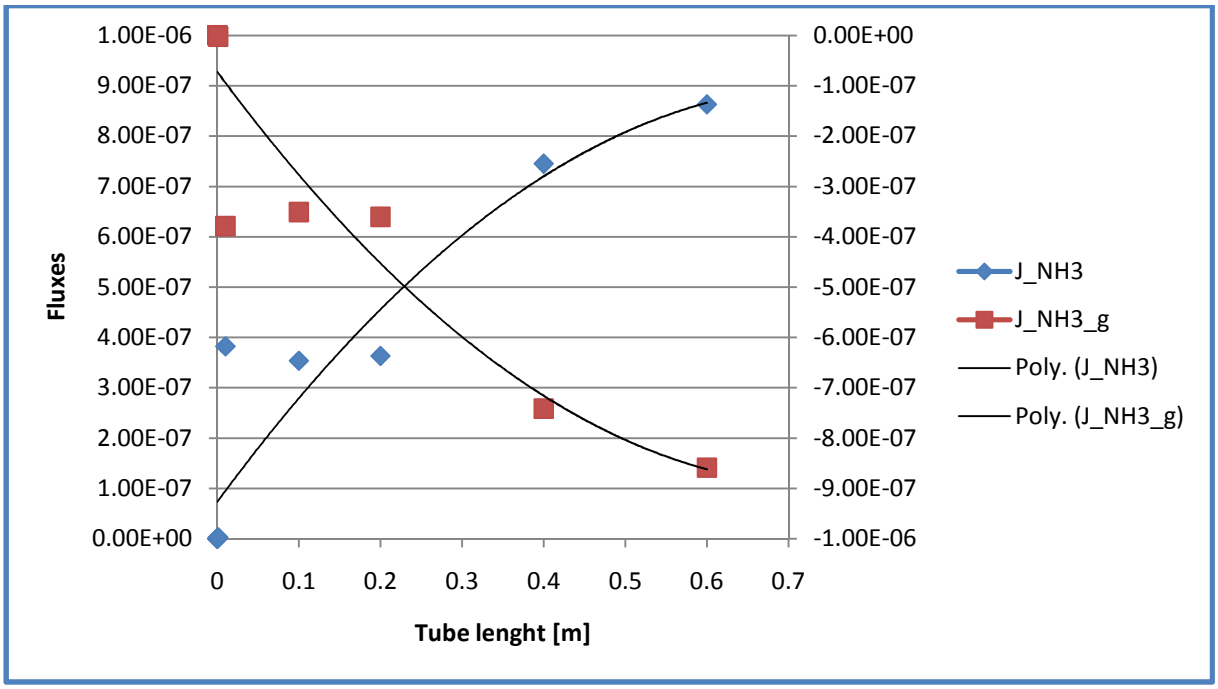

Figure 5.23 – Heat and mass fluxes

At last the values of the fluxes, resistivities and driving forces at the end of the tube are presented in table 5.5.

Table 5.5 – Results of the irreversible thermodynamics model

$J_q^{'g}$	-8.59E-07
J_{NH3}	8.63E-07
r_{qq}^s	1.09E-07
$r_{qs}^s = r_{sq}^s$	0.0298
r_{ss}^s	-2.42E+06
$\Delta_{l,g}\left(\frac{1}{T}\right)$	1.44E-05
$\left[-\frac{1}{T^l}\Delta_{g,l}\mu_{NH3,T}(T^l)\right]$	1.8637